

THE ROLE OF CANCER STEM CELL PHENOTYPE
IN THE EMERGENCE OF EPIRUBICIN RESISTANCE
IN TRIPLE NEGATIVE BREAST CANCER

By Lashika Weerakoon

Under the Supervision of A. Prof Robyn Meech

Thesis Submitted to Flinders University for the Degree of

Master of Biotechnology

College of Medicine and Public Health

28th July 2021

Master of Biotechnology
College of Medicine and Public Health
Flinders University

Topic

BTEC9000A Biotechnology Research Project (Medicine) 2020_S2

Title of the Study

The Role of CSC Phenotype in the Emergence of Epirubicin Resistance in Triple-Negative Breast Cancer

Student Name

Lashika Weerakoon

Student ID

2225287

Supervisor Name

A. Prof Robyn Meech

Supervisor Address

CMPH, Flinders University, Flinders Medical Centre (6D:322)

Assessor 1 Name

Assoc. Prof. Karen Lower

Assessor 1 Address

CMPH, Flinders University, Flinders Medical Centre (6D:211.1)

Assessor 2 Name

Dr Suong Ngoc Thi Ngo

Assessor 2 Address

University of Adelaide, Roseworthy Campus, Floor/Room G 0

Thesis Due Date

28th June 2021

CONTENTS

LIST OF FIGURES	IV
LIST OF TABLES	IV
DECLARATION	V
ACKNOWLEDGEMENTS	VI
LIST OF ABBREVIATIONS	VIII
CLINICAL NOMENCLATURE	X
ABSTRACT	XI
INTRODUCTION	1
1.1.0.0. Resistance to Anti-cancer Drugs.....	1
1.2.0.0. Breast Cancer.....	7
1.3.0.0. Molecular Classification of Breast Cancer and Its Implications in Clinic.....	8
1.4.0.0 Current Treatment Landscape of Breast Cancer	9
1.5.0.0 Clinical Management of Triple-Negative Breast Cancer	10
1.6.0.0 Epirubicin in Treating Breast Cancer and the Emergence of Resistance	11
1.7.0.0. The Role of Cancer Stem Cell Phenotype in Drug Resistance	14
1.8.0.0. Molecular Signalling Pathways Orchestrating Drug Resistance.....	18
1.9.0.0. Molecular Biomarkers of Breast Cancer Stem Cells	21
1.10.0.0. MDA-MB-231 Cell line as an Invitro Model to Study TNBC.....	27
1.11.0.0. Rational for the Current Study, Preliminary Investigations, and the Experimental Design	28
1.12.0.0. Thesis Aims and Hypothesis.....	32
1.13.0.0. Significance to Medical Biotechnology.....	34
MATERIAL & METHODS	36
2.1.0.0. Research Facilities and Core Services.....	37
2.2.0.0. Material and Equipment.....	37
2.3.0.0. Cell Line.....	40
2.4.0.0. Methods.....	40
2.4.1.0. Maintenance of Mammalian Cell Cultures	40
2.4.2.0. Cryopreservation and Resurrection of MDA-MB-231 Cells.....	41
2.4.3.0. Epirubicin Treatment of MDA-MB-231 Cell Cultures	42
2.4.4.0. TRIzol Aided RNA Extraction	43
2.4.5.0. cDNA Synthesis by Reverse Transcription	44
2.4.6.0. Quantitative Real-Time PCR (qRT PCR).....	45
2.4.7.0. MTT Cell Proliferation Assay	46

2.4.8.0.	Mammosphere Formation Assay.....	48
2.4.9.0.	Establishment of an Epirubicin Resistant MDA-MB-231 Cell Subline	50
2.5.0.0.	Statistical Analysis	52
2.7.0.0.	Compliance with Ethical and Safety Standards	52
RESULTS	53
3.0.0.0.	Overview	54
3.1.1.0.	Adaptive Response of MDA-MB-231 cells to Epirubicin Treatment	54
3.1.1.1.	<i>ALDH1A1</i> , <i>OCT4</i> and <i>SOX2</i> Stemness Indicator Gene Expression	55
3.1.1.2.	<i>ABCB1</i> Transporter Gene Expression.....	58
3.1.2.0.	Stability of Gene Induction after Epirubicin Withdrawal	60
3.1.3.0.	Exposure to Epirubicin Reduces Mammosphere Formation Capacity.....	63
3.1.4.0.	Exposure to Epirubicin Inhibits Cell Proliferative Capacity	68
3.2.0.0.	Establishment of an Epirubicin Resistant MDA-MB-231 Sub-line.....	70
3.2.1.0.	Comparison of the Drug Selection Protocols.....	70
3.2.2.0.	Analysis of drug sensitivity by IC50 determination	72
3.2.3.0.	Stem Cell Markers in the Epirubicin Selected Population	74
DISCUSSION	77
4.1.0.0.	General Project Overview and Summary of Findings.....	77
4.2.0.0.	Upregulation of <i>ABCB1</i> , <i>ALDH1A1</i> , <i>OCT4</i> , and <i>SOX2</i> Genes in Short-term Epirubicin Exposed MDA-MB-231 Cells	80
4.3.0.0.	Stability of Epirubicin induced Gene Induction	87
4.4.0.0.	Diminished Mammosphere Formation Capacity	88
4.5.0.0.	Epirubicin Inhibits MDA-MB-231 Cell Proliferation Even After Four Days.....	89
4.6.0.0.	Selection of a Stably Epirubicin Resistant MDA-MB-231 Cell Population.....	90
4.7.0.0.	Variable IC50 of the Epirubicin Selected MDA-MB-231 Cells.....	92
4.8.0.0.	Epirubicin Selected MDA-MB-231 Cells and BCSC Markers	94
4.9.0.0.	Future Directions	95
BIBLIOGRAPHY	98
APPENDICES	115
5.1.0.0.	Material, Equipment and Software Tools Utilised in This Study.....	115
5.2.0.0.	Methods Elaborated	118
5.2.1.0.	Estimation of RNA Yield	118
5.2.2.0.	Establishment of the Standard Curve for the MTT Assay.....	118
5.3.0.0.	Calculations.....	119
5.4.0.0.	Epirubicin Treatment Alters UGT Enzyme Gene Expression Levels	123
5.5.0.0.	MDA-MB-231 Spheroid Generation By Liquid Overlay Method	125

LIST OF FIGURES

FIGURE 1.1.	SCHEMATIC REPRESENTATION OF CANCER EVOLVING TO BE TREATMENT-RESISTANT	4
FIGURE 1.2.	MULTIFACTORIAL NATURE OF ANTINEOPLASTIC DRUG RESISTANCE.	6
FIGURE 1.3.	CANCER STEM CELL MODEL.....	17
FIGURE 1.4.	STEMNESS AND ABC TRANSPORTER MRNA LEVELS OF EPIRUBICIN TREATED CELLS.....	30
FIGURE 1.5.	STEMNESS AND ABC TRANSPORTER MRNA LEVELS OF INDUCED BREAST CANCER STEM CELLS	31
FIGURE 3.1.	EXPRESSION OF BREAST CANCER STEM CELL MARKER GENES AFTER 48-HOUR EPIRUBICIN TREATMENT	57
FIGURE 3.2.	EXPRESSION OF ABC TRANSPORTERS UPON 48-HOUR EPIRUBICIN TREATMENT	59
FIGURE 3.3.	STEMNESS MARKERS AND ABC TRANSPORTER EXPRESSION UPON THE DRUG HOLIDAY	63
FIGURE 3.4.	MAMMOSPHERE FORMATION	67
FIGURE 3.5.	VARIATION IN THE PROLIFERATION AFTER DRUG TREATMENT + HOLIDAY	69
FIGURE 5.1.	STANDARD CURVE FOR THE MTT ASSAY	119
FIGURE 5.2.	DIFFERENTIAL EXPRESSION OF UGT2B7, UGT2B10 AND UGT2B15	124
FIGURE 5.3.	MDA-MB-231 SPHEROID CULTURING	127

LIST OF TABLES

TABLE 1.1.	AN OVERVIEW OF BREAST CANCER STEM CELL MARKERS USED IN THIS STUDY.....	22
TABLE 2.1.	CHEMICALS AND REAGENTS USED THROUGHOUT THIS STUDY AND RESPECTIVE SUPPLIERS	38
TABLE 2.2.	qPCR CYCLING CONDITIONS.....	45
TABLE 2.3.	PARAMETERS OF DIFFERENT STRATEGIES TO ESTABLISH AN EPIRUBICIN RESISTANT MDA-MB-231 SUBLINE.....	51
TABLE 5.1.	THE COMPOSITION OF THE REAGENTS AND BUFFERS USED IN THIS STUDY	115
TABLE 5.2.	EQUIPMENT'S AND APPARATUS USED IN THIS STUDY	115
TABLE 5.3.	CONSUMABLES USED IN THIS STUDY.....	116
TABLE 5.4.	OLIGONUCLEOTIDES USED IN MRNA QUANTIFICATION	117
TABLE 5.5.	SOFTWARE TOOLS USED IN THE STUDY	118
TABLE 5.6.	CROSS ANALYSIS OF THE STEMNESS MARKER MRNA LEVELS IN THE UNTREATED MDA-MB-231 CELLS	128

DECLARATION

I certify that this thesis does not incorporate without acknowledgment any material previously submitted for a degree or diploma in any university; that to the best of my knowledge and belief, it does not contain any material previously published or written by another person except where due reference is made in the text.

Lashika Weerakoon

28th June 2021

ACKNOWLEDGEMENTS

I would like to acknowledge and thank many people who have provided their invaluable support and encouragement throughout this project.

First and foremost, I would like to express my deepest and sincere gratitude towards my supervisor, Associate Professor Robyn Meech, for the golden opportunity extended to me to learn and grow under you. I never ceased to be inspired by your unparalleled knowledge and vision as a great scientist, in addition to your sincerity and compassionate heart. I owe many great teachers I have met in my life for any success that I have achieved as a student. However, the length that you go in supporting your students is comparable to none. I could not have asked for better guidance during the most crucial phase of my academic years. Thank you, Robyn.

Secondly, I cannot express enough thanks to the PhD students in my lab: Mr Radwan Ansar, Mr Quinn Martin, Mr Dylan Martin, and Mr Jai Mayers. I am incredibly grateful for the wise counsel, support, and companionship through each stage of this project. I would particularly like to mention Mr Radwan Ansar, who carried out the preliminary experiments that paved the path for this project, method optimization, and invaluable assistance when learning new techniques.

My sincere appreciation goes to Emeritus Professor Peter Mackenzie, Dr Dong Gui Hu, Dr Julie-Ann Hulin, Professor Ross McKinnon, Dr Pramod Nair, Dr Alex Haines, Dr Siti Mubarokah and especially Dr Sara Tommasi, the Department of Pharmacology. It was a great pleasure and honour to learn from you and be in your company. I must especially mention and thank Dr Lu

Lu for being always willing to help, whether it is learning laboratory techniques or orienting myself in the laboratory. I am also grateful to Associate Professor Munish Puri, Associate Professor Kirsten Heimann, Professor Chris Franco, Professor Wei Zhang, Dr Liu-Fei Tan, and other research staff in the Department of Biotechnology for their support throughout my time at Flinders.

Finally, my heartfelt gratitude goes to my fellow lab mate and my friend, Mr Jai Mayers, who was instrumental in every step in this project. My gratitude towards you is endless for the unwavering attention, continuous support, and much-needed reassurance extended towards me from you. Your companionship throughout this time was a true blessing.

Even though mentioned before, I would like to reiterate all the members of Prof Meech's lab. This year has been a remarkable year for me, and I owe all of you for that. I thank you again and again.

LIST OF ABBREVIATIONS

3D	Three Dimensional
ABC	ATP Binding Cassette (ABC)
ALDH	Aldehyde Dehydrogenase (ALDH)
ATCC	American Type Culture Collection
BC	Breast Cancer
BCSC	Breast Cancer Stem Cell
bFGF	Basic Fibroblast Growth Factor
BP	Base Pairs
CD44	Cluster of Differentiation 44
cDNA	Complementary DNA
CSC	Cancer Stem Cell
Ct	Cycle Threshold
DMEM	Dulbecco's Modified Eagle's Medium
DMSO	Dimethyl Sulfoxide
DNA	Deoxyribo Nucleic Acid
DNER	Delta/ Notch- Like Epidermal Growth Factor (EGF) Related Receptor
dNTP	Deoxy Nucleotide Tri Phosphate
EDTA	Ethylenediaminetetraacetic Acid
EMT	Endothelial Mesenchymal Transition
ER	Estrogen Receptor
FBS	Foetal Bovine Serum
G	Gauge
HCl	Hydrochloride Acid
hEGF	Human Epidermal Growth Factor
HER2	Human Epidermal Growth Factor Receptor 2
IC50	Half Maximal Inhibitory Concentration
ITS	Insulin Transferrin Selenium
mRNA	Messenger RNA
MTT	3-(4,5-dimethylthiazol-2-yl)-2,5-diphenyl tetrazolium bromide
OCT4	Octamer-Binding Transcription Factor 4

OD	Optical Density
PBS	Phosphate Buffered Saline
PC	Physical Containment
PC2	Physical Containment Level 2
PCR	Polymerase Chain Reaction
poly-HEMA	Poly-2-hydroxyethyl-methacrylate
PR	Progesterone Receptor
qRT PCR	Quantitative Reverse Transcription PCR
R2	Coefficient of Determination
RNA	Ribo Nucleic Acid
SC	Stem Cell
SOX2	Sex Determining Region Y (SRY)- Box 2
TNBC	Triple-Negative Breast Cancer
UGT	Uridine 5'-Diphospho-Glucuronosyltransferase
USA	United States of America
UV	Ultraviolet

CLINICAL NOMENCLATURE

Pathologic Complete Response (PCR) in breast cancer: The absence of neoplastic cells in the breast and the axillary lymph nodes after histology (Milani et al. 2017).

Neo-Adjuvant Chemotherapy: The use of systematic therapy prior to surgery (Korde et al. 2021).

Adjuvant Therapy: The use of systematic therapy after the primary treatment, such as surgery, to reduce the risk of disease recurrence (Ward et al. 2021).

Locoregional Recurrence: Re-emergence of the tumour at the primary site of initial diagnosis or in the regional lymph nodes following a disease-free period (Tse et al. 2021).

ABSTRACT

Despite the advances in treatment strategies, cancers remain fatal to most patients mainly due to tumour cell's remarkable ability to develop resistance to therapy. Epirubicin is an anthracycline, extensively utilised in the chemotherapeutic regimens for treating early as well as advanced breast cancer. Chemoresistance to epirubicin is a common occurrence and a major factor limiting the efficacy of epirubicin-incorporated regimens, which leads to treatment failure, disease progression, relapse, and mortality.

This study focuses on triple-negative breast cancer (TNBC), a biologically aggressive breast cancer subtype with few therapeutic options in the form of targeted therapies. TNBC may show primary or acquired resistance to epirubicin, and the development of collateral resistance to next in line therapy is an added complexity in the clinical management of TNBC. Elucidation of cellular mechanisms contributing to drug resistance is crucial to predict, prevent and overcome drug resistance in clinical settings.

The cancer stem cell (CSC) phenotype is a critical element of the multi-dimensional architecture of drug resistance. Resembling normal stem cells, CSCs are often slow-cycling and can survive cytotoxic treatments that target fast proliferating cancer cells. They can subsequently expand due to their inherent self-renewal capacity and cause tumours to re-emerge with a heightened resistance driven by enhanced plasticity. These secondary tumours are often more aggressive and multi-drug resistant. Targeting the CSC population and stemness pathways that promote drug resistance may reduce cancer recurrence.

This study aimed to investigate the role of BCSCs in the emergence of resistance to the chemotherapeutic agent epirubicin in TNBC. In the first Aim, quantitative gene expression analysis data indicated an upregulation of key stemness markers ALDH1, OCT4, and SOX2 along with the drug transporter ABCB1, upon a short term (48 hours) epirubicin treatment of MDA-MB-231 TNBC cells. These adaptive expression responses to epirubicin exposure were partly sustained after a period of drug withdrawal, and notably, ALDH1 expression showed further upregulation following the drug withdrawal. Despite showing sustained expression of stemness markers, the cells did not show enhanced self-renewal capacity when tested using a mammosphere formation assay. However, this finding appeared to relate to the diminished proliferative capacity of epirubicin treated cells. In the second Aim, an MDA-MB-231 sub-line was generated by long-term epirubicin selection and assessed for enhanced drug resistance and expression of stemness and drug resistance markers. While consistent IC50 values for epirubicin could not be defined, the drug-selected subline appeared less sensitive to high doses of epirubicin. However, it did not show enhanced expression of stemness markers or the drug efflux transporter.

The findings of this study lend support for the multifactorial nature of chemoresistance against epirubicin involving pathways that control drug exposure (such as drug efflux) and stem cell-associated survival pathways. Specifically, the results show that induction of these pathways may serve as a short-term adaptive response to epirubicin exposure; however, they may be dispensable in developing long-term stable drug resistance.

INTRODUCTION

1.1.0.0. Resistance to Anti-cancer Drugs

Cancer is a leading cause of death in Australia, with approximately one in two Australians diagnosed with cancer by the age of 85. Diagnosis of cancer triggers a necessity of eradicating or controlling the disease as quickly as possible, which typically involves more than one treatment approach. Surgery, radiotherapy, and/or drug treatment remain the conventional therapeutic approaches utilised in the management of cancer that is localized in a tissue or locally advanced (Gatenby & Brown 2020). For metastatic cancer that has disseminated to multiple parts of the body, systemic therapy is required, which involves the delivery of drugs that circulate through the bloodstream. Antineoplastic systemic therapy can include cytotoxic, hormonal, targeted, as well as modern immunotherapy agents. These are used in metastatic

settings, as well as neoadjuvant and adjuvant treatments (Gonzalez-Angulo et al. 2007). Neoadjuvant therapy is often used to reduce tumour bulk prior to surgery, while adjuvant therapy may be given after other treatments to reduce the risk of cancer recurrence. Despite being in the era of precision oncology and immunotherapy with the promise of potent and more tolerable therapeutic options to combat cancer, chemotherapy remains a cornerstone treatment option in managing advanced cancer.

Regardless of their importance, therapeutic regimens incorporating cytotoxic agents face many challenges in clinical settings. The natural emergence of resistance to agents remains the frontline hurdle in curing or achieving disease-free survival in cancer patients. Moreover, treatment-related toxicity in non-malignant tissues is another significant trade-off in cytotoxic-based therapeutic regimens. These effects may be dose-limiting, with therapeutic doses too toxic for the patient to withstand. Thus, modern oncology is in dire need of efficient therapeutic modalities that can overcome resistance using tolerable drug doses (Garcia-Mayea et al. 2020).

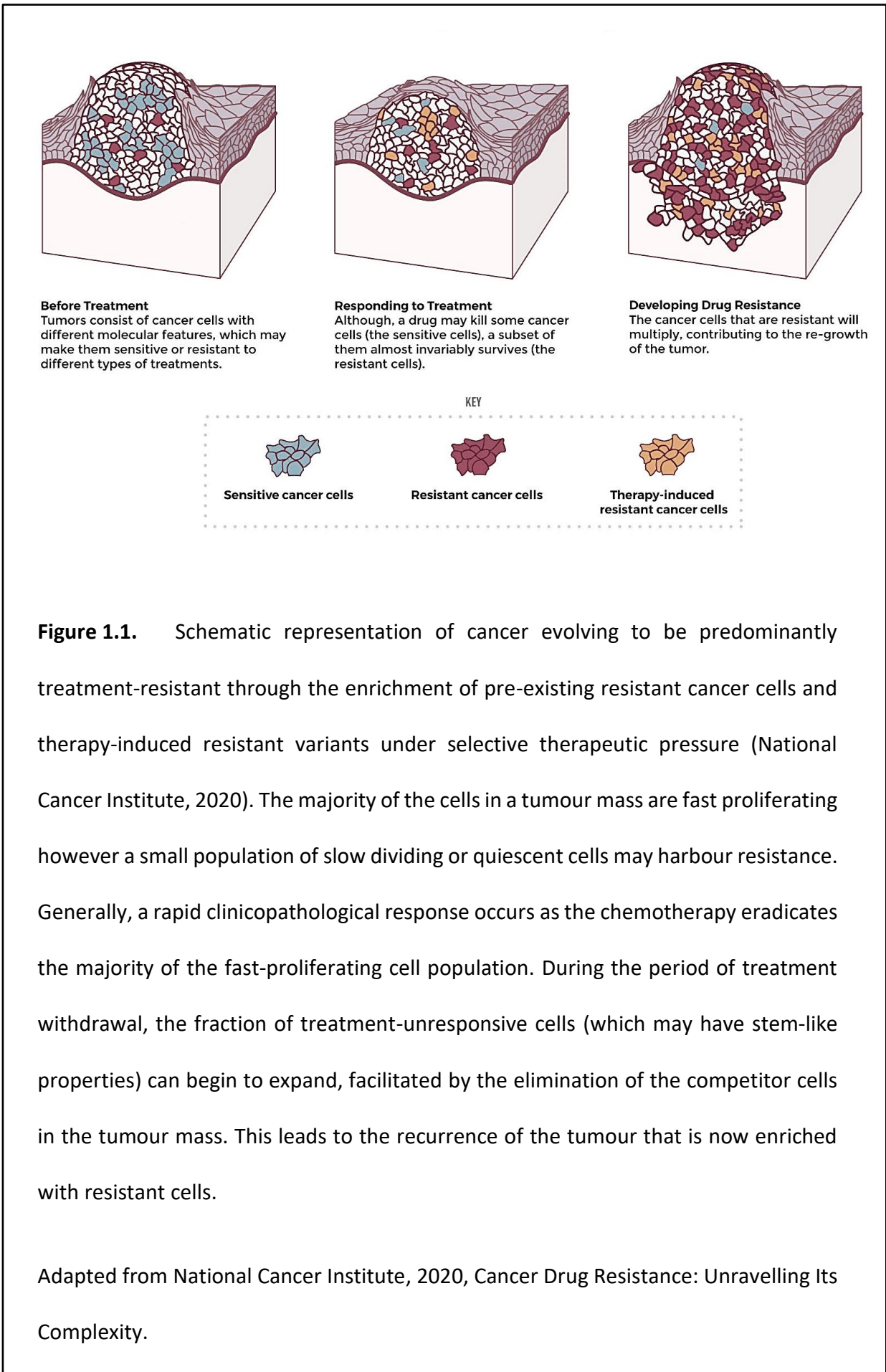
At the initial stages of treatment, 90% of primary cancers and 50% of metastases respond to treatment. However, after variable periods following the initial course of drug administration, the recurrence of a treatment-unresponsive, more aggressive tumour is a common and primarily inescapable occurrence in all the types of neoplasms that collectively cause up to 90% of cancer mortality (Wang, X et al. 2019).

Therapy failure can occur when the tumour becomes insensitive to one, or more broadly, to multiple drugs. The term multi-drug resistance describes the state where tumours become

irresponsive to multiple drugs with distinct functionalities (i.e. different targets) and chemical structures (Györfy et al. 2006).

Contributing to its complexity, drug resistance can be intrinsic as well as acquired. Although there is some controversy over the precise definitions of intrinsic and acquired resistance, from a clinical perspective, intrinsic resistance is generally defined as a lack of response to initial therapy; in contrast, tumours that initially responded to treatment and later relapsed are typically described as showing acquired resistance. At a cellular and molecular level, intrinsic resistance suggests the presence of pre-existing resistant subclones that prevent the complete eradication of the tumour in the early stages of treatment. Acquired resistance may involve the development of genetic or epigenetic changes during treatment, as well as the selection and overgrowth of drug-resistant cells (Hayashi & Konishi 2020). In general, drug resistance involves a combination of evolutionary events that leads to the advancement of sub-populations enriched with pre-existing resistant cells and the emergence of new resistant mutants with a survival advantage: both thriving under drug exposure. Ultimately, under the therapeutic selection pressure, drug-sensitive tumour cells are eradicated while resistant cells with enhanced survival advantage are released from the competition and expand, forming a predominantly resistant tumour (Figure 1.1).

Cancer cells are generally considered more plastic than non-cancer cells, meaning they possess an enhanced capability to change phenotypically due to genetic and epigenetic alterations. This enhanced plasticity plays a vital role in the evolution of tumours towards drug resistance. Targeting these plasticity pathways during the initial therapy stages could be a strategy for sustaining a more favourable therapeutic response.



The multidimensional architecture of tumour cell drug resistance is contributed to by a range of processes: increased drug efflux, decreased drug uptake, altered drug metabolism, sequestration of drugs, functional/structural alteration of drug targets, activation of detoxifying systems, enhanced repair of drug-induced DNA damage, disruption of signalling pathways, alterations of cell cycle regulation factors, and inhibition of apoptosis (e.g. Figure 1.2) (Baguley 2010; Filipits 2004; Mansoori et al. 2017). Almost all of these pathways have been reported to play some role in resistance to non-targeted cytotoxic therapies, while some are more commonly associated with resistance to targeted therapies (e.g., genetic/epigenetic alteration in the drug target). The presence of multiple pathways involved in drug resistance, which may act concurrently and/or synergistically, is a significant challenge for overcoming resistance. All these elements contribute to defining clinical drug resistance as a complex and multifactorial phenomenon. Elucidation of these cellular mechanisms is crucial in order to predict, prevent and overcome drug resistance in clinical settings.

Drug regimens comprising two or more drugs with different chemical and functional characteristics, administered either simultaneously or sequentially, contribute more effectively to overcome the multiple survival pathways used by tumour cells. Combination therapy refers to the co-administration of different agents and may cause more significant initial tumour cell kill. It may allow (and in some cases necessitate) the utilisation of lower doses of each drug while reducing the side effects and potentially also lowering the likelihood of developing resistance (Ibiyeye et al. 2019). In contrast, sequential use of single agents can allow for higher dosing than is tolerable in combination therapy. Generally, the efficacy of these approaches varies by cancer and drug type and must be determined empirically. All of these strategies will be hindered by the development of cross-resistance. In sequential therapy, this may involve tumours becoming unresponsive to the drugs used in the latter

phases of treatment, driven by resistance mechanisms induced by the first-line agents. This is sometimes called collateral resistance, as it is a ‘collateral effect’ of treatment. Multi-drug resistance is generally driven by mechanisms independent of the specific mode of drug action.

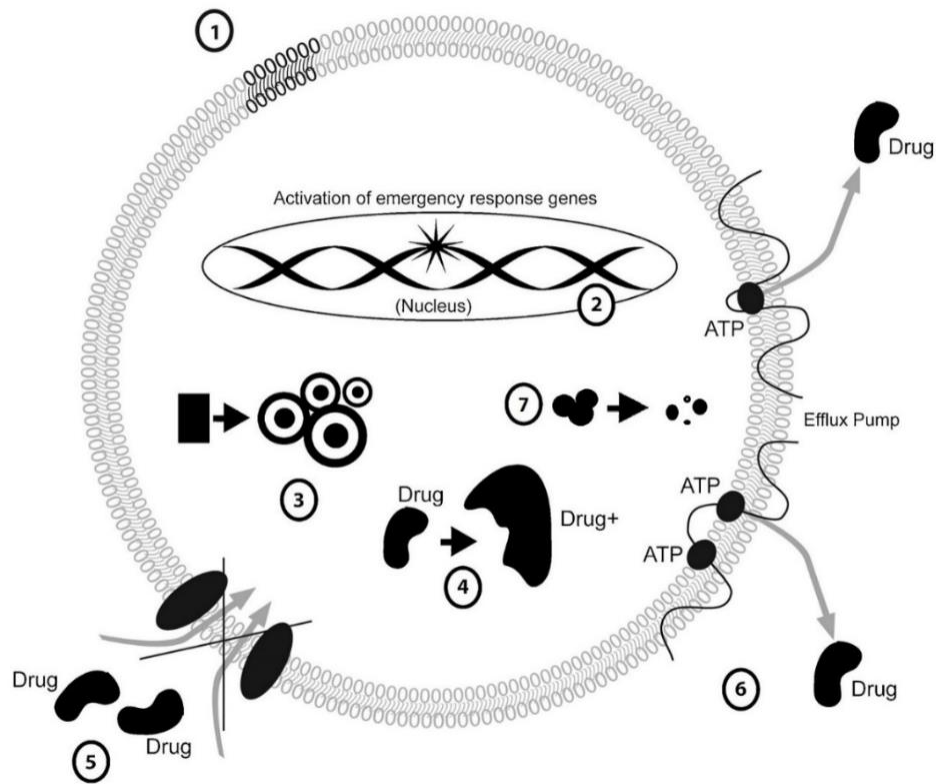


Figure 1.2: Multifactorial nature of antineoplastic drug resistance. Treatment-resistant cancer cells bypass the inhibition of proliferation and apoptosis induced by a therapeutic agent using multiple mechanisms contributing to antineoplastic drug resistance including 1) Tumour microenvironment 2) increased repair of DNA, 3) Modifying the drug target, 4) Enhanced drug metabolism 5) downregulated drug uptake 6) Upregulated drug efflux, 7) Enhanced reactive oxygen species scavenging.

Adapted from *Molecular Cancer Therapeutics*, 2010, 9/12, 3126-36, Kristi E. Allen, Glen J. Weiss, Resistance May Not Be Futile: microRNA Biomarkers for Chemoresistance and Potential Therapeutics, with permission from AACR.

1.2.0.0. Breast Cancer

Breast cancer (BCa) is the most prevalent cancer type among women worldwide. It accounts for 25% of all cancers, with approximately 1.7 million cases diagnosed worldwide each year (Sung et al. 2021). The incidence of BCa has slightly increased since 2004, which can be attributed to increased screening and lifestyle changes (Pfeiffer et al. 2018). More positively, BCa morbidity and mortality rates have decreased since 1989, which mirrors the advances in diagnosis and treatment (Siegel et al. 2020). Still, the ever-changing global BCa landscape demands increased research attention, notably as BCa recently surpassed lung cancer as the most common form of cancer and the leading cause of cancer death among women, according to the latest 2021 data (Sung et al. 2021).

Neoplastic transformation of the mammary gland initiates as an accumulation of genetic and epigenetic modifications that collectively alter critical elements of cell signalling. These mutations create an autonomously dividing cell, which will eventually establish a colony of pathologically abnormal cells. Oncogenic mutations can be inherited (e.g. *BRCA1*, *BRCA2*), induced by extrinsic agents (e.g. viruses, chemical agents, irradiation) or arise spontaneously during cell mitosis (Godet & Gilkes 2017). Because BCa is very phenotypically and molecularly diverse, the drivers of malignancy are also diverse. Although, they frequently include mutation of genes encoding ubiquitous tumour suppressors such as p53, p16, pTEN, p27, caveolin-1, and factors that control DNA repairs such as the aforementioned *BRCA1* and *BRCA2* (Wren 2007).

1.3.0.0. Molecular Classification of Breast Cancer and Its Implications in Clinic

BCa portrays a remarkable degree of both histopathological and molecular heterogeneity, defined by genetic, epigenetic, and transcriptomic variation (Viale 2012). Thus, BCa cannot be treated as a sole clinicopathological entity and is instead dissected into multiple subtypes to facilitate oncologic decision making.

Based on the expression of estrogen (ER) and progesterone (PR) hormone receptors and the amplified expression of the human epidermal growth factor receptor 2 (ERBB2/HER2), BCa patients have been classically stratified into three distinct clinical subtypes; hormone receptor-positive (HR+/ ER+, PR+/- and HER-), HER2 positive (HER2+) and triple-negative (ER-, PR- and HER2-). About 80% of all BCa are ER+ with 65% being PR+ (indicating that ER is transcriptionally active), 20% are HER2+, and 10-20% are classified as triple-negative (TNBC). Later analysis of BCa using a 50-gene-expression signature called PAM50 led to stratification into five distinct molecular subtypes: Luminal A, Luminal B, HER2 enriched, basal-like and normal-like BCa (Perou et al. 2000). These different subtypes have distinct clinical outcomes and response to treatment. However, there remains considerable heterogeneity within these subtypes, and additional biomarkers such as proliferation marker Ki-67, cytokeratin, cyclin D and claudin expression are utilised to refine clinical decision making (Gusterson et al. 2005; Prat et al. 2010). In particular, TNBC is further categorised into basal-like 1, basal-like 2, mesenchymal, mesenchymal stem-like, immunomodulatory and luminal androgen receptor types based on the distinct molecular profile, which prompt employing different treatment strategies (Wahba & El-Hadaad 2015).

1.4.0.0 Current Treatment Landscape of Breast Cancer

While ~70-80% of early-stage non-metastatic BCa has a higher chance of successful clinical management, advanced BCa with distant organ metastasis is considered incurable yet treatable with currently available treatment options (Harbeck et al. 2019). Therapeutic decisions in the clinical management of BCa differs with multiple molecular and histological variables, including tumour size, nodal status, histological grade, ER, PR and HER2 expression.

Locoregional (surgery and radiation therapy) and systemic treatment are the principal elements of modern BCa therapy (Guiu et al. 2012). Breast-conserving surgery or mastectomy followed by radiation therapy and adjuvant drug therapy are routinely administered in early-stage BCa patients. Adjuvant therapies, including hormonal/targeted therapies or chemotherapies, are designed to kill any residual cancer cells to lower the chances of relapse. Neoadjuvant therapy describes the administration of drugs, including chemotherapies prior to the primary treatment. It is routinely employed in BCa treatment regimens and contributes to treatment success by increasing the duration of event-free survival while increasing the probability of breast-conserving surgery by shrinking the tumour (Schmid et al. 2020). Also, the in-vivo preview of the response to neoadjuvant chemotherapy aids in therapeutic decision making of the post-operative treatment strategy and acts as a powerful prognostic marker for the recurrence risk (Bellon et al. 2020; Milani et al. 2017).

For advanced BCa, which is considered incurable, surgery remains an option. Although systemic treatment involving hormonal therapy, targeted therapies, and chemotherapy continues to be the primary therapeutic choices to control disease progression and reduce symptom burden.

1.5.0.0 Clinical Management of Triple-Negative Breast Cancer

Despite some variabilities in clinical course, TNBC is a highly lethal (5-year mortality > 75%) malignancy with a poor prognosis including shorter disease-free interval, higher recurrence rate, aggressive metastasis, and more frequent drug resistance, as compared to other stage-equivalent BCa subtypes. As discussed further below, limited therapeutic targets add to the complexity of the clinical management of TNBC. Furthermore, the unmet medical needs of managing TNBC is mainly represented by limited persistence of the clinical response, inadequate survival benefit and challenging toxicology profiles (Li, CH et al. 2019).

Surgical management and radiation therapy are administered to TNBC patients similarly to other BCa subtypes. TNBC patients with a tumour >0.5cm or nodal involvement (regardless of the size) are given adjuvant and/or neoadjuvant chemotherapy in nonmetastatic settings. An array of factors including tumour size, lymph node involvement, grade, overall performance, and other comorbidities are typically considered when defining chemotherapeutic regimens for patients. TNBC is immunohistochemically defined by not expressing estrogen receptor (ER) and progesterone receptor (PR) and by the absence of overexpression/amplification of human epidermal growth factor receptor 2 (ERBB2/HER2). Thus, TNBC patients do not qualify as candidates for hormonal (e.g., anti-estrogen) and HER2-targeting treatment regimens (e.g. trastuzumab and selective kinase inhibitors). As a result, chemotherapy incorporating cytotoxic drugs remains a fundamental systemic treatment option in the standard of care for metastatic TNBC (Alkaraki et al. 2020).

Despite chemotherapy being the standard of care for metastatic TNBC, no agent has been specifically approved for this BCa subtype. Nevertheless, Chemotherapy regimens

incorporating a taxane (docetaxel, paclitaxel), an anthracycline (epirubicin, doxorubicin) and alkylator (cyclophosphamide) remain the gold standard chemotherapy regimen for node-positive TNBC in either adjuvant or neoadjuvant settings (Mayer & Burstein 2016). However, half of the patient population with localised TNBC who receive neoadjuvant chemotherapy fails to show adequate clinicopathological response (Symmans et al. 2017). Instead, they end up with a substantial residual tumour burden with a risk of severe adverse effects. Overall, only around 30% of TNBC patients demonstrate pathologic complete response (Von Minckwitz et al. 2012), primarily associated with chemoresistance.

1.6.0.0 Epirubicin in Treating Breast Cancer and the Emergence of Resistance

Anthracyclines are a vital component of standard combinatorial chemotherapeutic regimens utilised in the clinical management of early as well as advanced BCa. Epirubicin (Ellence® or Pharmorubicin®; Pfizer Pharmaceuticals, New York) and doxorubicin (Adriamycin®; Bedford Laboratories, Bedford, OH) are the most established anthracyclines incorporated in the majority of standard chemotherapy combinations (Khasraw et al. 2012). Following its FDA approval in 1999, epirubicin hydrochloride has been marketed in over 80 countries (Peng et al. 2020).

A semisynthetic anthracycline antibiotic, epirubicin is the 4' epimer of doxorubicin. Epirubicin is among the most potent chemotherapeutics utilised in treating an array of tumours (Khasraw et al. 2012). While being extensively used in the clinical management of early as well as advanced BCa, epirubicin is also used in the treatment of a broad spectrum of malignancies that include ovarian, thyroid, gastric and lung cancers, acute leukemia, non-Hodgkin's

lymphoma, advanced soft tissue sarcoma and superficial bladder cancer (Peng et al. 2020). However, clinical use of anthracyclines may be limited by complications of adverse haematological and cardiac effects, which is a common problem in anthracycline-incorporating treatment regimens. Still, epirubicin is favoured over doxorubicin as it has a preferable toxicology profile with an equivalent potency (Ormrod et al. 1999).

Antimitotic and cytotoxic activity of epirubicin, similarly to other anthracyclines, results from its interference with DNA, RNA, and protein synthesis, slowing down and stopping the growth of tumour cells and inducing apoptosis. Epirubicin targets DNA topoisomerase II- α which plays a crucial role in maintaining the topological status of chromosomes during DNA replication, repair, and transcription (Tarpgaard et al. 2021). Epirubicin inhibits topoisomerase II activity by stabilising the complex between the cleaved DNA and the topoisomerase II protein, preventing the re-ligation step, and preventing enzyme turnover. This mechanism leads to DNA strand breakage, which in turn triggers apoptosis (Ormrod et al. 1999). Epirubicin also intercalates between DNA strands, can induce the formation of DNA adducts, and inhibits DNA helicase, which further interferes with DNA replication and transcription and promotes apoptosis. The consequences of these effects are most significant for rapidly dividing cells such as those that make up the bulk of the tumour. However, rapidly dividing normal cell populations are also adversely affected, leading to classical chemotherapy side effects such as hair loss and gastrointestinal and haematological toxicity. Anthracyclines also perturb cellular calcium and iron level and induce free-radical generation, which causes toxicity to both cancer cells and non-cancer cells and is the major cause of its cardiotoxicity at high doses.

Multiple randomised trials incorporating epirubicin in poly-chemotherapy showed a significant reduction in mortality and recurrence rates. In particular, several randomised

studies in BCa have indicated high rates of complete pathological response to chemotherapeutic regimens incorporating anthracyclines with taxanes in a neo-adjuvant setting (Group 2012; Trudeau et al. 2005). Thus, currently, epirubicin is administered alone or as a component of combinatorial regimens alongside other antineoplastic agents in varying dosages. The standard epirubicin dose ranges from 75 to 90 mg/m², administered as single intravenous injections at 21-day intervals. Higher doses, up to 135 mg/m² in monotherapy and 120 mg/m² as a component of combination therapy, have also been effective in treating BCa (Plosker & Faulds 1993). The treatment schedule for a TNBC patient in a neoadjuvant setting typically includes multiple cycles (up to 6) of anthracycline combined with a taxane. The elimination half-life of epirubicin is reported to be around 24 hours and is affected by liver function as it is subject to hepatic metabolism, including glucuronosyltransferases (Robert & Bui 1992).

The overall therapeutic potency of anthracyclines in cancer patients remains highly variable, with response rates ranging from 42-79% (Ejlertsen et al. 2004; Nielsen et al. 2000). This reflects the large proportion of anthracycline treated patients that gain no benefit from the treatment, nonetheless, experiencing the adverse effects and potential delays in more effective treatment. To worsen this unfavourable situation, a tumour can be primed by previous failed therapeutic attempts to show diminished sensitivity to treatments that are administered subsequent in line.

Cellular resistance to the cytotoxic activity of epirubicin and other anthracyclines may occur via several intratumoural mechanisms, including increased drug efflux mediated by P-glycoprotein, increased drug metabolism, increased levels of intracellular glutathione or glutathione-S-transferase, alterations in topoisomerase-II activity, induction of heat shock

proteins, and blockade of apoptotic pathways (Ormrod et al. 1999). However, to date, there has been a minimal success in predicting or preventing epirubicin resistance based on analysis or manipulation of the aforementioned pathways. This may be due to combinatorial and/or redundant effects of these pathways on epirubicin response; alternatively, it may indicate that these pathways are not the most critical regulators of the response, and other unknown mechanisms are involved.

1.7.0.0. The Role of Cancer Stem Cell Phenotype in Drug Resistance

During the past few decades, there has been a significant increase in research into the biology of stem cells and their potential application to tissue regeneration therapy. In addition, stem cells have attracted attention from researchers due to their prominent roles in tumorigenesis and therapeutic resistance properties in cancers (Douville et al. 2009). Thus, the development of the cancer stem cells (CSC) hypothesis stands as a significant milestone in decoding therapeutic resistance and disease recurrence in cancer.

The traditional model for tumorigenesis is the clonal evolution or stochastic model. This model outlined by Nowel (1976) describes how random mutations occurring during the lifespan of a cell, coupled with clonal selection processes wherein cells with selectively advantageous mutations (i.e., more 'fit' cells) outcompete less fit cells, causes the accumulation of tumorigenic cells and thus cancer progression (Nowell 1976). Clonal evolution indicates no differentiation hierarchy, and tumour progression occurs via selection and expansion of adapted subclones either in a linear and/or branched fashion [Figure 1.3 (A)]. A single clone acquiring stepwise novel mutations is described by the linear evolution model, while multiple

subclones arising from a common ancestor and evolving in a parallel and nonlinear fashion is described in the evolutionary model (Lang et al. 2015).

In 1977, Hamburger and Salmon first suggested that a stem cell population can be responsible for tumorigenesis (Hamburger & Salmon 1977). Moreover, observations that a population of cells within a tumour show stem-like properties led to the cancer stem cell (CSC) model. This challenged the classical stochastic model by proposing that a small subpopulation of CSC sitting at the highest level of the cancer cell hierarchy drives tumorigenesis. CSCs functionally resemble somatic stem cells as they maintain the stem cell pool by exclusive self-renewal, give rise to all differentiated cell lineages in the tumour mass, and possess the capacity to re-establish a tumour following its regression under therapy. Their inherently tumorigenic properties are also considered to be central to the process of metastasis. Notably, the stochastic evolution and CSC models are not mutually exclusive, and a combination of both is currently thought to contribute to the origin, heterogenic differentiation, and post-therapeutic relapse of tumours.

Following these initial discoveries, models involving CSCs have evolved to give new insights into the molecular and cellular basis of initiation, progression and therapeutic resistance in cancers (Garcia-Mayea et al. 2020). Amongst solid cancers, breast cancer stem cells (BCSC) were the first to be identified. These BCSC were defined functionally by their potent tumour initiating capacity in immune-deficient (NOD/SCID) mice (Al-Hajj et al. 2003). Collective studies since the initial identification of BCSCs suggest that they account for between 0.1-1% of the cells within primary breast tumours and breast cancer cell lines, with variation in frequency related to the BCa subtype. The eradication of this rare population of cells as a treatment strategy has increased cancer research attention (Bao & Prasad 2019).

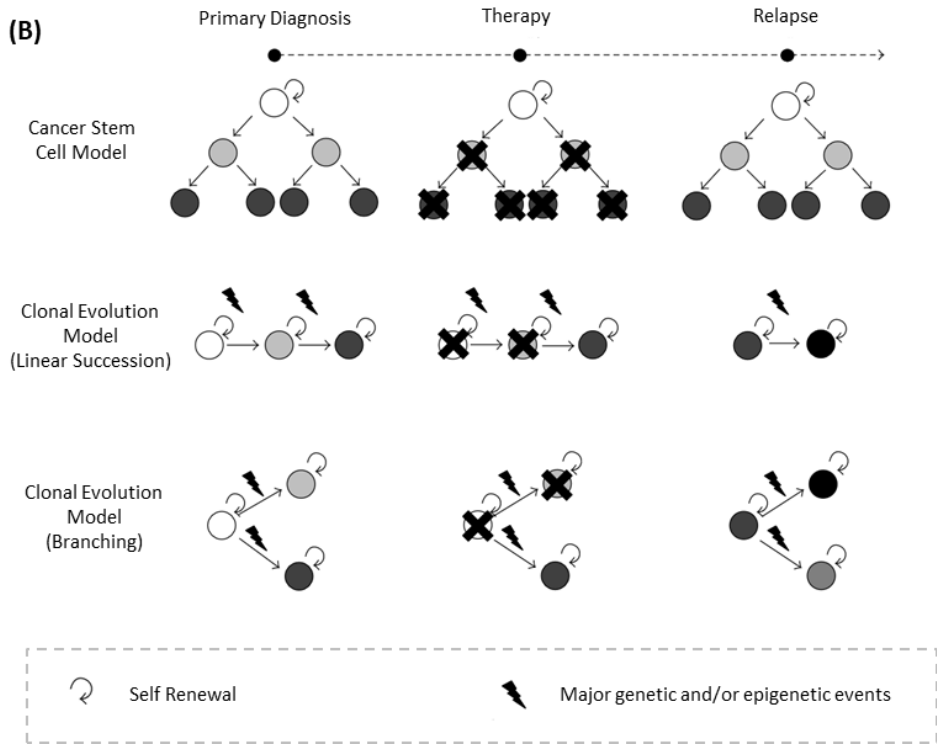
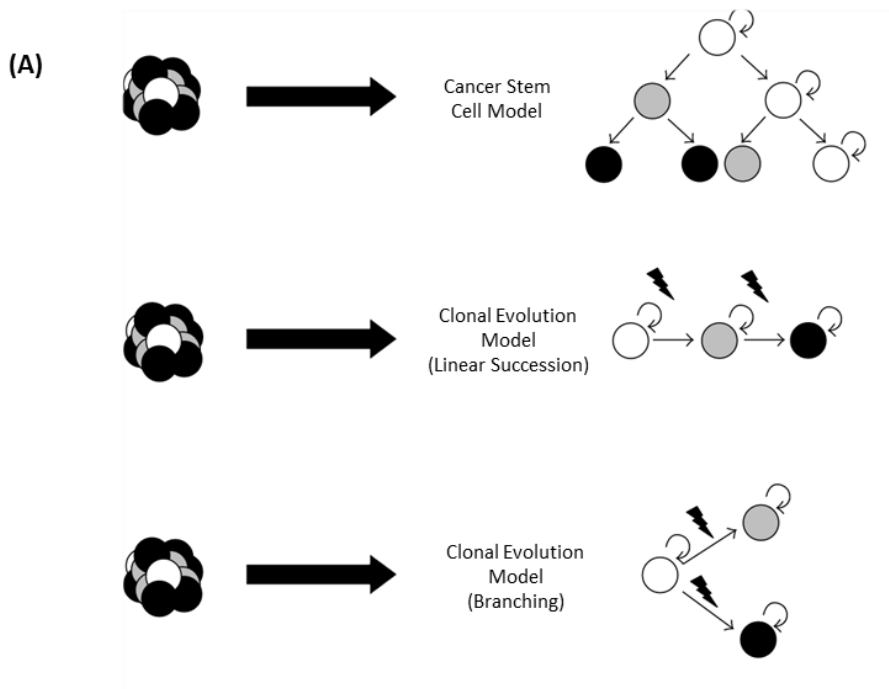


Figure 1.3. (A) Modelling initiation and heterogeneous differentiation in tumours with cancer stem cells, linear succession, and branched evolution. A single clone acquiring stepwise novel mutations is explained in a linear evolution model. The branched model give rise to a parallel and nonlinear subclonal architecture that evolves from a common ancestor.

(B) Treatment escape and relapse explained with cancer stem cell (CSC) and clonal evolution models. In the CSC model, bulk tumour cells are eradicated by therapy while the surviving CSC population act as a reservoir for tumour re-initiation. In the clonal evolution model, distinct subclones with mutations that endow survival advantages persist after therapy and reinitiate the tumour.

Adapted from Hindawi Publishing Open Access Journals, 2015, 137164-13, Lang, Fabian ; Wojcik, Bartosch ; Rieger, Michael A, Stem Cell Hierarchy and Clonal Evolution in Acute Lymphoblastic Leukemia.

Defined by strong self-renewal capacity and epigenetic plasticity, normal adult stem cells are responsible for maintaining normal tissues and organs (Zhang, X et al. 2020). Stem cells are often relatively slow dividing or even quiescent and provide a long-term reservoir for regeneration and repair. Given of the critical need to preserve the integrity of the stem cell reservoir, these cells are protected from damage and death by a variety of extrinsic and intrinsic mechanisms. These include the stem cell niche and various protective metabolic features such as highly efficient detoxification processes and DNA repair pathways that reduce

the risk of accumulating DNA damage and consequent apoptotic death. CSCs utilise these same mechanisms to avoid cell death induced by antitumour therapy. Upon exposure to a therapeutic cytotoxic agent that targets highly proliferative cells, the significant proportion of the bulk tumour is eradicated, resulting in a decrease in tumour mass, but CSCs typically survive. This leads to an alteration in the composition of the heterogeneous tumour. This phenomenon can explain the recurrence of a more aggressive and drug-resistant tumour mass enriched with CSCs that emerge following the treatment.

In-depth elucidation of molecular pathways involved with stemness-driven drug resistance could enable the design of therapeutic strategies to target these cell subpopulations, either by developing novel therapies or increasing their sensitivity to conventional therapies (Zhang, Mei et al. 2017). Many cellular mechanisms have been proposed to underlie stemness-driven chemoresistance, including but not limited to upregulated expression of membrane transporters, activation of pro-survival pathways, superior DNA repair capacity, evasion of apoptosis, enhanced protection against ROS, and cell plasticity, including the ability to adopt a quiescent state (Batlle & Clevers 2017; Garcia-Mayea et al. 2020). These mechanisms may simultaneously operate in orchestrating therapeutic resistance. Targeting these mechanisms might help overcome CSC mediated chemoresistance.

1.8.0.0. Molecular Signalling Pathways Orchestrating Drug Resistance via Cancer Stemness

Persistent activation of one or more highly conserved signal transduction pathways is one of the main oncogenic drivers linked to tumour development. These signalling pathways are identified as key factors contributing to stemness-driven drug resistance. PI3K/AKT signalling,

receptor tyrosine kinase (RTK) activity, transforming growth factor- β (TGF- β) signalling and embryonic developmental pathways such as Wnt, Notch, and Hedgehog, are among the myriad of pathways that are correlated to drug resistance through stem cell signalling (Habib & O'Shaughnessy 2016; Monteiro et al. 2014).

The TGF- β pathway is recognised as a quiescence promoter, a metastasis inducer and a stemness promotor that plays roles in drug resistance (Najafi et al. 2019). PI3K/AKT signalling promotes the CSC phenotype by regulating the antioxidative machinery and fostering quiescence.

Notch, Wnt and Hedgehog are the multitasking signalling cascades that are involved in a range of crucial biological and cellular processes during embryonic development and adult tissue homeostasis and repair. These include maintaining stem cell pools by self-renewal and controlling cell fate determination and regulating cell migration and morphogenesis (Bao & Prasad 2019). In BCa, the same signalling cascades appear to be involved in the evolution and maintenance of the CSC population and its niche, as well as enhancing invasion, suppressing apoptosis, and stimulating survival pathways that can contribute to therapy resistance (Chou et al. 2015; De Sousa e Melo & Vermeulen 2016; Mamaeva et al. 2016).

TNBC basal phenotype is characterised by elevated activity of the Notch pathway compared to other BCa subtypes (D'Angelo et al. 2015). Notch ligands bind to the Notch receptor, which releases the receptor's intracellular domain, which translocates to the nucleus, activating a downstream signalling cascade involved in maintaining the stem cell phenotype (Al-Hussaini et al. 2011). In CSCs, aberrant Notch activation was linked to the acquisition of EMT and self-renewal that further contributes to drug resistance (Najafi et al. 2019). A recent study (Xiao et

al. 2019) indicated that silencing the Notch pathway in TNBC cell-line MDA-MB-231 leads to the suppression of the AKT pathway along with EMT, which subsequently enhances sensitivity to doxorubicin, an epimer of epirubicin.

TNBC cells show high nuclear accumulation of β -Catenin, indicating activation of the Wnt/ β -Catenin signalling pathway, linked to enhanced migration, colony formation, chemoresistance, and other stem-cell-like features. Furthermore, upregulated expression of Wnt receptors detected in TNBC and knockdown of the same has led to tumour suppression (King et al. 2012). Furthermore, a preclinical study involving mouse models has indicated that targeting upregulated Wnt signalling pathways in BCSCs may lead to diminished metastatic potential (Jang et al. 2015).

Increased Hedgehog signalling due to overexpression of the core Hedgehog pathway transcription factors (GLI1 and GLI2) was shown to enhance mammosphere formation by BCSC, supporting its involvement in self-renewal in this population (Liu, S et al. 2006). Furthermore, studies investigating the role of Hedgehog signalling in drug resistance have indicated that the pathway promotes post-treatment tumour regrowth (Arnold et al. 2015). In addition to controlling self-renewal of CSC, the Hedgehog pathway has been shown to promote drug resistance in cancer cells by regulating ALDH1 activity and activity of the ABCG2 drug efflux transporter (Justilien & Fields 2015; Zhang, Mary et al. 2012).

Current interest in elucidating signalling pathways underpinning stemness of cancer cells is based on the potential for clinical application in overcoming therapeutic resistance. Combinatorial therapeutic approaches using CSC-targeting agents with conventional therapeutics have entered clinical trials, although efficacy is still to be fully defined (Shibata &

Hoque 2019; Yang et al. 2020; Zhou, H-M et al. 2021). Further in-depth investigation of these cascades could lead to novel target identification and new drug development to further advance the goal of overcoming clinical drug resistance.

1.9.0.0. Molecular Biomarkers of Breast Cancer Stem Cells

CSC marker genes can signify cellular mechanisms that promote the maintenance of tumours and therapy resistance. Inhibition of some of these crucial stemness markers has been reported to sensitize the tumour cells to cytotoxic therapy (Kozovska et al. 2018; Rodrigues et al. 2018; Saygin et al. 2017). The majority of the CSC studies have indicated a positive correlation with the expression of these markers with chemoresistance while emphasising an inverse relationship with prognosis. Thus, modulating the activity of these molecular markers may be harnessed in targeted therapy, and the expression of these genes in patients may have substantial prognostic value in the clinic.

BCSCs are known to be heterogeneous among different BCa subtypes (Zhou, J et al. 2019), suggesting biomarker profiles and their potential for diagnostic, therapeutic or prognostic use are context-dependent. Therefore, a panel of molecular markers is generally used for the specific identification and isolation of stem cells in both research and therapeutic settings (Douville et al. 2009). Molecular markers genes expressed by, but not limited to BCSC, include *CD44* (Cluster of differentiation 44, Hyaluronan receptor), *ALDH1* (Aldehyde Dehydrogenase), *CD133* (Cluster of differentiation 133, prominin 1, cell surface antigen), *OCT4* (Octamer-binding Transcription Factor 4), *DNER* (Delta/ Notch- like epidermal growth factor (EGF) related receptor), *SOX2* (Sex determining region Y (SRY)- box 2), *Nectin-4* (Nectin cell adhesion molecule 4) (Siddharth et al. 2017), and homeobox protein *Nanog* (Wang, M-L et al. 2013). Among this array of markers, surface-expressed and enzymatic markers are the most useful

for prospective identification of BCSCs, with the $CD44^+/CD24^{-/low}$ surface marker profile or the activity of the ALDH enzyme serving as the gold standard signature for isolation of BCSCs (Zhou, J et al. 2019).

It is also important to note that BCSCs are a heterogenous population even within a single tumour, and different combinations of these molecular markers may be expressed in different BCSC subpopulations, and these may also show spatial and temporal variability. Hence it is also of current interest to identify whether specific marker combinations can identify more ‘pathogenic’ BCSC, i.e., those that may be more responsible for drug resistance, relapse, and/or metastasis. Elucidating this information remains crucial for BCSC markers to be utilised in clinical settings.

Table 1.1. An overview of breast cancer stem cell markers used in this study

ALDH1 (Ginestier et al. 2007)	
Annotation	Aldehyde dehydrogenase 1 (ALDH1) is a member of the ALDH enzyme superfamily that consists of 19 isoenzymes discovered up to date (Chang et al. 2018). It is extensively used as a functional marker for both normal and cancer SCs with several tumour origins.
Molecular Functionalities	Primarily localised in the cytosol, the ALDH1 enzyme is involved in aldehyde detoxification and retinoic acid synthesis that are critical cellular mechanisms. As a detoxifying enzyme, it is involved in protecting cells from oxidative stress by metabolizing various endogenous and exogenous aldehydes into their corresponding carboxylic acids. ALDH1 is involved with the early-stage differentiation of stem cells through the oxidation of retinol to retinoic acid.

Significance in BCa	<p>The ALDH1 enzyme decreases the level of reactive oxygen species and reactive aldehydes in CSCs, leading to the initiation of carcinogenesis and the promotion of tumour growth. Many published studies indicate a positive correlation of induced ALDH1 expression with drug resistance in various cancers. Furthermore, it is involved in self-renewal, differentiation, and self-protection (by acquired drug resistance) of BCa cells leading to poor prognosis and survival outcomes, particularly in luminal B and TNBC subtypes.</p>
References	<p>(Tomita et al. 2016) (Althobiti et al. 2020b) (Toledo-Guzmán et al. 2019)</p>
CD44 (Al-Hajj et al. 2003)	
Annotation	<p>The cluster of differentiation 44 (CD44) is a transmembrane receptor protein ubiquitously expressed in a variety of human tissues. In addition to the standard molecular form (CD44s), multiple CD44 variant isoforms facilitate a dynamic range of cellular functions. Being extensively studied in relation to carcinogenesis, CD44 is a principal molecular marker for CSCs.</p>
Molecular Functionalities	<p>The multifunctional surface adhesion molecule is activated by binding its primary ligand hyaluronic acid (HA) and several other ligands. CD44 is a part of many vital cellular functions such as cell division, adhesion, migration, signalling and lymphocyte homing. CD44-HA complex has established a critical functional role in the acquisition and maintenance of the stemness and induces drug resistance via multiple functionalities, including induction of EMT, oxidative stress resistance, secretion of exosomes and regulation of epigenetic alterations.</p>
Significance in BCa	<p>Involved in oncogenic signal transmission, CD44 stands as the most prominent surface marker for CSCs. CD44 is predominantly overexpressed in tumorigenic BCa cells, and silencing CD44 expression is correlated with downregulation of proliferation, migration, and invasiveness in BC. While CD44 is prominently involved in cellular</p>

	<p>mechanisms that are critical for the physiological functioning of the normal cells, they also drive the pathological characteristics of the neoplastic cells. Adhesive and cell signalling capabilities of CD44 are integrated to modulate the progression and the metastasis of invasive BC. The overexpression and the dysregulation of the CD44 receptor have positively correlated with tumour initiation and progression of cancers. A study by Kong et al. (2018) has linked stemness characteristics defined by the CD44+/CD24- phenotype to be more invasive, metastatic, and proliferative indicating aggressive tumour cell behaviour (Kong et al. 2018).</p>
References	(Medrano-González et al. 2021) (Chen, C et al. 2018) (Goodison et al. 1999) (Nam et al. 2015)
OCT4	
Annotation	<p>Octamer-binding Transcription Factor 4 (OCT4) is a homeodomain transcription factor of the Pit-Oct-Unc (POU) family. OCT4 is identified as a master regulator of self-renewal and maintenance of pluripotency in embryonic stem cells as well as CSCs.</p>
Molecular Functionalities	<p>Generally expressed in embryonic and adult stem cells, OCT4 was first shown to be involved in regulating early-stage mammalian embryogenesis and pluripotency. Later studies discovered the oncogenic role of OCT4 contributing to stemness, self-renewal and disease recurrence. This well-established stemness marker is also a factor essential for in vitro somatic cell reprogramming. OCT4 forms complexes with other stemness regulators; SOX2, c-Myc and KLF4 (collectively identified as Yamanaka factors) to be utilised as a reprogramming cocktail.</p>
Significance in BCa	<p>The enrichment of OCT4 in a subpopulation of undifferentiated cells has been identified as one factor contributing to tumour initiation, metastasis, and chemoresistance in BC. However, despite the strong</p>

	correlation of expression in CSCs, chemoresistance and poor prognosis, the functional role of OCT4 in cancer is yet to be fully interpreted.
References	(Fultang et al. 2021; Mohiuddin et al. 2020; Sen et al. 2021)
SOX2	
Annotation	Sex determining region Y (SRY)- box 2 (SOX2) is a cell fate-determining transcription factor that belongs to the SOX superfamily.
Molecular Functionalities	SOX2 pluripotency factor is responsible for maintaining an undifferentiated cellular phenotype, facilitating self-renewal and pluripotency: critical features of the stem cell phenotype. This transcription factor acts in conjunction with other cofactors such as OCT4 in the maintenance of stemness defined by self-renewal and pluripotency in undifferentiated embryonic stem cells while facilitating the maintenance of self-renewal. It is also used in the reprogramming of somatic cells.
Significance in BCa	SOX2 overexpression is linked to stemness in cancer that associates with disease progression, metastasis, recurrence, and chemotherapeutic resistance. Despite the primarily restricted expression in embryonic and somatic stem cells, SOX2 (along with OCT4) expression in CSCs appears to be important for their drug resistance.
References	(Schaefer & Lengerke 2020) (Metz & Rizzino 2019)
DNER (Eiraku et al. 2002)	
Annotation	Delta/Notch-like epidermal growth factor (EGF) related receptor, DNER is a multi-domain transmembrane protein extensively expressed in the central nervous system.
Molecular Functionalities	The early studies on DNER function recognized it as a molecule vital in neural (cerebella) maturation. DNER is defined as a Notch ligand that

	participates in intercellular interactions regulating self-renewal and cell fate in normal stem cells and CSC.
Significance in BCa	Functioning as an oncogene, <i>DNER</i> promotes stemness facilitating progression, metastasis and chemoresistance in BCa. While <i>DNER</i> mediated induction of EMT is correlated with metastasis, it is responsible for preventing chemosensitivity by blocking cell apoptosis via the indirect activation of the Wnt/ β Catenin pathway. Also, the recent study done by Wang L et al. revealed the role of Girdin/PI3K/AKT signalling in the BCa pathology with the subsequent link in regulating several other CSC genes.
References	(Wang, Z et al. 2020) (Wang, L et al. 2019) (Saito & Takeshima 2006)
<i>ABCB1, ABCC1, ABCG2</i>	
Annotation	ATP binding cassette (ABC) transporters are a superfamily of membrane proteins that consists of 49 members in seven subfamilies. Among these, Permeability associated-glycoprotein (P-gp) encoded by the <i>MDR1/ABCB1</i> gene, multidrug resistance-associated protein 2 (MRP2) encoded by the <i>ABCC2</i> gene, and BCa resistance protein (BCRP) encoded by the <i>ABCG2</i> gene are identified as leading contributors to the evolution of multi drug resistance in tumours.
Molecular Functionalities	ABC transporters mediate the active efflux of various bioactive molecules, including xenobiotics, across the cell membrane using ATP hydrolysis. They protect cells against cellular toxins and xenobiotics. All three of these transporters contain hydrophobic domains that allow broad substrate specificity, hence allowing the efflux of various structurally and functionally distinct drug molecules. Flow cytometry-based identification of ABC transporter enriched cell populations is generally done by measuring the exclusion of Hoechst 33342 dyes.
Significance in BC	Overexpression of ABC transporters is a crucial mechanism involved in the evolution of multidrug resistance in cancer, driven by the elevated

	efflux of chemotherapy drugs out of the cells modulating the pharmacokinetics of the drugs, lowering the intracellular drug concentration. The resulting drug insensitivity restricts the prolonged and effective use of antineoplastic drugs. The broad and overlapping substrates range of different ABC transporters makes tumours cross-resistant to a vast array of chemotherapeutic drugs.
References	(Liu, F-S 2009; Sridharan et al. 2019) (Ween et al. 2015)

1.10.0.0. MDA-MB-231 Cell line as an Invitro Model to Study TNBC

The MDA-MB-231 cell line is used in this project to investigate mechanisms of TNBC resistance to the chemotherapeutic drug epirubicin. The MDA-MB-231 cell line has a molecular profile defined by lack of ER, PR, HER and E-cadherin expression, but overexpression of EGFR. They are highly proliferative epithelial cells with a spindle-shaped morphology that grow as an adherent monolayer that can become confluent. The line was derived in 1974 from a pleural effusion of metastatic adenocarcinoma of a 51-year-old patient (Cailleau et al. 1974). Being of metastatic origin, the MDA-MB-231 cell line can migrate and invade into the extracellular matrix and is commonly used in studying the molecular behaviour of aggressive and invasive BCa (Mohammed et al. 2020). MDA-MB-231 cells are near triploid with a chromosome number ranging in 52-68; there are genomic aberrations and mutations involving numerous tumour suppressors and oncogenes, including *BRAF*, *CDKN2A*, *KRAS*, *NF2* and *TP53* genes. In particular, the cell line is characterised by the presence of a single mutant copy of *TP53* which encodes the classical tumour suppressor protein p53, and deletion of *CDKN2A* that encodes tumour suppressor protein p16 that plays a critical role in regulating cell cycle progression. Tumours that arise from basal-like progenitors have poorer clinical outcomes in contrast to BCa of luminal origin. Microarray profiling has categorised the MDA-MB-231 cell line into the basal subcategory of BCa, consistent with its aggressive phenotype.

1.11.0.0. Rational for the Current Study, Preliminary Investigations, and the Experimental Design

Synergistic eradication of the CSC population along with the bulk tumour has the potential to block tumour drug resistance and relapse. Unravelling the mechanisms underpinning CSC-driven chemoresistance could pave the path to create combinatorial regimens and other treatment modalities that can successfully target bulk tumour cells and CSCs simultaneously. However, the genomic and molecular basis of chemoresistance remains incompletely understood due to a deficiency of methods with the capability to assess heterogeneous tumours harbouring treatment-persistent CSC subpopulations.

As mentioned previously, different subtypes of BCa express different CSC marker profiles and different CSC abundancies. Moreover, an enriched stem cell signature has been identified in TNBC tissues compared to non-TNBC tissues revealing a positive relationship between TNBC aggressiveness and the enriched stemness profile (Honeth et al. 2008; Li, H et al. 2013; Ma et al. 2014). In the current study, we sought to investigate the relationship between CSC markers and the development of resistance to the chemotherapeutic agent epirubicin using MDA-MB-231 cells as an in-vitro model system for TNBC

An unpublished previous study carried out by the Flinders Molecular Pharmacology Research Group provided preliminary evidence that treatment of MDA-MB-231 cells with epirubicin increases the expression of genes associated with drug metabolism, drug efflux, and the CSC phenotype (Figure 1.12.0.0. A). Because gene expression was increased by short-term drug treatment at subtoxic doses, it was presumed that the response was due to gene induction rather than the enrichment of pre-existing drug-resistant CSC. In a related study performed in this laboratory, two BCSC-like cell lines were generated using reprogramming technology (see

Figure 1.12.0.0. B). These reprogrammed cell lines, called induced (i)BCSC, were found to overexpress multiple CSC marker genes and ABC transporters when compared to the parental control line. These two studies in combination suggested that 1) cytotoxic drug treatment induces the activity of stemness pathways in TNBC cells, and 2) that induction of stemness increases the activity of drug resistance pathways (such as drug efflux). The current project expands upon this previous work by first confirming the preliminary finding that epirubicin treatment induces genes associated with both stemness and drug resistance, and then further examines the role of this gene induction process in the development of long term drug resistance and potentially in the cross (or collateral)-drug resistance.

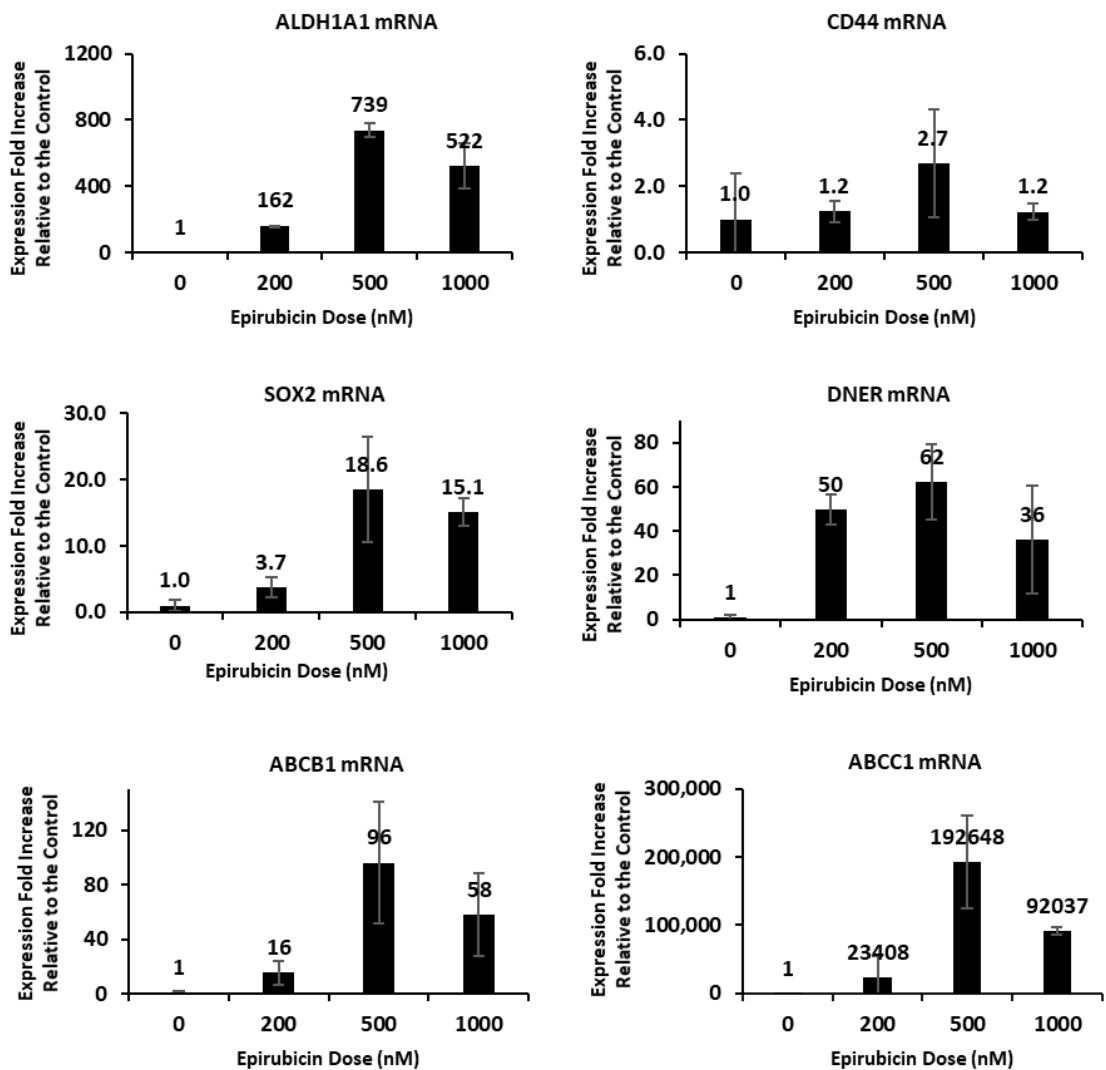


Figure 1.4. The fold induction of mRNA levels of stem cell marker genes *ALDH1A1*, *CD44*, *SOX2*, and *DNER* along with ABC drug transporters *ABCB1* and *ABCC1* in MDA-MB-231 BCa cells upon the treatment with 200, 500, and 1000 nM epirubicin along with vehicle (ethanol) negative control (denoted by 0 epirubicin dose) for 72 hours. Induction of each gene is represented as a fold over the control. All gene expression values were normalized to the 18S housekeeping gene. Only one biological replicate with two technical replicates was performed, and the target genes were amplified in duplicate. Standard deviation between the technical replicates is represented by the error bars (+/-).

ALDH1A1: Aldehyde dehydrogenase, CD44: Cluster of differentiation 44, SOX2: Sex determining region Y (SRY)- box 2, DNER: Delta/ Notch- like epidermal growth factor (EGF) related receptor, ABCB1: Adenosine triphosphate (ATP) binding cassette family B1, ABCC1: Adenosine triphosphate (ATP) binding cassette family C1, BCa: Breast Cancer.

Figure 1.4 is generated using the data collected by Mr. Radwan Ansar during his study where the role of UGT enzymes in the evolution of chemoresistance in BCa was also analysed (UGT gene data: Appendix 5.4.0.0).

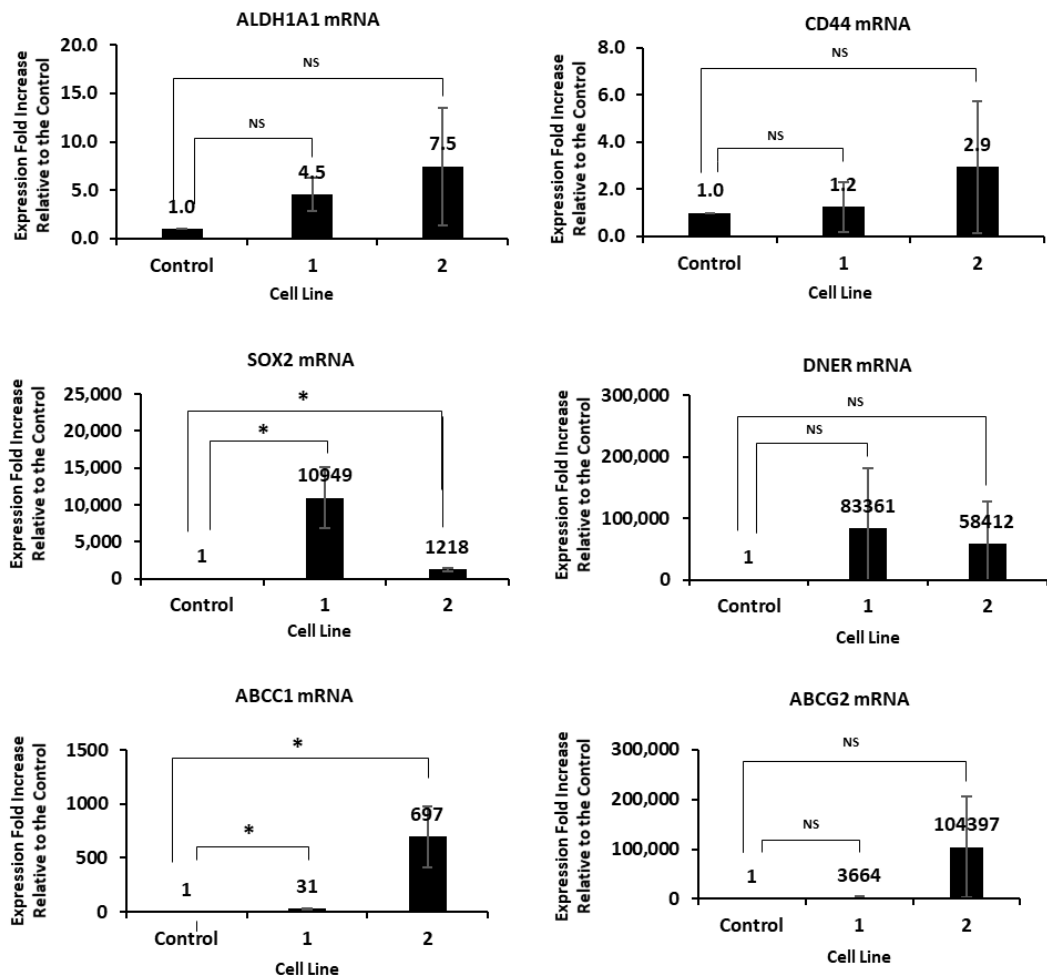


Figure 1.5. Fold induction of mRNA levels of stemness marker genes *ALDH1*, *CD44*, *SOX2*, and *DNER* along with ABC Transporters *ABCC1* and *ABCG2* in induced MDA-MB-231 breast cancer stem cells. Two independently derived cell lines, denoted as 1 and 2, were assessed. Induction of each gene is represented as a fold over the control. All gene expression values were normalized to the 18S housekeeping gene. Three biological replicates with two technical replicates for each were performed. The target genes were amplified in duplicates. Standard deviation between the technical replicates is represented by the error bars (+/-). Statistical Significance ($P < 0.05$) is denoted by an asterisk (*).

ALDH1A1: Aldehyde dehydrogenase, CD44: Cluster of differentiation 44, SOX2: Sex determining region Y (SRY)- box 2, DNER: Delta/ Notch- like epidermal growth factor (EGF) related receptor, ABCC1: Adenosine triphosphate (ATP) binding cassette family C1, ABCG2: Adenosine triphosphate (ATP) binding cassette family G2.

Figure 1.5 is generated using the data collected by Mr. Radwan Ansar during his study where the role of UGT enzymes in the evolution of chemoresistance in BCa was analysed (UGT gene data: Appendix 5.4.0.0).

1.12.0.0. Thesis Aims and Hypotheses

The overarching objective of this study was to evaluate the role of the CSC phenotype in the emergence of resistance to the chemotherapeutic drug epirubicin in the context of TNBC. The study had two main components. In the first component, the capacity of short-term epirubicin treatment to induce the expression of drug resistance and stemness markers was examined. In the second component, a cell line with stable epirubicin resistance was established via long-term drug treatment, and the model was evaluated for similar changes in drug resistance and stemness markers. If time permitted, I also sought to determine whether stable resistance to epirubicin also led to collateral resistance to other drugs. These main aims were advanced in a set of sub-aims, each of which addressed a defined hypothesis as stated below.

Aims

1.0.0 Evaluate the response of MDA-MB-231 cells to transient (48 hours) epirubicin treatment.

1.1.0. Quantitative expression analysis of genes associated with stemness and drug resistance.

1.2.0. Determination of the stability of gene expression changes upon drug withdrawal.

1.3.0. Assessment of the self-renewal capacity of epirubicin treated cells using mammosphere assays.

2.0.0 Establish and characterise an MDA-MB-231 subline with stable resistance to epirubicin.

2.1.0. Development of a method to establish an MDA-MB-453 sub-line with stable resistance to epirubicin.

- 2.2.0.** Characterisation of the long-term treated epirubicin-resistant subline.
 - 2.2.1** Determination of epirubicin sensitivity (defined by IC50 value).
 - 2.1.1.** Quantitative expression analysis of genes associated with stemness and drug resistance.
 - 2.1.2.** Assessing collateral-resistance in epirubicin-resistant cells (possible future study).

Hypotheses

- 1.0.0.** Short-term epirubicin treatment of MDA-MB-231 cells induces adaptive responses that promote stemness and drug resistance.
 - 1.1.0.** Short-term (48 hours) epirubicin treated cells will show upregulated expression of genes associated with stemness and drug resistance (efflux) pathways.
 - 1.2.0.** Alterations in gene expression will be sustained for a limited period after drug withdrawal.
 - 1.3.0.** Epirubicin treated cells will show enhanced self-renewal capacity as indicated by mammosphere formation capacity.
- 2.0.0** A long-term cyclical epirubicin treatment regimen will generate an MDA-MB-231 cell population with stably enhanced stemness and drug resistance properties.
 - 2.1.0** Long-term treated cells will show lower epirubicin sensitivity (defined by IC50 value) relative to the parental drug-sensitive line.
 - 2.2.0** Long-term treated cells will show enhanced expression of stemness genes even after a drug withdrawal.
 - 2.3.0** Long-term treated cells that show stable resistance to cytotoxic drugs will also show resistance to other classes of anti-cancer drugs (potential future study).

1.13.0.0. Significance to Medical Biotechnology

Even in the era of precision medicine and immunotherapeutic approaches, chemotherapy remains an indispensable therapeutic option to combat BCa. Especially subtypes such as TNBC have limited therapeutic options due to their lack of expression of molecular targets for the most common targeted therapies. However, the therapeutic usefulness of chemotherapeutic agents is limited by intrinsic and acquired resistance to many clinically used drugs. Chemoresistance in tumour cells can lead to treatment failure, cancer progression and relapse, contributing to increased mortality rates.

Lack of pathological complete response upon first-line chemotherapy treatment is a common occurrence in TNBC, and optimal drug regimens to address this predicament remain debated. However, most studies suggest that anthracycline-incorporating chemotherapeutic regimens achieve higher pathological complete response rates in TNBC than other regimens, making anthracyclines such as epirubicin important chemotherapeutics for these patients (Lee et al. 2019).

The identification and characterisation of molecular mechanisms mediating chemoresistance could provide avenues to improve the response to current therapies. Identifying and targeting key players in drug resistance pathways could circumvent primary resistance and avoid the evolution of collateral resistance to secondary antineoplastic agents. Such data could also help clinicians by providing biomarker profiles that could be used to personalise chemotherapeutic regimens in future. There is ample evidence that cancer stemness plays a crucial role in drug resistance and recurrence of TNBC. Identification of druggable targets within the CSC population is thus an emerging approach in the cancer treatment landscape. Eradication of

this rare population of cells along with the tumour mass might achieve more favourable outcomes in TNBC patients. This study will contribute to these long term goals by helping to understand the process by which drug treatment promotes the acquisition of cancer cell stemness and the role of both drug clearance and stemness pathways in multi-drug resistance.

MATERIAL & METHODS

2.1.0.0.	Research Facilities and Core Services.....	37
2.2.0.0.	Material and Equipment.....	37
2.3.0.0.	Cell Line.....	40
2.4.0.0.	Methods.....	40
2.4.1.0.	Maintenance of Mammalian Cell Cultures.....	40
2.4.2.0.	Cryopreservation and Resurrection of MDA-MB-231 Cells.....	41
2.4.3.0.	Epirubicin Treatment of MDA-MB-231 Cell Cultures	42
2.4.4.0.	TRIzol Aided RNA Extraction.....	43
2.4.5.0.	cDNA Synthesis by Reverse Transcription	44
2.4.6.0.	Quantitative Real-Time PCR (qRT PCR).....	45
2.4.7.0.	MTT Cell Proliferation Assay.....	46
2.4.8.0.	Mammosphere Formation Assay	48
2.4.9.0.	Establishment of an Epirubicin Resistant MDA-MB-231 Cell Subline	50
2.5.0.0.	Statistical Analysis	52
2.7.0.0.	Compliance with Ethical and Safety Standards	52

2.1.0.0. Research Facilities and Core Services

The experiments in this study were mainly conducted in the Department of Clinical Pharmacology, Flinders University. All protocols involving cytotoxic drug treatments were carried out in the level two physical containment (PC2) facility in the same Department using a Biosafety cabinet that is approved for the handling of cytotoxics. Flinders University Proteomics Facility was utilised when carrying out MTT assays using the Beckman Coulter DTX 880 plate reader. Cell imaging using the EVOS® FL cell imaging microscope was carried out in the Ian Gibbins Microscopy Suite, Flinders Medical Centre.

2.2.0.0. Material and Equipment

All the chemicals and reagents utilised throughout this project were of analytical grade. A list of chemicals, reagents and respective suppliers is provided in Table 2.1 below. Detailed buffer and reagent compositions are specified in Appendices Table 5.1 (reagents denoted with an asterisk in Table 2.1 are detailed in Appendix Table 5.1). Equipment used and the respective manufacturers are listed in Appendix Table 5.2.

Table 2.1. Chemicals and reagents used throughout this study and respective suppliers

Detailed composition of the reagents denoted with an asterisk (*) is given in Appendix Table 5.1.

Chemical/ Reagent (Concentration)	Supplier
General Chemicals	
Ethanol	Chem Supply, South Australia, Australia
Glycerol	Amresco, Ohio, United States
Mammalian Cell Culturing	
Dulbecco's Modified Eagle's Medium (DMEM)	Life Technologies, Victoria, Australia
Foetal Bovine Serum (FBS)	Sigma-Aldrich, Saint Louis, United States
Phosphate Buffered Saline (PBS) (1%)	Life Technologies, Victoria, Australia
Trypsin-EDTA (0.5%)	Life Technologies, Victoria, Australia
Penicillin Streptomycin Glutamine (100x)	Sigma-Aldrich, Saint Louis, United States
DMSO Freezing Media*	Refer to Appendix Table 5.1
In-vitro Drug Treatment	
Epirubicin Hydrochloride (E9406)	Sigma-Aldrich, Saint Louis, United States
RNA Isolation and RT-qPCR	
TRIzol Reagent	Life Technologies, Victoria, Australia
Chloroform	Chem Supply, South Australia, Australia
Isopropanol	Chem Supply, South Australia, Australia
Nuclease Free Water	Promega, USA
RNase Inhibitor	Astral Scientific, New South Wales Australia
DNase Enzyme	Life Technologies, Victoria, Australia
DNase Buffer	Life Technologies, Victoria, Australia
EDTA (25 mM)	Sigma-Aldrich, Saint Louis, United States
Deoxynucleotide-triphosphate (dNTP) mix (10 mM)	Life Technologies, Victoria, Australia
Random Hexamers (50µM)	Life Technologies, Victoria, Australia
NxGen® M-MuIV Reverse Transcriptase	Astral Scientific, New South Wales

	Australia
Reverse Transcriptase Buffer	Astral Scientific, New South Wales Australia
GoTaq Master Mix 2X	Promega, USA
MTT Assay	
Thiazolyl Blue Tetrazolium Bromide (MTT)	Sigma-Aldrich, Saint Louis, United States
Hydrochloric acid (HCl)	Chem Supply, South Australia, Australia
Nonidet P-40 (NP 40)	Sigma-Aldrich, Saint Louis, United States
Isopropanol	Chem Supply, South Australia, Australia
Mammosphere Formation Assay	
Poly-2-hydroxyethyl methacrylate (Poly-HEMA)	
Advanced DMEM/F12	Life Technologies, Victoria, Australia
B27 Supplement	Life Technologies, Victoria, Australia
Human Epidermal Growth Factor (hEGF)	PeptoTech, New Jersey, United States
Basic Fibroblast Growth Factor (bFGF)	PeptoTech, New Jersey, United States
Insulin Transferrin Selenium (ITS)	Sigma-Aldrich, Saint Louis, United States
Trypan Blue	Sigma-Aldrich, Saint Louis, United States
Methyl Cellulose	Life Technologies, Victoria, Australia
3D Cell Culture	
Matrigel®	Sigma-Aldrich, Saint Louis, United States
Agarose	Astral Scientific, New South Wales Australia

2.3.0.0. Cell Line

The MDA-MB-231 breast carcinoma cell line was originally obtained from American Type Culture Collection (ATCC® HTB26™). Defined by the absence of ER, PR, and HER overexpression along with a mutated *p53* gene, this invasive basal-like cell line is a suitable tool to study the behaviour of aggressive late-stage TNBC.

2.4.0.0. Methods

2.4.1.0. Maintenance of Mammalian Cell Cultures

Mammalian cell culture was carried out under aseptic conditions using a tissue culture hood or biosafety cabinet. Equipment and consumables used were sterilised with 70% ethanol prior to use. MDA-MB-231 cells were maintained as adherent monolayer cultures in complete DMEM supplemented with 10% FBS, usually in T75 flasks. The detailed formulation of the culture medium is provided in the Appendices Table 5.1. Cell cultures were maintained at 37°C temperature and 5% CO₂ in a humidified incubator. Future mentions of culture conditions in this thesis will refer to the aforementioned conditions if not specified otherwise. The media was renewed 2-3 times a week or as needed.

Cells were regularly monitored using an Olympus CK2 microscope. Upon reaching approximate 80-90% confluence, the cells were subcultured (passaged) or harvested to be used in the experiments. Subculturing or harvesting involved aspirating the media from the flask and washing the cell layer with Phosphate Buffered Saline (PBS) to remove the remaining media and cell debris. Following the removal of PBS, trypsin EDTA solution (10% of the original culture volume) was added to the flask to induce the dissociation of the adherent cell culture. Dissociation of cells from the flask was monitored with a microscope to avoid the selection of

cells with varying adherence. After 2-5 min trypsin exposure, the trypsin activity was halted by adding complete DMEM and resuspending by gently pipetting up and down three times. Cells were passaged at ratios between 1:2- 1:10 in fresh T75 flasks as needed or were seeded in multiwell plates for experiments.

Cell seeding in a specified density required cell counting using a haemocytometer under a microscope. The cells within the four sets of the 16 squares on the haemocytometer were counted at 100x magnification. The average cell count was applied to the equation below to calculate the final cell concentration.

$$\text{Cell Density (cells per ml)} = \text{Average Cell Count} \times \text{Dilution Factor} \times 10^4$$

2.4.2.0. Cryopreservation and Resurrection of MDA-MB-231 Cells

The early passage cell culture stocks were maintained by cryopreservation in the vapour phase of a liquid nitrogen tank. Cryopreservation involved centrifuging cells that had been harvested using trypsin at 1500 rpm for 5 mins. The supernatant was carefully aspirated, and the cell pellet resuspended in 1 ml of cryopreservation medium, which was comprised of FBS supplemented with 10% dimethyl sulfoxide (DMSO) (v/v) as the cryoprotectant. The cell suspension was transferred to cryovials and subjected to slow freezing by incubation a -80°C freezer before moving to the liquid nitrogen tank for extended storage.

Resurrecting cryopreserved cells for experiments involved rapid thawing of vials in a 37°C water bath (approximately 1-2 minutes) and immediately transferring the contents to a tube containing 10 ml warm complete DMEM. After centrifugation of the cell suspension at 1500 rpm for 5 mins, the diluted cryopreserving media was removed. The cell pellet was resuspended in complete DMEM (10 ml) and added to a fresh culture flask (T75).

2.4.3.0. Epirubicin Treatment of MDA-MB-231 Cell Cultures

A stock solution of epirubicin at 10 mM was prepared by dissolving 5 mg of epirubicin hydrochloride (Sigma-Aldrich) in 862 μ l of absolute ethanol. This solution was diluted in complete DMEM when treating the MDA-MB-231 cell cultures at varying epirubicin concentrations. The solubility of epirubicin in an aqueous solution is 0.093 mg/ml (approximately 171 micromolar).

Trypsinised cells in suspension were counted using the haemocytometer and seeded in six-well plates at a density of 6.25×10^5 cells per well. After a 24h adherence period, the media in the wells was removed and replaced with media containing the vehicle (0.1% ethanol) or epirubicin at specified concentrations (100 nM and 200 nM or 250 nM and 500 nM). The cells were treated in duplicates for each condition. Treated plates were incubated with the drug for defined exposure periods (see Results section) before the cells were harvested for analysis.

In a subset of experiments, epirubicin treatment was withdrawn for a defined period before the cells were harvested for analysis. This is referred to as a 'drug holiday' and was designed to assess the stability of cell responses induced by the drug exposure. At the end of the epirubicin exposure period (48 h), the media containing epirubicin was removed, and the adherent cultures were washed twice with PBS to remove traces of the drug and dead cell debris. Fresh complete DMEM was added to the cultures before further incubation. Future references to drug withdrawal or drug holiday protocols in this thesis will refer to the steps mentioned above.

In all experiments involving treatment of cells with epirubicin, pre-established Safe Work Method Statements (SWMS) and associated Risk Assessments for cytotoxic drug handling were followed. The safety precautions included appropriate use of personal protective equipment (PPE), working only within the Biosafety cabinet approved for cytotoxic handling, layering working surfaces with disposable plastic-backed absorbent liners, and disposing of all liquid and solid waste in a cytotoxic containment bin.

2.4.4.0. TRIZOL Aided RNA Extraction

Total cellular RNA in the cell cultures was extracted using Trizol (Life Technologies, Victoria, Australia) (Chomczynski & Sacchi 1987). At the end of the drug treatment period or the drug holiday, the culture media was aspirated, followed by a PBS wash. The cells were lysed by adding TRIZOL reagent (1 ml per 10-25 cm²) directly to the wells. The cell lysis was aided with homogenisation by pipetting up and down vigorously. The TRIZOL lysates were transferred to 1.5 ml Eppendorf tubes and incubated for 5 mins at room temperature to dissociate ribonucleoprotein complexes before adding 200 µl chloroform, vortexing for 15 s, and centrifuging at 11500 rpm for 15 mins to enable phase separation.

The upper aqueous layer was collected in fresh 1.5 ml Eppendorf tubes, carefully avoiding contaminations by the interphase or organic layers. The aqueous solution was combined with 500 µl isopropanol and mixed well by inversion to facilitate RNA precipitation. Following a 10 min incubation, the RNA pellet was collected by centrifuging the samples at 11500 rpm for 10 mins at 4°C. The supernatant was discarded, and the pellet resuspended in 1 ml of 70% ethanol before centrifuged at 7500 g for 5 mins at 4°C. The supernatant from this wash step was discarded, and the RNA pellet was air-dried for 0.5-2 hours to evaporate the remaining

ethanol, ensuring not to overdry the pellet. The RNA pellet was redissolved in 20 μ l nuclease-free water and was stored at -20 °C until cDNA synthesis.

The yield and the purity of the extracted RNA were spectrophotometrically estimated with NanoDrop™ 2000 (Thermo Scientific™) using the absorbance measured at 260 nm and 280 nm. The samples with a 260/280 ratio between 1.8-2 were considered sufficiently pure to be processed for cDNA synthesis.

2.4.5.0. cDNA Synthesis by Reverse Transcription

A total of 2.5-5 μ g of RNA was used to make cDNA, which was calculated using the estimated RNA concentration values from the NanoDrop (Appendix 5.2.1.0). The process involved DNase treatment to degrade residual genomic DNA, followed by reverse transcription with random primers.

For DNase treatment, a predetermined amount of RNA dissolved in 16.5 μ l nuclease-free water was combined with 1 μ l of DNase (2,000 units/ml), 2 μ l of 10 x DNase buffer and 0.5 μ l of RNase inhibitor (40,000 units/ml). The 20 μ l reaction was incubated at 37°C for 10 mins before the DNase was inactivated by adding 1 μ l of 25 mM EDTA (2.5 mM final concentration) and incubation at 75°C for 10 mins.

For cDNA synthesis, half of the above reaction mixture (10 μ l) was combined with 1 μ l of 10 mM dNTPs (0.625 mM final), 1 μ l of 50 μ M random hexamers (3.125 μ M final), and nuclease-free water (4 μ l). The annealing reaction mixture (16 μ l) was incubated at 65°C for 10 mins and then on ice for 10 mins. In the reverse transcription step, the annealing reaction mixture

was combined with 1 μ l NxGen[®] M-MuLV Reverse Transcriptase (200,000 units/ml), 2 μ l of 10x reverse transcriptase buffer, and 1 μ l of RNase inhibitor (40,000 units/ml). The 20 μ l reaction mixture was incubated at 42°C for 1 hour, and the reaction stopped by heating at 90°C for 10 mins. Synthesised cDNA was diluted 5-fold by adding 80 μ l of sterile nuclease-free water and stored at -20°C until PCR analysis.

2.4.6.0. Quantitative Real-Time PCR (qRT PCR)

Real-time Quantitative Reverse Transcription Polymerase Chain Reaction (qRT PCR) with SYBR-green dye incorporation was used to determine the mRNA levels of selected genes in the epirubicin-treated MDA-MB-231 cells as compared to the vehicle-treated control. 20 μ l reaction mixture comprised 2 μ l of diluted cDNA, 6 μ l nuclease-free water, 10 μ l of 2x GoTaq MasterMix, and 2 μ l of a 5 μ M stock of the target-specific forward and reverse primers (0.25 μ M each). Thermal cycling was performed using the Rotor-Gene 6000 thermocycler (Corbett Research) under the conditions shown in Table 2.2.

Table 2.2. qPCR Cycling Conditions

Cycle	Temperature	Time (seconds)
Hold	95°C	120
Cycling (40 repeats)	95°C	10
	60°C	15
	72°C	25
Melt	55°C- 95°C (Rising by 1°C each step)	90 seconds pre-melt 4 seconds post-melt

Each amplification reaction was performed in duplicate. The human 18s rRNA was amplified as a reference (housekeeping) control. Previous studies in the laboratory had shown good correspondence of the 18s rRNA gene with other housekeeping genes, including GAPDH, in

this cell line under various cytotoxic treatments (Dr. Dong Gui Hu, personal communication). No-template controls that contained nuclease-free water *in lieu* of cDNA were incorporated to monitor for possible contamination. Master mixtures for each separate gene were used to minimise pipetting errors. The SYBR-green fluorescence signal was acquired at the end of the 72°C extension step using Rotor-Gene 6000 software. The threshold value at which fluorescence was measured in each cycle was set at 0.08, within the linear phase of the reaction plot, when the log of the reporter (SYBR-green) signal is plotted against the cycle number. The threshold cycle (C_t) for each reaction was defined as the intersection between the amplification curve and the threshold value; this provides a relative measure of the concentration of the target in the reaction. Primer sequences are presented in Appendix Table 5.4. The primers had been used in previous studies and had been shown to have good specificity and amplification efficacy.

2.4.6.1. Data Analysis

The data from the Rotor-Gene 6000 software was exported to an excel file for analysis. All data analysis was performed using the $2^{-\Delta\Delta CT}$ method (Livak & Schmittgen 2001). Gene expression levels were normalised to the expression of the *18s* housekeeping gene. The induction or repression of gene expression due to treatment was calculated as a fold change relative to the vehicle (ethanol) treated control.

2.4.7.0. MTT Cell Proliferation Assay

The Thiazolyl Blue Tetrazolium Blue (MTT) metabolic viability assay (Mosmann 1983) was utilized to evaluate MDA-MB-231 cell proliferation and viability after exposure to epirubicin. To prepare the MTT solution, 3-(4,5-dimethylthiazol-2-yl)-2,5-diphenyl-2H-tetrazolium

bromide was dissolved in phosphate-buffered saline PBS at a final concentration of 5 mg/ml, filter sterilized, and stored at -20°C covered with foil. MTT cell solvent was prepared by adding 4 mM HCL to 0.1% NP40 in isopropanol.

The MTT assay was used to assess the proliferation rate of cells that had been previously exposed to epirubicin or vehicle for 48 hours. For each MTT experiment, three 96-well plates were seeded with pre-treated MDA-MB-231 cells (5000 cells in 200 µl complete DMEM per well), and each plate was subsequently assayed at a different time point (day 1, 2, and 3). The cells were given a 24h adherence period, where the day of cell seeding was defined as day 0. On day 1, 20 µl MTT solution was added to the media in each well of one plate. The exact process was carried out on days 2 and 3. The plate was incubated for four hours at 37°C, covered with foil to allow MTT to form formazan crystals by reduction inside metabolically active cells. After the incubation, media and MTT solution in each well were removed carefully, avoiding any disturbance to the cells. 150 µl of MTT solvent was added to each well, and the foil-wrapped plate was agitated for 15 mins on an orbital shaker. The absorbance at 590 nm was measured using a Beckman Coulter DTX 880 Multimode Detector. The absorbance values were corrected for the background signal produced by the media alone.

Response of MDA-MB-231 cells to epirubicin treatment with respect to cell proliferation was reported using the proliferation index (PI). PI is calculated based on a model that predicts cell numbers in a population to double at a fixed rate (Munson 2010). The sum of total cells in each condition, including the originally seeded cells, was determined using a standard curve (5.2.2.0. Appendices). PI is the fold increase of the cell number over a selected period, which is calculated according to the below equation. The population doubling time of MDA-MB-231

cells has been previously estimated at approximately 25-30 hours, which was taken into account when designing experiments.

$$\text{Proliferation Index (PI)} = \frac{\text{Sum of the Cells}}{\text{Number of Originally Seeded Cells}}$$

2.4.8.0. Mammosphere Formation Assay

Anchorage-independent growth in serum-free media with defined growth factors is a classical assay for stemness and self-renewal capacity (Shaw et al. 2012). For both primary mammary stem cells and BCa-derived BCSC, the mammosphere formation assay has been established to assess these properties (Dontu et al. 2003). When applied to a mixed population of BCSC and non-BCSC, it can quantify the proportion of cells in the population with stem-like self-renewal capacity. In the current study, the effect of epirubicin treatment on the ability of MDA-MB-231 cells to form mammospheres was quantitatively evaluated using the protocol described below.

2.4.8.1. Preparation of the Non-adherent Culture Plates

Tissue culture plates were coated with poly-2-hydroxyethyl-methacrylate (poly-HEMA) to create a non-adherent surface. A 10x solution was prepared by dissolving 2.4 g of poly-HEMA in 20 ml of 95% ethanol, sealing with parafilm and incubating overnight on a rotator at 65°C before storing at room temperature. The 1x solution with final concentration at 12 mg/mL was made by diluting the 10x poly-HEMA in 95% ethanol. Each well of a 24-well plate was coated with a volume of 300 µl poly-HEMA solution. The plates were placed at room temperature for 2-3 days to allow complete evaporation of ethanol. Prior to use, the dried plates were sterilized by exposure to UV light in the laminar flow hood for 30 mins, followed by three washes in sterile PBS to remove any loose polymer particles.

Before the assay, MDA-MB-231 cells were exposed to varying epirubicin concentrations (0, 100 nM and 200 nM) for 48 hours, followed by a 72-hour drug holiday. Each drug treatment was performed in duplicate. Cells were harvested and counted as described in the Methods section 2.4.1.0. Mammosphere assays were performed in quadruplicate using 4000 cells/well in poly-HEMA coated 24-well plates. The total number of cells required for each treatment condition was calculated with a ~ 5% excess to allow for cell losses during processing (i.e. [4000 x 4] +1000 cells); these cells were washed with serum-free DMEM twice using centrifugation at 800 rpm for 5 mins. The cells were resuspended in mammosphere media at a concentration of 4000 cells/ml and passed through a 28G needle three times, ensuring the formation of a single cell suspension before seeding at 4000 cells (1 ml) per well.

Mammosphere media was comprised of serum-free DMEM/F12 (1:1) supplemented with 1 x B27 supplement, 20 ng/ml human epidermal growth factor (hEGF), 10 ng/ml basic fibroblast growth factor (bFGF), 1x insulin transferrin selenium (ITS) supplement and 0.5% methylcellulose to create a semi-solid medium. Methylcellulose solution was prepared by dissolving autoclaved methylcellulose in serum-free DMEM with overnight agitation at 4°C. Prior to use, the methylcellulose solution was centrifuged at 7000 rpm for 30 mins to eliminate any precipitate present. Culture plates were incubated at 37°C at 5% CO₂ in a humidified incubator for up to 3 weeks. Every three days, each well was supplemented with 200 µl fresh mammosphere media. Development of the mammospheres was monitored weekly and imaged using an EVOS® FL cell imaging microscope for quantification. Mammosphere formation efficiency was calculated using the equation below (Cioce et al. 2010).

Mammosphere Formation Efficiency

$$= \frac{\text{Average Number of Mammospheres Formed per Well}}{\text{Original Number of Cells Seeded per Well}} \times 100\%$$

2.4.9.0. Establishment of an Epirubicin Resistant MDA-MB-231 Cell Subline

2.4.9.1. Long-term Epirubicin treatment

The establishment of an epirubicin resistant sub-cell line was attempted using a range of different epirubicin concentrations applied to MDA-MB-231 cells at different cell densities (confluence) guided by previously published studies (Table 2.4.9.0). The cultures were initially maintained in T75 flasks and downscaling to T25 flasks was carried out as needed following the drug treatments. In each case, after a 48-hour drug exposure period, the drug was removed, cells washed twice with PBS and media without drug was added. Two days following drug withdrawal, cells were trypsinised and replated to accelerate the detachment of dying cells. Cell cultures were maintained in media without drug until reaching the desired confluency (see Table 2.4.9.0), replenishing media every three days or as needed. Media renewal was carried out more frequently when many dead cell debris was present following the treatment. When cells had 'recovered' from treatment, they were treated again with epirubicin (generally at a high dose) using the same protocol. The details of dosage escalation are shown in Table 2.4.9.0. Untreated MDA-MB-231 cell culture was maintained in parallel as the parental control line. Prior to experimental analysis of the long-term drug-treated cells, they were withdrawn from epirubicin treatment for at least two passages.

Table 2.3. Parameters of different strategies to establish an epirubicin resistant MDA-MB-231 subline

Attempt	01.	02.	03.	04.
Culture confluency when treating	~60%	~80%	~80%	~95%
Starting epirubicin concentration	5 nM	5 nM	100 nM	400 nM
Subsequent epirubicin concentrations	NA	15, 50, 100 nM	200, 400 nM	3 x 400 nM
References	(Alkaraki et al. 2020) (Xu et al. 2018) (Chittaranjan et al. 2014) (Braunstein et al. 2016) (Chen, X et al. 2016) (Zhong et al. 2016) (Hembruff et al. 2008)		(Knowlden et al. 2003)	

2.4.9.2. Determination of epirubicin sensitivity defined by IC50

The sensitivity of long-term treated MDA-MB-231 cell lines to epirubicin was determined using the MTT assay. A 96-well plate was seeded with 1.6×10^4 cells in 200 μ l complete DMEM in each well. In each plate, 48 wells were seeded with long-term epirubicin treated MDA-MB-231 cells, and the remaining 48 wells were seeded with the parental MDA-MB-231 line. Following a 24-hour incubation, the media in the plates were replaced with 0, 25, 50, 100, 200, 400, 800, and 1200 nM epirubicin in DMEM (6 wells per dose). After a 72-hour drug treatment period in standard incubation conditions, an MTT assay was carried out following the method described in 2.4.7.0.

$$\text{Percent Inhibition \%} = 100 - \left(\frac{OD (Test)}{OD (Un - treated)} * 100 \right)$$

Three biological replicates were performed for each model, with six technical replicates per drug dose. The vehicle control was denoted as 0 epirubicin concentration and contained 0.1% ethanol in complete DMEM. The maximal inhibitory concentration (IC50), the drug concentration required to reduce the cell population by 50% (relative to control) at a specified initial cell number, was used to measure the chemo-sensitivity of the cell lines. IC50 values were calculated using GraphPad Prism 9.1.2.

2.5.0.0. Statistical Analysis

All data reported represent a minimum of three independent biological replications except for the IC50 determination (n=2) and the gene expression (mRNA) analysis of the long-term epirubicin treated cell models (n=1). The results are presented as the mean \pm standard deviation. The significant differences between groups were analysed using the paired t-test and one-way ANOVA with Tukey post hoc testing where appropriate. A value of $p < 0.05$ were considered statistically significant. Biological and technical replications of each experiment are defined in the figure legends.

2.7.0.0. Compliance with Ethical and Safety Standards

No human participants or animals were involved in the study. Approval had been granted from the Flinders Institutional Biosafety Committee for Exempt dealings involving human cells, including those used in this study. However, this study did not involve any genetic manipulation of the cells. Administration of cytotoxic drug epirubicin hydrochloride (Category 2 mutagen and carcinogen) was carried out in a PC2 containment facility, using approved protocols as described in section 2.4.3.0.

RESULTS

3.0.0.0.	Overview	54
3.1.1.0.	Adaptive Response of MDA-MB-231 cells to Epirubicin Treatment	54
3.1.1.1.	ALDH1A1, OCT4 and SOX2 Stemness Indicator Gene Expression	55
3.1.1.2.	ABCB1 Transporter Gene Expression.....	58
3.1.2.0.	Stability of Gene Induction after Epirubicin Withdrawal	60
3.1.3.0.	Exposure to Epirubicin Reduces Mammosphere Formation Capacity.	63
3.1.4.0.	Exposure to Epirubicin Inhibits Cell Proliferative Capacity	68
3.2.0.0.	Establishment of an Epirubicin Resistant MDA-MB-231 Sub-line	70
3.2.1.0.	Comparison of the Drug Selection Protocols.....	70
3.2.2.0.	Analysis of drug sensitivity by IC50 determination.....	72
3.2.3.0.	Stem Cell Markers in the Epirubicin Selected Population	74

3.0.0.0. Overview

Critical analysis of the literature shows that resistance to different anticancer agents correlates with misexpression of a diverse range of genes that reflect the heterogeneous mechanisms involved in drug resistance. However, within this heterogeneity, the upregulation of genes that modulate drug exposure and promote the stemness phenotype is relatively consistent. The first part of this Results Section presents a quantitative expression analysis of key BCSC genes and ABC efflux transporters after short-term epirubicin treatment of MDA-MB-231 cells. Whether this rapid adaptive transcriptional response to drug treatment is sustained after drug withdrawal is then assessed. Moreover, whether the transcriptional response corresponds to a stemness phenotype is evaluated using assays of mammosphere formation capacity and general proliferative capacity.

This project aims to determine whether the short-term adaptive responses of TNBC cells to drug treatment are linked to the mechanisms by which tumours evolve to be drug-resistant after long-term drug treatment. The second part of this Results Section describes the development of protocols to generate and characterise a stably drug-resistant MDA-MB-231 sub-line by long-term treatment of MDA-MB-231 cells with epirubicin. These cells are subsequently assessed for changes in drug sensitivity and gene expression relative to untreated parental MDA-MB-231 cells.

3.1.1.0. Adaptive Response of MDA-MB-231 cells to Short-term Epirubicin Treatment

MDA-MB-231 cells cultured as monolayers were treated with 0, 250 nM and 500 nM epirubicin for 48 hours as described in Methods. The adaptive transcriptional response to this

relatively short-term drug exposure was evaluated by quantitative expression analysis of selected target genes using qRT-PCR. The genes of interest for this analysis were stemness marker genes as well as efflux transporter genes. The data shown in this section were derived from three independent biological replicate experiments.

3.1.1.1. *ALDH1A1*, *OCT4* and *SOX2* Stemness Indicator Genes are Significantly Upregulated by Short-term Epirubicin Treatment

BCSCs are characterised by the overexpression of a set of genes that are considered indicative of the stemness phenotype. *ALDH1A1* and *CD44* are the most established BCSC marker genes, while *OCT4*, *SOX2*, and *DNER* are core regulators of normal stem cells that have also been reported to be elevated in BCSC by some studies.

ALDH1A1, a classical marker gene for BCSC, demonstrated the highest fold increase after epirubicin treatment compared to the control. The 250 nM and 500 nM treatments produced ~113 (+/-49) and ~191 (+/- 20) fold increases, respectively, which were both significantly different to the vehicle-treated control ($p < 0.05$). While the response showed a trend toward dose-dependence, the induction was not significantly different between the 250 nM and 500 nM treatments, primarily due to inter-experimental variation.

CD44 is another classical BCSC marker gene that is frequently assessed alongside *ALDH1A1*. Surprisingly, *CD44* was not significantly induced following epirubicin exposure. Epirubicin concentrations 250 nM and 500 nM produced 1.2 (+/- 0.37) fold changes and no change, respectively.

OCT4 is a marker of embryonic stem cells shown to be elevated in BCSC in several studies. *OCT4* mRNA was significantly upregulated compared to the control at both epirubicin doses ($p < 0.05$). The 250 and 500 nM treatments produced 6.4 (+/- 2) and 9.9 (+/- 5) fold increases, respectively. As with *ALDH1A1*, there was no statistically significant difference between the 250 and 500 nM doses, although the response showed a trend towards dose-dependence.

SOX2, another embryonic stem cell marker, showed statistically significant induction upon epirubicin exposure ($p < 0.05$). At 250 and 500 nM epirubicin treatment doses, *SOX2* mRNA levels were upregulated 2.6 (+/- 0.5) and 5.0 (+/- 2.5) fold. As with *ALDH1A1* and *OCT4*, there was no statistically significant difference between the 250 and 500 nM doses, although the response showed a trend towards dose-dependence.

DNER is involved in Notch signalling and has been linked to BCSC phenotypes. There was no significant change in the expression level of *DNER* after epirubicin treatment. At 250 nM and 500 nM epirubicin, *DNER* mRNA levels were 1.8 (+/- 0.9) and 1.4 (+/- 0.5), fold higher than those in the vehicle-treated control; however, these were not significant differences.

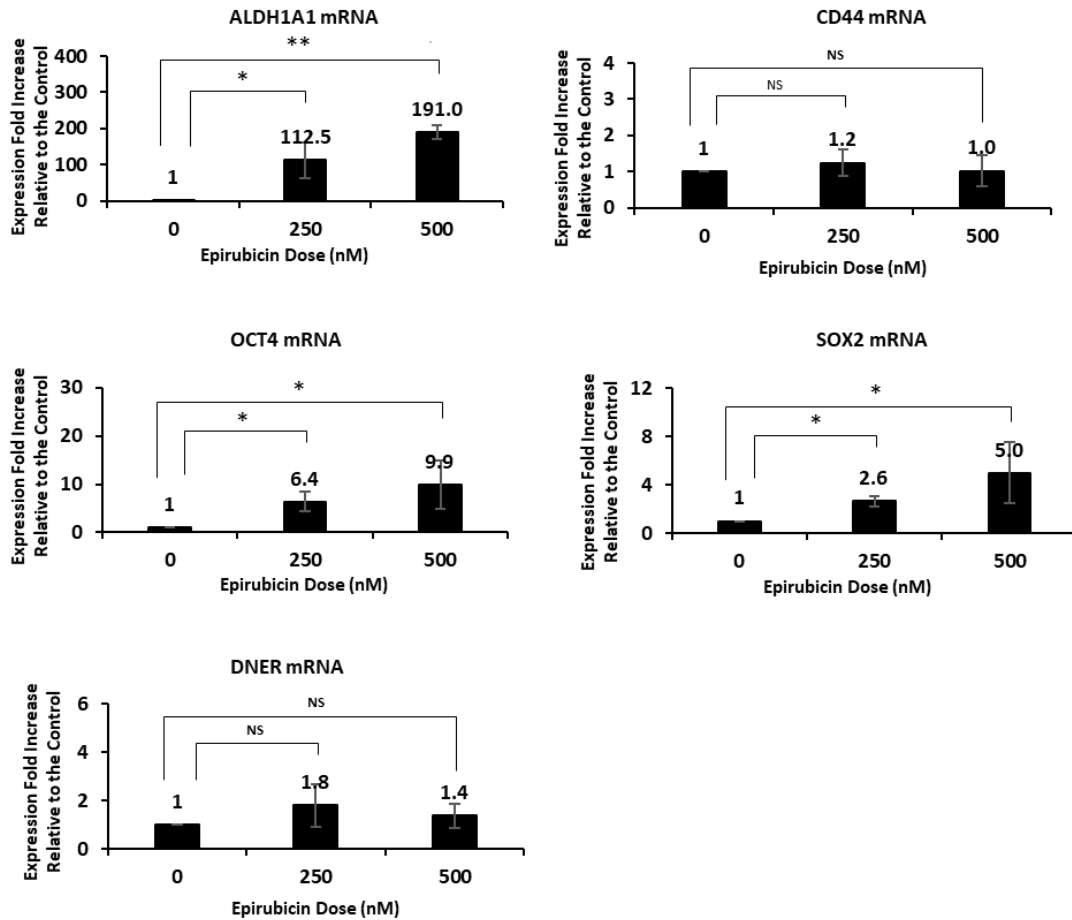


Figure 3.1. Differential expression of BCSC marker genes *ALDH1*, *CD44*, *SOX2*, *OCT4* and *DNER* in MDA-MB-231 cells after treating with 250 nM and 500 nM epirubicin for 48-hour duration. Ethanol vehicle control is indicated as 0 nM epirubicin treatment in the graphs. The cells at an initial density of 6.25×10^5 cells per well in 2 mL media were seeded in a six-well plate. Cells were treated after a 24-hour adherence period. The target genes were amplified in duplicates. The Human 18S gene was used as the endogenous control in the double delta calculation.

The standard deviation is represented by the error bars (+/-). For all data, statistical significance from the controlled condition was assessed using Student's t-test denoted as * when $p < 0.05$ and ** when $p < 0.01$. The graphs indicate the results of three independent biological replicates with two technical replicates.

ALDH1A1: Aldehyde dehydrogenase, *CD44*: Cluster of differentiation 44, *OCT4*: Octamer-Binding Transcription Factor 4, *SOX2*: Sex determining region Y (SRY)- box 2, *DNER*: Delta/ Notch- like epidermal growth factor (EGF) related receptor, NS: Not Significant.

3.1.1.2. *ABCB1* Transporter Gene Expression is Significantly Upregulated by Short-term Epirubicin Treatment

Changes in the expression of genes encoding three main ABC transporters after short-term epirubicin exposure were investigated. Permeability associated-glycoprotein (P-gp encoded by the *ABCB1* gene), multidrug resistance-associated protein 2 (MRP2 encoded by the *ABCC2* gene) and BCa resistance protein (BCRP encoded by the *ABCG2*) were selected due to their role in drug efflux, which can contribute to multidrug resistance.

ABCB1 expression was significantly upregulated by epirubicin treatment ($p < 0.05$). The 250 nM and 500 nM treatments produced a 77.8 (+/- 41.5) and 288.4 (+/- 282.5) fold change, respectively. However, the response at 500 nM was not statistically significant due to high inter-experimental variation. There was no statistically significant difference between the two doses, although again, there was an apparent trend towards dose-dependence.

ABCC1 expression was significantly upregulated by epirubicin treatment ($p < 0.05$). The 250 nM and 500 nM treatments produced a 2.2 (+/- 0.3) and 1.6 (+/- 0.3) fold increase, respectively. However, there was no dose-dependent trend.

ABCG2 expression was also significantly upregulated by epirubicin treatment ($p < 0.05$). The 250 nM and 500 nM treatments produced a 2.2 (+/- 0.3) and 1.3 (+/- 1.0) fold increase, respectively. However, the response at 500 nM was not statistically significant due to high inter-experimental variation, and there was no dose-dependent trend.

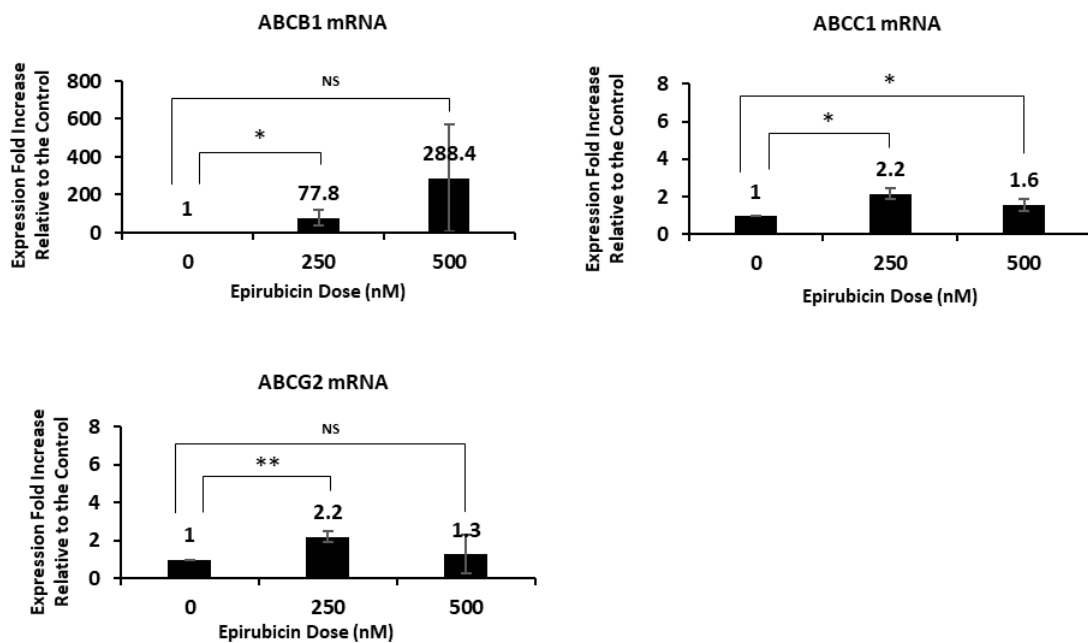


Figure 3.2. Differential expression of ABC transporter genes *ABCB1*, *ABCC1* and *ABCG2* in MDA-MB-231 cells after treating with 250 nM and 500 nM epirubicin for 48 hours. Ethanol vehicle control is indicated as 0 nM epirubicin treatment in the graphs. The cells at an initial density of 6.25×10^5 cells per well in 2 mL media were seeded in a six-well plate. Cells were treated after a 24-hour adherence period. The target genes were amplified in duplicates. The Human *18S* gene was used as the endogenous control in the delta-delta Ct calculation.

The standard deviation is represented by the error bars (+/-). For all data statistical significance from the controlled condition was assessed using Student's t test denoted as * when $p < 0.05$ and ** when $p < 0.01$. The graphs indicate the results of three independent biological replicates with two technical replicates.

ABCB1: ATP Binding Cassette (ABC) sub-family B member 1, *ABCC1*: ATP Binding Cassette (ABC) sub-family C member 1, *ABCG2*: ATP Binding Cassette (ABC) sub-family G member 2, NS: Not Significant.

3.1.2.0. Stability of Gene Induction after Epirubicin Withdrawal

Stemness marker genes *ALDH1A1*, *OCT4* and *SOX2*, along with the *ABCB1* transporter gene, were significantly upregulated in epirubicin treated MDA-MB-231 cells as shown in the Results Sections 3.1.1.1 and 3.1.1.2. We next sought to determine whether this gene induction profile represented a reversible state or if would it be sustained after the drug was withdrawn. Thus, the experiments shown in the previous sections were repeated; however, after the 48-hour drug treatment, cells were either harvested immediately or cultured for a further 72 hours in the absence of drug (drug holiday). As previously, three biological replicate experiments were performed, and all data shown in this Section is the average of these three experiments. As a minor modification to the previous experiment, two lower epirubicin concentrations were chosen: 100nM and 200 nM. The rationale for this change was twofold: first, there was a concern that 48 hours at higher epirubicin doses may cause too much cell stress, and hence cells may not be transcriptionally active during the next 72 hour drug holiday; second, we wanted to investigate gene expression responses at epirubicin doses more similar to those used in the long-term drug treatment experiments described in Section 3.2.

After 48 hours of epirubicin treatment at 100 and 200 nM, all four genes showed increased expression compared to the vehicle-treated control. Although the data did not always reach statistical significance due to inter-experiment variation, it generally confirmed the observations in the previous section when 250 and 500 nM epirubicin concentrations were used. At 72 hours post drug withdrawal, all genes except *SOX2* continued to show elevated expression relative to the vehicle-treated control. The precise details of these responses are described below and shown in Figure 3.3.

ALDH1 showed 7.6 (+/- 0.2) average fold induction after 48-hour treatment at 100nM epirubicin. Notably, this was increased to 14.9 (+/- 8.2) fold after the 72 hour drug holiday, although the difference between these values was not statistically significant. Similarly, after 48-hour treatment at 200 nM epirubicin, *ALDH1* expression increased 26.7 (+/- 9.7) fold; this was further increased to 53.1 (+/- 4.2) fold after the 72 hour drug holiday, and the difference between the two values was statistically significant ($p < 0.05$).

OCT4 showed 4.8 (+/- 1.8) fold, and 7.8 (+/- 2.1) fold induction after 48-hour treatment at 100nM and 200nM epirubicin, respectively, relative to vehicle control. After the 72 hour drug holiday, these values decreased slightly to 3.1 (+/- 2.4) and 5.0 (+/- 1.8) fold, respectively, but the differences were not statistically significant.

SOX2 showed 2.3 (+/- 0.4) fold and 3.5 (+/-0.8) fold induction after 48-hour treatment at 100nM and 200nM epirubicin, respectively, relative to vehicle control. After the 72 hour drug holiday, these values decreased to 1.2 (+/- 0.2) and 1.1 (+/-0.1) fold, respectively, and the changes were statistically significant ($p < 0.05$), demonstrating a loss of induction.

ABCB1 showed 67.8 (+/- 104.2) and 117.7 (+/- 143.2) fold induction after 48 hour treatment at 100nM and 200nM epirubicin respectively, relative to vehicle control. These values were not statistically significant due to high inter-experiment variation. After the 72 hour drug holiday, *ABCB1* showed 61.4 (+/- 28.4) and 125.5 (+/- 70.1) fold elevation, respectively. While this suggests that gene induction was sustained, firm conclusions cannot be drawn because of the high variation and lack of statistical significance.

The overall observation was that the induction of these genes at the 100nM and 200nM epirubicin doses was lower and more variable than at the higher doses used in Sections 3.1.1.1 and 3.1.1.2. The second major observation was that the expression of these genes was generally sustained at a similar level after the 72 hour drug holiday (with the exception of *SOX2*). Moreover, one gene (*ALDH1*) showed greater elevation after the drug holiday; the mechanism that may underlie this is yet to be determined.

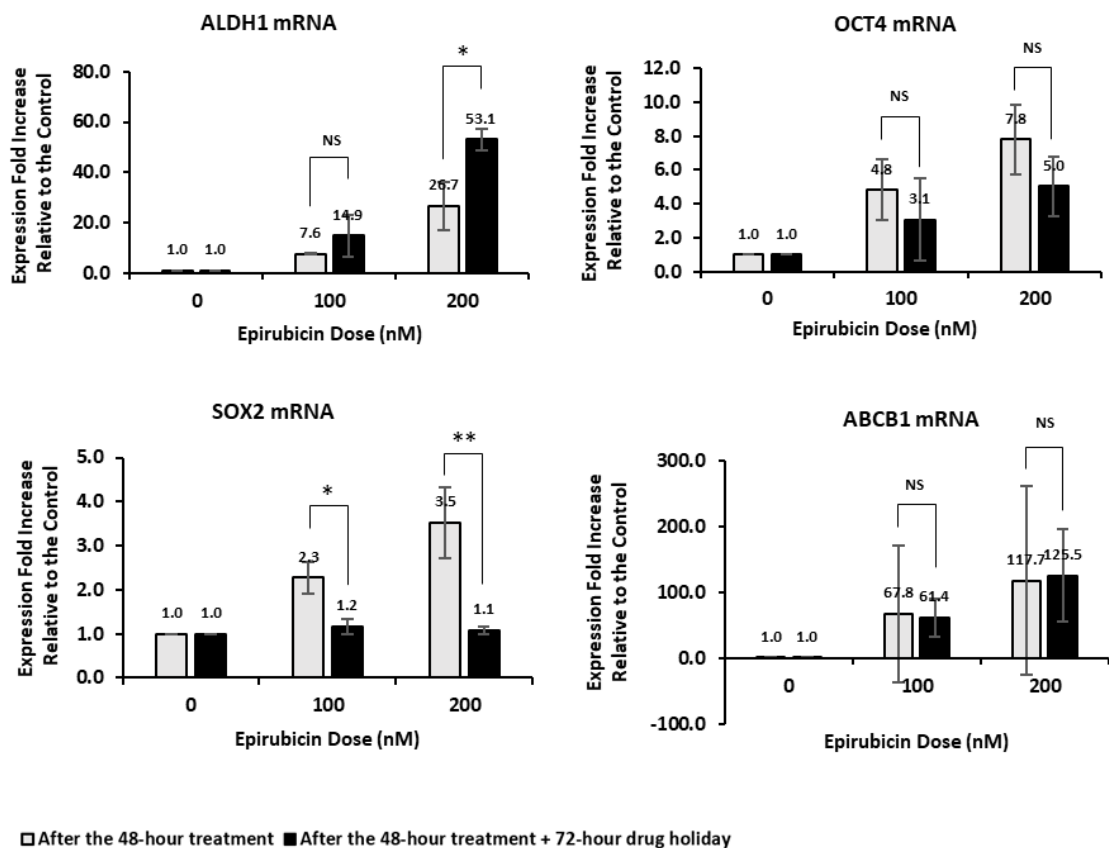


Figure 3.3. Comparison of expression levels of ALDH1, SOX2, OCT4 and ABCB1 genes after 48-hour treatment and the same treatment+ 72-hour drug holiday. MDA-MB-231 cells were treated with 250 and 500 nM epirubicin and ethanol vehicle control is indicated as the 0 nM epirubicin treatment.

The target genes were amplified in duplicates. The Human 18S gene was used as the endogenous control in the delta-delta Ct calculation. The standard deviation is represented by the error bars (+/-). For all data statistical significance between the two time points was assessed using Student's t test denoted as * when $p < 0.05$ and ** when $p < 0.01$. The graphs indicate the results of three independent biological replicates with two technical replicates.

ALDH1A1: Aldehyde dehydrogenase, OCT4: Octamer-Binding Transcription Factor 4, SOX2: Sex determining region Y (SRY)- box 2, ABCB1: ATP Binding Cassette (ABC) sub-family B member 1, NS: Not Significant.

3.1.3.0. Exposure to Epirubicin Reduces Mammosphere Formation Capacity.

Given that short-term (48 hours) epirubicin treatment increased expression of stemness genes in MDA-MB-231 cells, and this was at least partly sustained after drug withdrawal, we next sought to determine whether the transcriptional response was associated with a greater number of cells displaying a stemness phenotype. The capacity for anchorage-independent growth in serum-free conditions (i.e., mammosphere formation) is one functional indicator of stemness, specifically self-renewal capacity. Hence mammosphere assays were performed using MDA-MB-231 cells that had been treated with 0, 100 and 200 nM epirubicin for 48 hours and then maintained without drug for 72 hours (drug holiday) as described in Section 3.1.2.0. The mammosphere cultures were established as described in the Methods and maintained for 21 days before quantitative analysis. For this analysis, all mammospheres with a size $> \sim 20$ μm were counted, and the mammosphere forming efficiency was calculated as a percentage of the initially seeded cell number.

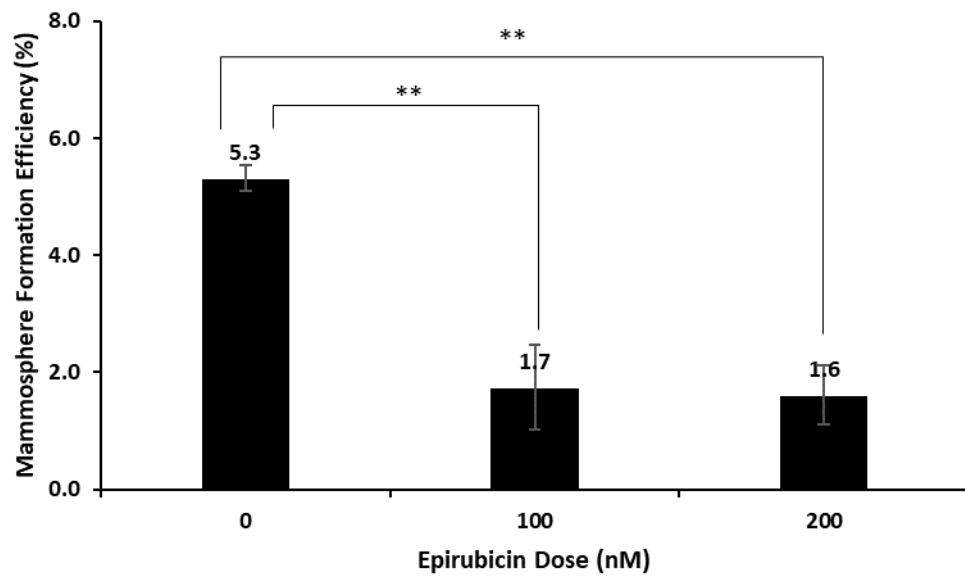
Mammosphere formation capacity of epirubicin treated cells (48-hour treatment plus 72 hour drug holiday) was found to be diminished when compared to the vehicle-treated control. Specifically, the 100 and 200 nM epirubicin treated samples showed mammosphere formation efficiencies of 1.7% (+/- 0.7) and 1.6% (+/- 0.5), respectively; these values were significantly lower than the 5.3% (+/- 0.2) mammosphere formation efficiency value of the vehicle-treated control cells.

It was also noted that mammospheres formation by the epirubicin treated cells was delayed relative to the control cells. On day 7 of the mammosphere assay, only the control cells had

started to form mammospheres. Mammospheres appeared in the 100 nM treated cultures within the second week and 200 nM treated cells within the third week. On day 21, wells seeded with control cells were enriched with mammospheres with sizes ranging from 20- 200 μ M. In contrast, cells seeded with epirubicin treated cells had generally smaller mammospheres with many < 20 μ m.

The observation that epirubicin treated MDA-MB-231 cells show increased expression of stemness genes led us to predict that they may also show enhanced mammosphere formation; however, this was not observed. The mammosphere assay measures two parameters: 1) the ability of cells to *survive* in non-attached, growth factor deprived conditions, and 2) the ability of cells to continuously *proliferate* in these same conditions allowing them to form spheres >20 μ m in size. The observation that the epirubicin treated MDA-MB-231 did not show enhanced mammosphere formation might be explained by a reduction in the proliferative rate of these cells. At the beginning of the mammosphere formation assay, it was noted that the vehicle control (0nM) and epirubicin treated samples were at different confluency levels, with control cells at high confluency and drug-treated cells at low confluency. This suggested that the drug-treated cells were proliferating much more slowly than the control cells, even after the 72 hour drug holiday. Thus, we next examined the effect of epirubicin treatment on subsequent proliferative capacity as described in Section 3.1.4.0.

(A)



(B)

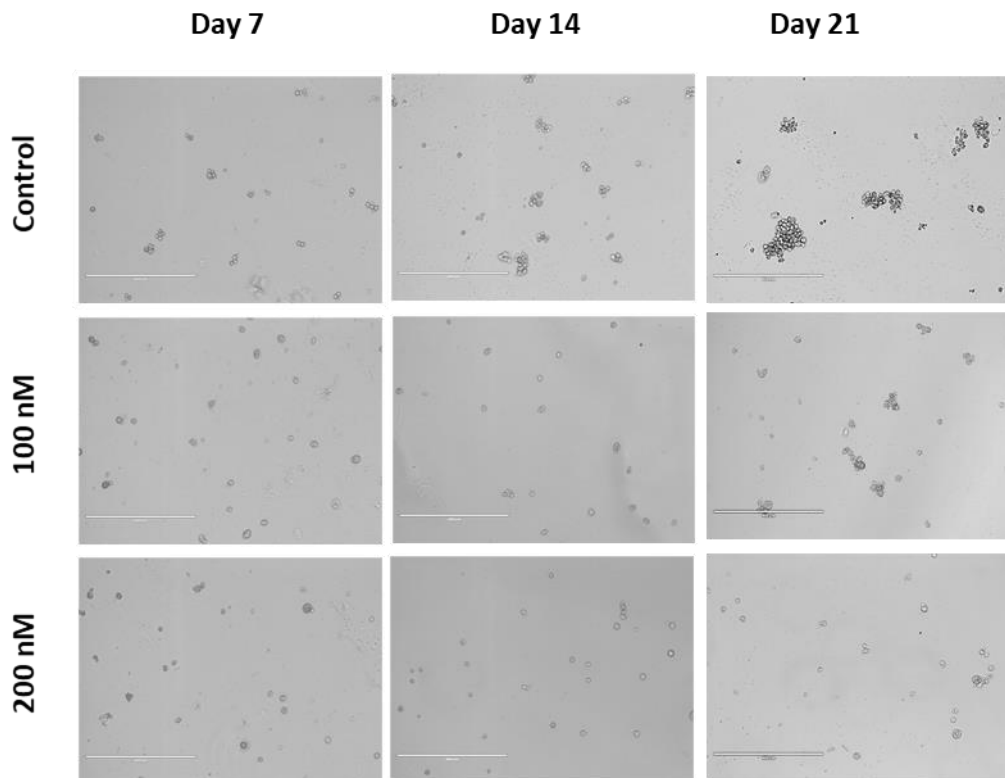


Figure 3.4 (A) Mammosphere formation efficiency of epirubicin treated MDA-MB-231 cells. Following a 24h adherence period, cells seeded in six-well plates were treated with 100 and 200 nM epirubicin and the ethanol vehicle control was used as the 0 nM epirubicin treatment. After 48 hour treatment with epirubicin, the drug was removed, and the cultures were further grown for 72 hours in fresh media. After this drug holiday, cells were assayed for mammosphere formation. On day 21 of the assay, mammospheres formed in size $> \sim 20 \mu\text{m}$ were counted and the mammosphere formation efficiency was calculated as the percentage of the originally seeded cell number.

The standard deviation is represented by the error bars (+/-). Statistical significance was assessed by one-way ANOVA with Tukey post hoc testing where appropriate. Statistical significance ($P < 0.01$) is denoted by asterisks (**). Cells were treated having two technical replicates for each treatment and the mammospheres were grown in quadruplicates for each sample. The graphs indicate the results of three independent biological replicates.

(B) Representative panels from each treatment on day 7, 14, and 21 of culture to compare the quantity and the size of the mammospheres formed. Magnification was at 10X; the bar in the panels indicates $400 \mu\text{m}$.

3.1.4.0. Exposure to Epirubicin Inhibits Cell Proliferative Capacity

Alterations in the proliferative capacity of MDA-MB-231 cells induced by epirubicin exposure were investigated in this section. MDA-MB-231 monolayer cultures were treated with 100 and 200 nM epirubicin for 48 hours, then the drug was withdrawn, and the cultures further maintained in drug-free media for 72 hours as described in the previous sections. Following the 72 hour drug holiday, the cells from each condition were subjected to proliferation analyses using the MTT assay. Proliferation was measured over three days as described in the Methods. The linear relationship between the formazan colourimetric signal produced and the viable cell number allowed the quantification of cell numbers at each time point using a standard curve. The effect of epirubicin treatment on the proliferative capacity of MDA-MB-231 cells was reported using the proliferation index (PI) as described in the Methods. As previously, three biological replicate experiments were performed, and the data shown in this section is the average of these three experiments.

MDA-MB-231 cells treated with epirubicin for 48 hours prior to a 72 hour drug holiday showed suppressed proliferation compared to the control cells. This suppression was statistically significant ($p < 0.05$) only on day 3. The vehicle-treated control sample showed an essentially linear growth curve over the course of the 3-day assay. In contrast, in both epirubicin pre-treated samples, cell numbers increased only slightly between day 1 and day 2 and plateaued thereafter (Figure 3.1.4.0). This suppression of proliferative capacity may partly explain the reduction in the formation of mammospheres $>20 \mu\text{m}$ in size by epirubicin treated cells in the mammosphere assay.

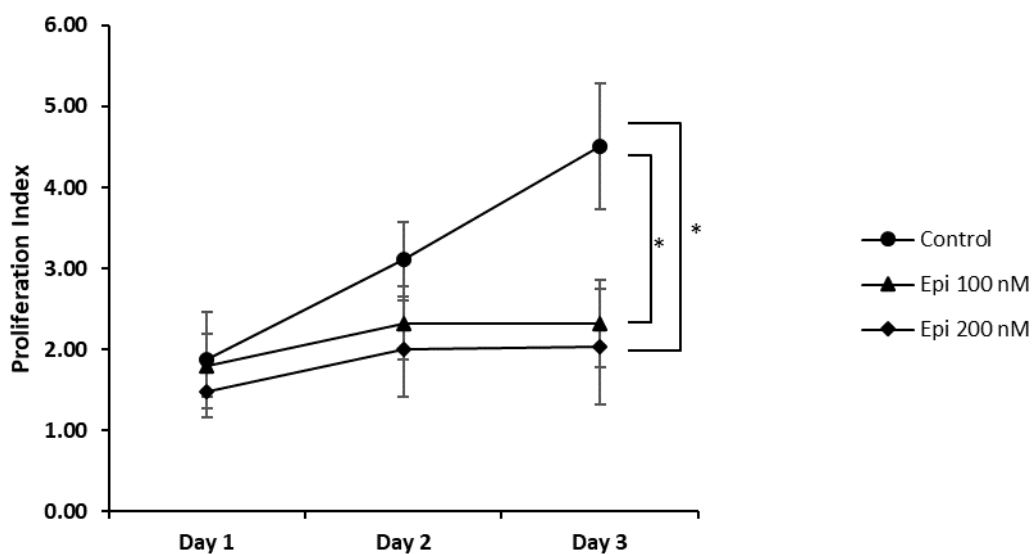


Figure 3.5. Variations in the proliferation of MDA-MB-231 cells after 48 hour epirubicin treatment (100 and 200 nM) and a 72-hour drug holiday at three time points; day 1,2 and 3. Ethanol treated samples were used as the vehicle control. Optical density values at 590 nm recorded from the MTT assay was converted to the cell number using a standard curve (Appendix Figure 5.1). Proliferation index was calculated as the fold change of viable cell number at any point compared to the originally seeded cell number.

The standard deviation is represented by the error bars (+/-). For all data statistical significance from the controlled condition was assessed using Student's t test denoted as * when $p < 0.05$. The graphs indicate the results of three independent biological replicates with two technical replicates.

3.2.0.0. Establishment of an Epirubicin Resistant MDA-MB-231 Subline

3.2.1.0. Comparison of the Drug Selection Protocols

The overall goal of this part of the project was to develop an epirubicin-resistant subline of MDA-MB-231 cells in order to better understand the role of stemness and drug clearance pathways in the stable long-term resistance of tumour cells to this drug. The development of drug-resistant cancer cell lines has been widely reported in the literature; however, there are few if any definitive protocols for the establishment of anthracycline (e.g. epirubicin) resistant models. Based on an analysis of literature, four different strategies were trialled. All strategies used a cyclical treatment approach that partly reflects the cyclical treatment protocols used clinically. In each cycle, the cells were drug-treated for 48 hours, followed by a drug holiday of variable length to allow cells to return to a proliferative state (defined empirically by reaching a specified level of confluence). The cycle was then repeated, and in most protocols, the epirubicin dose was escalated in each cycle. The four strategies varied according to the starting epirubicin dose, subsequent epirubicin doses used, and the culture confluences at the time of drug treatment. Each strategy was attempted a minimum of two times. The qualitative findings from these studies are described below.

Strategy 01. MDA-MB-231 cells were treated with 5 nM epirubicin for 48 hours at ~60% initial confluency. At this low epirubicin, concentration cells were predicted to continue to proliferate; hence a low confluency culture was used to provide space for cell growth in the same flask. However, following the initial drug treatment, the confluency of the cell culture continued to decline until the population was eliminated within a week of the drug

withdrawal. The flasks were maintained in the incubator for two more months to allow re-growth of any resistant clones, but no such re-growth was observed.

Strategy 02. MDA-MB-231 cells were treated with 5 nM epirubicin for 48 hours at initial cell confluency of 80%. This was followed by a drug holiday that was maintained until the cells recovered and again reached ~80% confluency. At this stage, the cells were treated with 15 nM epirubicin for 48 hours, followed again by a drug holiday until cells re-established ~80% confluence. This was repeated twice more using doses of 50 and 100 nM epirubicin. Substantially greater cell death was observed upon the 50 and 100 nM treatments relative to the lower doses. The 50 nM treated cells recovered after a sustained drug holiday to reach ~80% confluence again. However, after treatment with 100 nM epirubicin, the culture did not recover, and all cells were lost over the course of the final drug holiday, with no emergence of clones within two months.

Strategy 03. MDA-MB-231 cultures were treated with 100 nM epirubicin for 48 hours at ~80% initial confluency. This caused a high level of cell death similar to that observed in Strategy 02. However, after a sustained drug holiday, a viable cell population re-emerged and reached ~80% confluency. The process was repeated, escalating to 200 nM epirubicin and again, the cells recovered after a sustained drug holiday and reached 80% confluence. However, when the process was repeated with escalation to 400 nM epirubicin, the culture did not recover, and all cells were lost over the course of the final drug holiday, with no emergence of clones within two months.

Strategy 04. MDA-MB-231 cultures were treated with a 400 nM epirubicin for 48 hours at ~95% initial confluency. This caused significant cell death; however, after a sustained drug

holiday, a viable cell population re-emerged and reached ~95% confluency. The process was repeated three times in cultures using 400 nM epirubicin (no dose escalation) and allowing cells to reach ~95% confluency before each subsequent treatment. The last drug treatment cycle was observed to lead to less cell detachment than the previous cycles, suggesting that cells may be more drug-resistant. This population was further characterised as described in Section 3.2.2.0 to determine its relative drug resistance/sensitivity and any associated changes in gene expression.

3.2.2.0. Analysis of drug sensitivity by IC50 determination

The long-term epirubicin selected population established using Strategy 04 in Section 3.2.1.0 was characterized relative to untreated parental MDA-MB-231 cells. Epirubicin sensitivity was measured for each cell population using the MTT assay with a range of epirubicin concentrations: 0, 25, 50, 100, 200, 400, 800, and 1200 nM, and single 72-hour exposure duration. Of the three biological replicates carried out, one experiment had to be omitted from the analysis due to inconsistency of the technical replicates within the MTT assay. The data gathered from the other two biological replicates were processed using GraphPad Prism to derive values for the half-maximal inhibitory concentration (IC50) of epirubicin. The IC50 was calculated for each biological replicate independently, as shown in Figure 3.2.2.0.

In replicate 1, the drug selected population showed a lower IC50 for epirubicin than the control cells (50.71 nM vs 87.7 nM). This suggested that the drug-selected cells were more sensitive to epirubicin. However, in replicate 2, the drug-selected population showed a much higher IC50 for epirubicin than the control cells (1416 nM vs 230.1 nM). This would be consistent with reduced drug sensitivity.

Despite the discrepancies in the calculated IC50 values between the two replicate experiments, analysis of the proliferation curves shown in Figure 3.2.2.0 shows that in both replicates, the drug selected cells show *less growth inhibition at higher doses* of epirubicin when compared to the control cells.

For replicate 1, the drug selected cells show less growth inhibition at the two highest doses (800 and 1200 nM). However, the drug-selected cell population shows more inhibition than control cells at low doses, and the epirubicin dose at which 50% inhibition is observed is lower in the drug-selected population.

For replicate 2, the drug selected cells show less growth inhibition at the five highest doses (100, 200, 400, 800, and 1200 nM), and the epirubicin dose at which 50% inhibition is observed is *higher* in the drug selected population.

Overall, these patterns are generally consistent with the idea that the drug selected cells are *less sensitive to high doses of epirubicin* (because they show less growth inhibition than control cells at the high doses). However, because the two replicate experiments gave inconsistent IC50 values, they require further replication, which was unfortunately prevented by time constraints. It should be noted that the coefficient of determination (R^2) values for the interpretation of the goodness in the fit are excluded from the result analysis as IC50 determination incorporates a non-linear model, which cannot be validated by R^2 (Spiess & Neumeyer 2010).

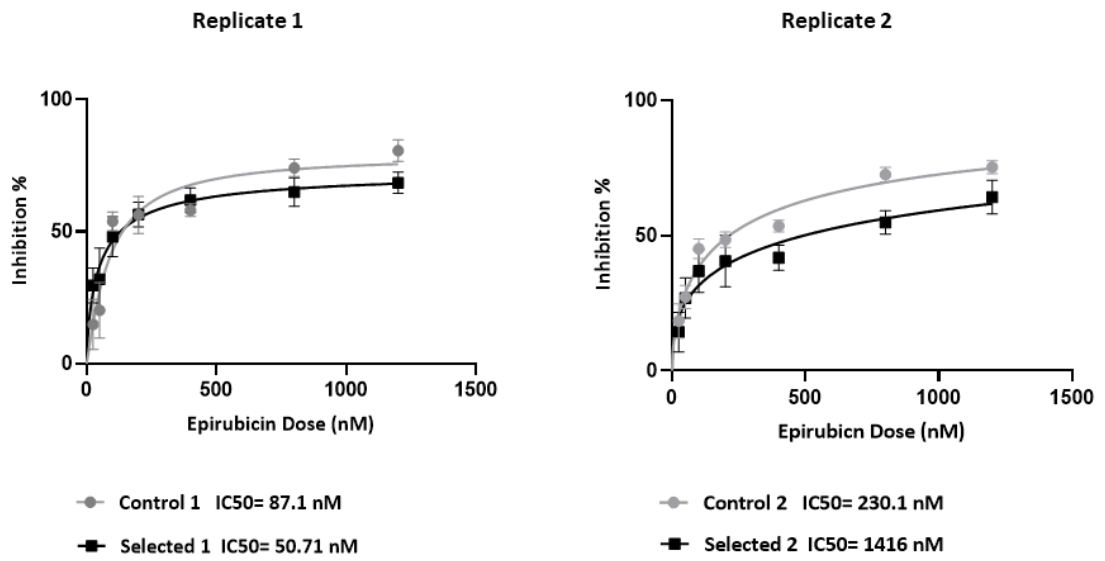
3.2.3.0. Stem Cell Markers in the Epirubicin Selected MDA-MB-231

Population Indicate No Change

The long-term epirubicin selected population established using Strategy 04 in Section 3.1.2.0 was examined for any gene expression changes consistent with stemness and drug resistance. The drug-selected cultures were passaged twice after the final drug holiday, and then both the drug-selected and untreated parental MDA-MB-231 cells were seeded into plates at defined densities for RNA isolation. The expression levels of the *ALDH1*, *OCT4*, and *ABCB1* genes were compared between the drug-selected and parental cells. These genes were selected for analysis because they all showed induction as an adaptive response to short term epirubicin treatment (Section 3.1.1.0 and 3.1.2.0)

As indicated in figure 3.6 (B), the expression of the *ALDH1* and *ABCB1* genes in the drug selected population was slightly decreased relative to the parental cell line (0.6- and 0.5-fold change, respectively). Expression of the *OCT4* gene was not different between the drug selected and parental cell lines. As time constraints did not allow more than one biological replicate experiment, no statistical analysis was performed. Overall, this data suggests that the long-term drug selection strategy did not produce a population with sustained upregulation of these specific stemness and drug resistance markers. However, this finding requires replication.

(A)



(B)

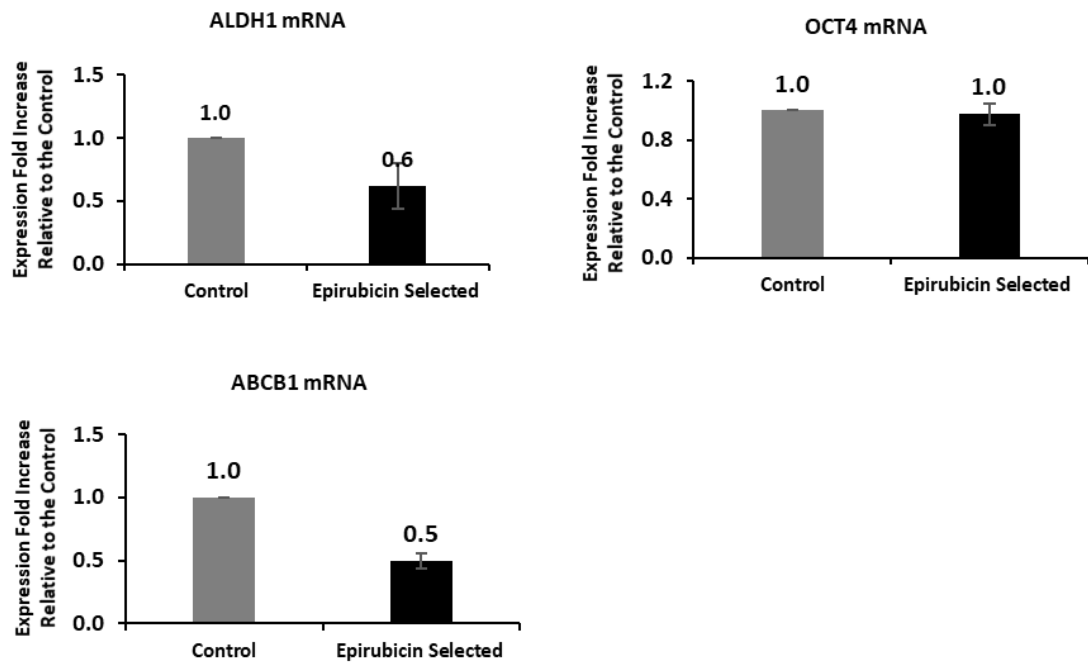


Figure 3.6 (A) Dose-response curve indicating epirubicin mediated inhibition of cell growth. The black and grey lines show the response of the epirubicin selected cell population and the untreated parental cell line respectively. The drug selected cell population was established as described in section 3.2.1.0 (Strategy 04). MDA-MB-231 cells were seeded in a 96-well plate with 1.6×10^4 cells per well. Inhibition response was assessed using an MTT assay measuring the optical density at 590 nm. Percent Inhibition = $100 - [(OD_{\text{Test}}/OD_{\text{Non-treated}}) \times 100]$. Each epirubicin treatment had six technical replicates and the graphs show two independent IC₅₀ determination assays carried out using the same sub-line at different passages. The standard deviation is represented by the error bars (+/-).

(B) Expression levels of ALDH1, OCT4, and ABCB1, in epirubicin-selected MDA-MB-231 cells relative to the parental MDA-MB-231 cells. The cells were passaged twice before seeding for the mRNA analysis. The cells at an initial density of 6.25×10^5 cells per well in 2 mL media were seeded in a six-well plate and grown to confluence before RNA harvest. The Human *18S* gene was used as the endogenous control in the delta-delta Ct calculation. Results of one biological replicate with two technical replicates are shown in the graphs. The target genes were amplified in duplicates. The standard deviation is represented by the error bars (+/-).

ALDH1A1: Aldehyde dehydrogenase, *OCT4*: Octamer-Binding Transcription Factor 4, *ABCB1*: ATP Binding Cassette (ABC) sub-family B member 1

DISCUSSION

4.1.0.0. General Project Overview and Summary of Findings

Elucidation of mechanisms underlying drug resistance in tumours could provide new avenues to predict, prevent and overcome unfavourable clinical responses in patients. Current literature indicates that pathways to drug resistance are highly heterogenous and involve mechanisms that relate to both drug pharmacokinetics and pharmacodynamics.

In pharmacology, the term pharmacokinetics refers to modulation of the drug by the body that involves the processes of absorption, distribution, metabolism, and elimination (ADME) both at a systemic level and within the target tissue/cell type. There is evidence that local (intratumoral) ADME processes alter drug exposure and thus response in cancer. In this

project, the ADME genes specifically investigated were those involved in drug efflux, and the findings were consistent with previous work showing that drug efflux is induced in cancer cells by drug treatment as part of an adaptive survival response that lowers drug exposure. Specifically, upon 48-hour epirubicin exposure, MDA-MB-231 TNBC cells increased expression of three efflux transporters *ABCB1*, *ABCC1*, and *ABCG2*, with *ABCB1* the most highly induced. This finding was consistent with previous *in vitro* work and with reports that levels of these efflux transporters are correlated with clinical outcomes, as discussed in more detail in subsequent sections.

Pharmacodynamics is the term used to describe the molecular, biochemical, and physiological effects of drugs on the body. It includes drug-target binding and all of the subsequent downstream events. The on-target effects of anti-cancer drugs are generally intended to be local (affecting mainly the tumour cells), although this selectivity is hard to achieve with cytotoxic drugs that may have multiple targets involved in ubiquitous cellular processes such as DNA replication and cell division. Previous work has shown that drug resistance is linked to a variety of changes in pharmacodynamic processes. For molecularly targeted therapies, these are often genetic/epigenetic changes in the direct drug target and/or its associated pathways. For cytotoxic chemotherapy, the relevant changes are those that affect general proliferative and survival signalling. Stemness pathways are known to control the ability of cells to proliferate in the absence of external cues, to survive in stressful environments, and to evade and/or repair genetic and cellular damage. They also give plasticity to cells, which allows them to change phenotypically to exploit changing environments; this may include adopting slow-cycling or quiescent states in contexts of anti-proliferative drug treatment. The expression of stemness markers is thus closely linked to drug resistance through what would be broadly considered pharmacodynamic effects. In this project, a set of stemness markers were found

to be rapidly induced by drug treatment. Specifically, upon 48-hour epirubicin exposure, MDA-MB-231 TNBC cells increased expression of the *ALDH1*, *OCT4*, and *SOX2* genes, with *ALDH1* the most highly induced. This finding was consistent with some previous *in vitro* work from this laboratory, although the rapid induction of stemness genes by short term drug treatment is not a widely reported outcome in literature, as discussed in more detail in later sections.

It was hypothesized that the rapid induction of genes that control drug exposure and stemness could contribute to the longer-term development of drug resistance, particularly if they were sustained even after the drug was removed, suggesting a phenotypic shift in the population. These changes were partly sustained over a 72-hour drug holiday, with the expression of most of these genes still elevated relative to untreated cells, but in most cases declined from the levels seen immediately after the 48-hour drug treatment. Interestingly, *ALDH1* was the exception, showing greater induction at 72 hours after drug withdrawal, as discussed further later.

It was hypothesized that the increased expression of stemness genes after epirubicin treatment indicated that cells had, at least transiently, adopted a BCSC-like phenotype. This was assayed functionally with the mammosphere formation assay, using cells that had been exposed to epirubicin for 48 hours, followed by a 72 hour drug holiday. However, there was a significant decline in mammosphere formation by drug-treated cells relative to control cells. Follow-up studies suggested that this was due to a generally reduced proliferative rate in the cells. Limitations of the mammosphere assay, and other ways to functionally assess stemness, are discussed in subsequent sections.

The second part of this project involved establishing a stably epirubicin resistant MDA-MB-231 sub-cell line using various long-term cyclical drug treatment protocols. Only one of the protocols trialled produced a cell line that could be sustained under drug treatment. Characterization of this line suggested that the drug selected subline was less sensitive (more resistant) to epirubicin; however, the IC50 value could not be determined reproducibly within the time constraints of the study. Interestingly, the preliminary analysis found that the drug selected subline did not have elevated expression of any of the genes that were shown to be induced by short-term epirubicin treatment (*ALDH1*, *OCT4*, *ABCB1*). This may indicate that long-term drug resistance is maintained by different processes to those involved in the short-term adaptive response to the drug. It is also possible that different drug treatment protocols induce different molecular pathways to resistance. These ideas are expanded on subsequently in this Discussion section.

4.2.0.0. Upregulation of *ABCB1*, *ALDH1A1*, *OCT4*, and *SOX2* Genes in Short-term Epirubicin Exposed MDA-MB-231 Cells

Cancer is a fundamentally heterogeneous disease at all levels (different cancers, same cancer-different patients, same cancer-different subtypes, different cells within the same tumour mass and at different times during tumour progression). Unsurprisingly, the mechanisms protecting tumour cells from the toxicity induced by antineoplastics are also diverse. This project examined both pharmacokinetic and pharmacodynamic mechanisms by measuring changes in genes associated with drug exposure and stemness.

Some of the most frequently examined molecular mechanisms contributing to epirubicin resistance are upregulated efflux of the drug out of the cell and increased activity of drug

metabolising/detoxifying enzymes (Appendix 5.4.0.0). Both of these processes lower the level of drug exposure. ABC family transporters are membrane efflux proteins with a broad capacity to transport exogenous and endogenous small molecules. Out of the known 49 ABC transporters, ABCB1, ABCC1, and ABCG2 play significant roles in actively exporting chemotherapeutic drug molecules out of the cell. In addition, elevated expression of ABC transporters has been described as one of the hallmark properties differentiating BCSC from the normal cells and contributing to their intrinsic drug resistance (Sridharan et al. 2019).

The finding in this project that short term epirubicin treatment increased expression of three ABC efflux transporters that are known to transport epirubicin was not surprising. However, most previous work has studied elevations of the transporters in long-term selected stably drug-resistant cell lines, mediated by promoter methylation changes, or by gene amplification or gene fusion events (Genovese et al. 2017; Reed et al. 2010). There is little insight from literature to explain the mechanisms by which epirubicin induced rapid transcriptional upregulation of these ABC transporter genes in the present study. The p53 tumour suppressor is known to regulate multiple drug efflux and metabolism genes. This has been previously linked to the induction of drug metabolic enzymes by epirubicin in hepatoma cells (Hu, DG et al. 2014). However, it must be noted that MDA-MB-231 cells harbour a mutant form of p53, and previous work in this laboratory showed that induction of drug metabolic *UGT* genes by cytotoxic drugs in this cell line was p53-independent (unpublished observations, personal communication Radwan Ansaar). This work could be expanded to define the mechanisms by which ABC transporters are induced by epirubicin in p53 mutant TNBC cells.

The *ABCB1* gene showed the greatest fold change among the genes screened in this study, while the induction of the *ABCC1* and *ABCG2* genes was relatively modest. This result suggests that *ABCB1* may be an important determinant of epirubicin response in MDA-MB-231 cells. Consistent with this idea, the *ABCB1* expression level was previously shown to be clinically correlated with survival outcomes in patients with locally advanced breast cancer receiving anthracycline (epirubicin or doxorubicin)-containing chemotherapy. Specifically, patients with elevated *ABCB1* mRNA levels within their tumours had much shorter disease-free (DSS) and overall survival (OS) than those without elevated expression (DSS: 13 vs 55 months, $p=0.0004$, and OS 21 vs 57 months, $p=0.0025$), respectively (Atalay et al. 2008). This study strongly suggested that *ABCB1* gene induction decreased survival in patients with breast cancer due to anthracycline resistance. In another study, MRP1 expression was only related to clinical outcomes in patients treated with an anthracycline-based regimen, not in those treated with a non-anthracycline regimen (Burger et al. 2003). Interestingly, very high-level *ABCB1* upregulation has also been shown in leukemic cells that were selected for doxorubicin resistance (Kadioglu et al. 2016). Moreover, gene fusions that increase *ABCB1* expression in patients who had received multiple anthracycline-containing chemotherapy cycles have been suggested to produce collateral resistance to other substrates of this transporter, including PARP inhibitors (Christie et al. 2019). These reports give clinical significance to our findings and suggest that understanding and preventing *ABCB1* induction might sustain more effective drug responses.

Of the stemness marker genes examined in the present study, *ALDH1* and *CD44*, the latter as part of the $CD44^+/CD24^{-/low}$ surface marker profile, have been established as gold standard identifiers for the BCSCs. Both can be used for the prospective identification of BCSC from tumours and cell lines. The results in this study indicated a significant increase in *ALDH1* mRNA

levels in short-term epirubicin treated cells, while *CD44* expression was unaffected. Previous studies suggest that CD44 is controlled post-transcriptionally and by regulated production of splice variants in CSC (Hu, Jing et al. 2017). The possibility that CD44 protein levels and/or selected splice variants can be induced by epirubicin cannot be discounted. This could be examined in future work using antibodies for immunoblotting analysis and by isoform-selective qRTPCR analysis. Previous studies have shown that the different BC cell lines used in research differ quantitatively in the proportion of cells with the CD44+/CD24- marker profile. MDA-MB-231 cells show a very high proportion of cells that are CD44+/CD24- (85%) (Sheridan et al. 2006). Hence the already high expression of CD44 in these cells may be another possible explanation for the lack of measurable induction by epirubicin.

ALDH1 is a metabolic enzyme that detoxifies reactive aldehydes that are derived from lipid peroxidation and that are initiated by and reciprocally amplify reactive oxygen species (ROS). Overexpression of ALDH1 increases detoxification of these reactive species protecting the cell from ROS mediated DNA damage and subsequent apoptosis (Raha et al. 2014). Epirubicin generates both drug and oxygen free radicals that cause the peroxidation of cell membrane lipids as a part of its cytotoxic mechanism. Overexpression of ALDH1 could therefore be part of a mechanism that circumvents the cytotoxic effect of epirubicin. In support of this idea, a clinical trial incorporating 234 neoadjuvant chemotherapy-treated BCa patients reported a significantly lower pathological complete response rate in patients that showed positive ALDH1 immunohistochemical staining in their tumours (13.5% vs 30.3%, $p=0.003$) (Kida et al. 2016).

BCSCs are heterogenous, and even the most established stemness markers such as CD44 or ALDH1 are not universal to all BCSC (Leccia et al. 2014). In fact, the ALDH1⁺ and CD44⁺/CD24⁻

$^{/low}$ marker profiles are proposed to represent two distinct BCSC subpopulations where $CD44^+/CD24^{-/low}$ accounts for a quiescent and mesenchymal phenotype while the $ALDH1^+$ phenotype accounts for proliferative and epithelial BCSC phenotype. The simultaneous evaluation of $ALDH1^+$ and $CD44^+/CD24^{-/low}$ phenotypes are not common; however, one study has indicated that in primary breast tumours, the overlap of the $CD44^+/CD24^{-/low}$ phenotype and $ALDH1$ expression is very low, at around 1% of cells (Ginestier et al. 2007). The $ALDH1^+$ phenotype has been positively correlated with high histological grade and larger tumours but has only been associated with survival outcomes in a subset of tumours (Althobiti et al. 2020a; Rabinovich et al. 2018). To better understand the cell-level heterogeneity of drug responses, the effect of epirubicin on $ALDH1$ and $CD44$ could be assessed simultaneously at the single-cell level using multi-colour flow cytometry with the Aldefluor fluorescence based $ALDH1$ activity assay and $CD44$ surface marker staining.

$OCT4$ is essential for the regulation of pluripotency (Mohiuddin et al. 2020). $OCT4$ is considered a promising drug target due to its unique abundance in cancer cells but not in normal (non-stem) cells (Sen et al. 2021). $OCT4$ overexpression has also been identified as one of the worse prognostic markers in TNBC patients (Zhang, J-M et al. 2018). Yousefnia et al. showed that MDA-MB-231-derived mammospheres had a 4.5 fold induction of $OCT4$ mRNA levels compared to the parental cell line (Yousefnia et al. 2019). The results described in this thesis indicated that epirubicin induced a significant increase in $OCT4$ expression (6.4 -fold at 250 nM and 9.9-fold at 500 nM) in MDA-MB-231 cells. Given that these levels are proportionate with the enrichment seen previously in mammospheres, this supports the idea that epirubicin induces a shift towards stemness in TNBC cells.

Despite being studied in many tumours, preclinical and clinical studies have shown inconsistent associations of OCT4 expression with aggressiveness and clinical outcomes (Mohiuddin et al. 2020). Kim et al. showed a higher *in vivo* tumorigenic capacity in OCT4-overexpressing BCa cells (Kim & Nam 2011). A clinical study involving 127 surgical patients with TNBC reported a positive correlation between high OCT4 expression and shorter overall survival (Zhang, J-M et al. 2018). However, another preclinical study using the hormone receptor-positive BCa cell line MCF7, found that silencing OCT4 induced EMT, migration and invasion (Hu, Jiajia et al. 2011). Apparently, in conflict with this finding, a study investigating 319 BCa cases found that OCT4 overexpression was positively correlated with poor survival outcomes in hormonal receptor-positive subtypes but not in the hormone receptor-negative sub-group (Gwak et al. 2017). Although data linking OCT4 expression with anthracycline treatment are not abundant, a study by Cheng et al. indicated high levels of OCT4 expression in doxorubicin selected resistant MDA-MB-468 TNBC cells (Cheng, C-C et al. 2018). The observation in the current study that epirubicin can rapidly induce OCT4 expression may or may not be mechanistically related to this finding.

SOX2 is another pluripotency factor that plays a crucial role in maintaining the stem cell state in embryonic, somatic, and cancer stem cells. In TNBC, SOX2 promotes proliferation and metastasis (Liu, P et al. 2018). A systematic meta-analysis incorporating 18 studies comprising 3080 patients stated that the SOX2 protein expression is not related to the overall survival of breast cancer patients but showed a close association with a worst disease-free survival (Hazard Ratio = 2.66, 95% CI= 1.20-5.91, $p = 0.016$) (Zhao et al. 2021). While there is limited data on the role of SOX2 in drug resistance, one study reported that silencing SOX2 in TNBC cells increased chemosensitivity to paclitaxel and diminished mammosphere formation (Mukherjee et al. 2017). The current study found a dose-dependent upregulation of SOX2 by

epirubicin in MDA-MB-231 cells; it is unknown whether this influences epirubicin sensitivity, but future studies could assess these using perturbation/knockdown methods.

A recent study by Wang et al revealed elevated expression of DNER in BCa tissues compared to adjacent normal tissues; moreover, TNBC expressed higher DNER levels compared to other BCa subtypes (Wang, Z et al. 2020). Increased expression of DNER is associated with poor survival of breast cancer patients, and previous work in MDA-MB-231 cells showed that it controls the expression of stemness markers as well as viability, migration and invasion (Wang, Z et al. 2020). In the current study, epirubicin did not induce DNER expression, suggesting that it may not play an essential role in the adaptive response to cytotoxic exposure. It is also possible that DNER levels are already sufficiently high in MDA-MB-231 cells that further expression provides no additional survival benefit.

Overall, the findings from the limited gene expression analysis performed in this study suggest that the adaptive response to short-term epirubicin treatment involves not only induction of factors that reduce drug exposure directly (e.g., ABC transporters) but also induction of stemness-associated survival pathways that are driven by pluripotency regulators (Oct4 and Sox2), and metabolic protection (e.g., ALDH1). The combined induction of drug clearance and survival pathways are likely not independent but driven by common stress response signalling pathways. Lack of induction of particular stem-cell associated genes by epirubicin might indicate that their specific functions are not relevant to the adaptive response. However, cross-analysis of the qRTPCR data demonstrates that the genes with a greater fold change are the least expressed genes and vice versa (Appendix Table 5.6); hence lack of induction may be simply because the genes are already maximally expressed and not a reflection of whether they are relevant to the drug-induced survival pathways.

4.3.0.0. Stability of Epirubicin induced Gene Induction

Multiple clinical studies indicate that drug resistance phenotypes can revert to being drug-sensitive upon the withdrawal of the treatment. In this study, the stability of epirubicin mediated gene induction was evaluated. Most of the changes were sustained to some degree after a three day drug holiday, although induction was trending downwards. This suggests that induction can be sustained for a period after drug withdrawal, but most cases would likely be lost over the longer term. Whether the induction of stem cell markers actually indicated functional enrichment of cells with BCSC properties in the population was tested using the mammosphere assay. Functional enrichment of BCSC could occur either because these cells were proportionately increased in number as non-BCSC died (or lost metabolic activity) under treatment or because non-BCSC acquired a BCSC phenotype.

The dynamic oscillation between stem cell and bulk tumour cells can be triggered by changes in signalling events that occur in the tumour micro-environment, including the introduction of stressors such as cytotoxic drugs. Upon drug withdrawal, the cancer cells may revert to the bulk tumour state. Thus, the cell population can be in different states of chemoresistance, proliferation, quiescence, and even epithelial to mesenchymal transition at any given time.

The studies herein prompt the conclusion that MDA-MB-231 TNBC cells may adopt a reversible drug-tolerant state under treatment driven by transient transcriptional and epigenetic mechanisms that allow cells to survive short term drug exposures. Relating the 48-hour treatment regimen used here to the plasma half-life of epirubicin in patients (~ 24 hours), it is possible that similar transient gene inductions are seen in patients after bolus treatment, but that most of this effect would likely be lost in the 3-week break before the next drug

treatment cycle is commenced. The only gene that showed fully sustained (in fact, increased) induction after the three day drug holiday in MDA-MB-231 cells was *ALDH1*. It would be interesting to determine how long this effect is sustained and whether *ALDH1* induction is also seen in patients during their treatment cycles.

4.4.0.0. Diminished Mammosphere Formation Capacity in Epirubicin Treated MDA-MB-231 Cells

The formation of mammospheres suggests anchorage-independent self-renewal, one of the most established characteristics of cancer stem cells. Supported by the overexpression of stemness related gene levels, it was hypothesised that the epirubicin treated cells might show an elevated mammosphere formation efficiency due to the enrichment of BCSC-like cells. However, mammosphere formation was inhibited by the epirubicin treatment.

The formation of mammospheres requires that single cells can overcome anoikis in the non-attachment culture, and also self-renew without the presence of serum factors and (at least initially) cell-cell contacts. However, as spheres continue to expand in size, they are receiving cell-cell signalling, and the daughter cells are typically thought to be less stem-like than the cells that initiated the sphere (Lombardo et al. 2015; Wang, R et al. 2014; Yousefnia et al. 2019). Because spheres were not counted unless they reached a minimum size, the reduced number of spheres in the epirubicin treated population could have reflected continued suppression of proliferative capacity by drug treatment that outweighed any enhanced stemness properties. This suppressed proliferative capacity was in fact demonstrated as discussed below.

4.5.0.0. Epirubicin Inhibits MDA-MB-231 Cell Proliferation Even After Four Days

Aberrant cell proliferation is a universal hallmark of all kinds of malignancies (Spoerri et al. 2017). Moreover, an increased or unchanged proliferation rate under drug treatment is considered an indicator of drug resistance. In contrast to this notion that drug resistance involves sustained proliferation, several studies have shown reduced proliferation rates in drug-resistant BCa cells (Chmielecki et al. 2011; Kreso et al. 2013; Moore et al. 2012).

This may be explained as a fitness cost, where survival can only occur at the expense of proliferation. For instance, upregulation of drug efflux pumps is a common occurrence in drug-resistant cancer cells. But synthesis, maintenance and operation of these pumps is a cost to the cancer cells, proposed to be used around 50% of the energy which would otherwise be reserved for other cellular mechanisms such as proliferation and migration (Kam et al. 2015). This resource delegation to drug resistance pathways may contribute to the diminished proliferation of even resistant cells under cytotoxic pressure. Hence, despite being often attributed to toxicity, a slower proliferation may in fact reflect the cost of resistance.

Two types of CSC, quiescent and proliferative, have been described in tumours. Yet, quiescence or proliferation do not obligatorily define stemness. Thus, while the finding of reduced proliferative rate after epirubicin treatment in the current study may help to explain the reduction in mammosphere formation, it should not be over-interpreted. It could reflect a wide range of effects, including toxicity, a cost of activating drug resistance pathways, or induction of a slow-cycling/quiescence stem-like state, all of which could be subjects for further study.

4.6.0.0. Selection of a Stably Epirubicin Resistant MDA-MB-231 Cell Population

Short term in vitro drug treatment assays using two-dimensional cell cultures do not well simulate the clinical response to cytotoxic treatments. Thus, cell cultures subjected to prolonged cytotoxic treatment were developed to better understand the pathways that may lead to clinical resistance. It was hypothesised that drug-resistant clones would emerge upon long-term treatment of the same cell population. The methodologies trialled involved exposing a cell population to epirubicin followed by extended drug holidays for cells to recover before the next cytotoxic insult.

The cyclical strategy was used to mimic other studies in literature and also to reflect the treatment strategy used clinically, where cycles (up to 6) are repeated until there is either complete response or no further response/tumour regrowth (suggesting resistance).

Under cytotoxic selective pressure, chemoresistance can emerge as a result of an expansion of pre-existing sub clonal populations or the clonal evolution and selection of drug-tolerant mutant variants in a heterogeneous tumour mass (Dagogo-Jack & Shaw 2018). CSCs and clonal evolution and selection are not mutually exclusive models in this process. However, cells that progress upon therapy are assumed to be permanently changed with a heritable resistance.

Different epirubicin doses and schedules were incorporated in this study, aiming to alter evolutionary dynamics and push the cell populations to develop stable drug resistance via mutations (or stable epigenetic changes) and clonal evolution of populations. In the first two strategies tested, the treatment was commenced with low drug doses to prime cells that were plated at low-moderate densities (60-80%). However, these cells did not survive, which

suggested that lower density cultures may be susceptible to toxicity. This effect appears non-linear as 60% of confluent cells did not recover from an epirubicin dose (5nM) that was 80-fold lower than the highest dose tolerated by a 95% confluent culture (400nM). Similarly, cells did not tolerate 100nM epirubicin at 80% confluence, even when 'primed' by a lower dose. Monolayer cultures lack the tumour supporting microenvironment of an actual tumour and are known to be involved in drug resistance. Density-dependent signalling that occurs only when cells are tightly packed may contribute to such non-linear effects on drug sensitivity.

Ultimately, a stable population was generated using a fixed high epirubicin concentration (400nM) to treat cells at high density, with comparatively fewer treatment rounds. This idea is an extrapolation from the observation that 100nM epirubicin induced resistance-associated genes to a lower level than higher (250nM, 500nM) doses in the short term drug treatment studies, although dose dependence wasn't precisely defined and the capacity of lower doses (below 100nM) to induce these genes was not directly tested. The success of the higher dose doses may suggest that lower doses were insufficient to induce the adaptive transcriptional responses that promote drug resistance (such as efflux).

"Hit hard and fast" is a popular notion in cancer therapy where the highest tolerated drug concentrations are often administered in the shortest possible period. But current study does raise a concern that high doses induce adaptive responses that allow cells to survive the treatment period and recover during the subsequent drug holiday. It may also enable resistant variants to expand due to the release from the competition of non-resistant cells. Such issues should be explored further in future work. It would also be valuable to use more naturalistic models in such studies, such as 3D tumour organoid models that better mimic tumour

conditions in terms of drug exposure, intercellular signalling events, and matrix interactions (see Future Directions).

4.7.0.0. Variable IC₅₀ of the Epirubicin Selected MDA-MB-231 Cells

The dose-response curves generated after epirubicin treatment of the epirubicin selected cell line, suggested that the cells were less sensitive to higher doses of epirubicin. Cytotoxicity of epirubicin in a variety of human cell lines in culture, including a number of BCa cell lines, increases exponentially with the drug dose and the duration of exposure (Ormrod et al. 1999). This exponential cytotoxicity was evident at epirubicin concentrations up to 200 nM. After that point, cells showed little further inhibition with higher doses. The derived IC₅₀ values demonstrated high variability between the biological replicates. Only one replicate showed a higher IC₅₀ supporting enhanced drug resistance. A comparison of the elucidated IC₅₀ values with those from literature was not shown, as these values are only comparable when using the same specific assay conditions. However, epirubicin inhibition in MDA-MB-231 cells did show a similar trend to published data (Carlisi et al. 2017; Cheng, W-J et al. 2020).

The MTT assay is the most extensively used method for the determination of IC₅₀. Yet, the inconsistency of the results gained from this assay prompts discussion of the biological and technical factors determining its reproducibility and replicability. Key elements include cell type, drug type, drug doses, and treatment duration, while medium replacement, medium type, seeding density and MTT assay incubation time affect the results to a lesser extent (Larsson et al. 2020). In this study, variations in epirubicin dosing, cell seeding, and media removal may be identified as contributors to inconsistency in the IC₅₀ estimation between experiments. Losing cells and formazan crystals in media removal prior to solubilization was

an observed issue, with empty patches sometimes evident in the bottom of the wells. In future work, MTT could be substituted with assays that generate soluble formazan crystals, i.e., 3-(4,5-dimethylthiazol-2-yl)-5-(3-carboxymethoxyphenyl)-2-(4-sulfophenyl)-2H-tetrazolium (MTS), also known as “one-step” MTT and water-soluble tetrazolium salts (WST-8) widely used as Cell Counting Kit 8 (CCK-8) (Barltrop et al. 1991; He et al. 2016; Ishiyama et al. 1997). To add to the artifacts incorporated with MTT assay, insufficient glucose, NADH and NADPH in the medium can interfere with MTT-formazan crystal formation leading to underestimates of viability. Another concern with all assays of mitochondrial dehydrogenase activity is the presence of intact mitochondria in dying cells that lead to overestimation of cell viability (Karakas et al. 2017). In the results of this study, the plateau in the latter part of all graphs, at high epirubicin doses is likely indicative of this issue. Other metabolic proliferation assays that may avoid this issue include the ATP assay (Lundin et al. 1986). This could be combined with morphological evaluation by phase-contrast microscopy and nuclei staining with Hoechst dye 33,342, which are recognised as compatible with the ATP assay results (Karakas et al. 2017).

Notably, the percent inhibition calculation used in this study relies on the cell number in the untreated wells ($\text{Percent Inhibition} = 100 - \left[\left(\frac{\text{OD}_{\text{Test}}}{\text{OD}_{\text{Non-treated}}} \right) \times 100 \right]$). But readings of the control wells are not free of variability that can arise due to inconsistencies in cell seeding and the variances in the proliferation potential of the cell lines. Thus, adopting control well-free methods to estimate cell viability, such as trypan blue-based cell counting and propidium iodide based apoptosis analysis, may be more appropriate for this study model (He et al. 2016). Based on the inherent density-dependence of drug sensitivity, inaccuracies in the cell seeding could be a major contributor to IC₅₀ variations.

4.8.0.0. Epirubicin Selected MDA-MB-231 Cells Show No Upregulation of BCSC Markers or Drug Efflux Genes

An unexpected finding was that cells that were selected by long-term treatment with epirubicin and had apparently lower sensitivity to high epirubicin doses did not show elevated expression of BCSC markers or ABCB1, even though these genes had been upregulated by short-term epirubicin treatment. It had been hypothesized that these adaptive changes would be part of the mechanism that ultimately led to long term stable resistance. There are a number of possible explanations for this finding. Firstly, the population may not be genuinely drug-resistant: in fact, until replicate studies resolve the discrepant IC50 data, this cannot be definitively concluded. Secondly, assuming the population is at least partly drug-resistant, these molecular pathways may not be relevant to its resistant phenotype. It is possible that the short term gene expression responses to cytotoxic treatment are only a transient step in the development of long term resistance and are supplanted later by other mechanisms. It is also possible that the pathways to drug resistance are very diverse and do not always involve these specific gene expression changes. As gene expression was not monitored throughout the drug selection process, it is unknown whether these genes were ever induced under this particular treatment modality. Such studies could be established with regular monitoring to define the pathways to resistance and incorporating not only genome-wide analysis of expression changes but potentially also single-cell transcriptomics to understand the range of different developmental trajectories that may exist in the population as it evolves towards resistance.

4.9.0.0. Future Directions

Several future directions for these studies have already been proposed. However, herein some of the key limitations of the current study and how they could be overcome in the future are summarized. Although several studies have examined the biochemical and cellular mechanisms involved in evading the cytotoxicity of epirubicin and other cytotoxic agents, the clinical relevance of most of these findings remains questionable due to the limitations of the models and assays used. The current study is limited similarly by focussing on cell lines and 2D culture systems and using a narrow range of analytical tools. Utilizing advanced preclinical models such as tumour spheroids, organoids, and patient-derived explant cultures or patient-derived xenograft mouse models would allow more sophisticated analyses that may have closer relevance to patient outcomes. However, a challenge that should be recognized with using patient samples is that they are highly heterogeneous, and a very large number of samples may be required to obtain a result that can be fit into a harmonious model.

Despite their stochastic distribution within tumours, CSCs often reside in the low pH, nutrient-deprived, and hypoxic region of the tumour (Mondal et al. 2018). Localised in this specialised microenvironment, CSCs receive many distinct cellular cues from their niche, contributing to orchestrating therapeutic resistance. Establishing spheroid/organoids models that recapitulate the CSC niche would give a more complete view of the role of stemness in epirubicin resistance. Within the course of this project, several attempts were made to grow MDA-MB-231 cells in an organoid model using Matrigel (Appendix 5.5.0.0); however, these were not wholly successful, and the experiments were curtailed due to lack of time. Using molecular tools to track these cells (such as GFP reporter genes) in 3D organoid models could help understand stem cell dynamics under drug treatment. Ultimately, such spheroid models

should also be complemented with vivo models that mimic physiological conditions more closely, including the processes that control tumour exposure to a systemically delivered drug.

The abundance of stem cells and the stem cell molecular marker profile is distinct in different subtypes of BCa and within functionally variant BCSC subpopulations (Sridharan et al. 2019). Studying different BCa subtypes and different BCSC subpopulations would be valuable. The latter could involve multi-colour flow cytometry to track different BCSC populations with varying marker profiles.

As mentioned above, a complete transcriptomic analysis of epirubicin treated cells would give a more profound insight into diverse processes involved in acquired drug resistance. One process that was not assessed in the current study is the epithelial-mesenchymal transition (EMT). EMT is a dedifferentiation programme that converts adherent epithelial cells to migratory mesenchymal cells (Chou et al. 2015). A link between epithelial-mesenchymal transition (EMT) and BCSC has been suggested where experimental activation of EMT has led to the induction of autocrine signalling loops associated with stemness profile (Park et al. 2019). Blocking these autocrine signals has eliminated the stemness properties from the cells (Shibue & Weinberg 2017). Furthermore, the EMT transcription factor Snail1 has been shown to mediate p53 repression, contributing to cell survival under cytotoxic stress (Ni et al. 2016). The TGF- β signalling pathway that promotes the CSC phenotype has been linked with the expression of EMT transcription factors Twist, Snail1 and Slug (Dongre & Weinberg 2019). A complete transcriptomic analysis would allow changes in EMT pathways to be correlated with changes in the stemness pathways during the acquisition of drug resistance.

In addition to using more clinically relevant model systems and addressing heterogeneity using single-cell level genome-wide analyses, it is also essential to consider that the correlation of mRNA levels with protein expression is often poor (Wegler et al. 2020). Thus, examining changes at the protein level is essential to understand the pathways to drug resistance, including stemness factors. This could be achieved using contemporary proteomics tools. It could also be useful to complement this with metabolomic analyses. This could include direct analysis of epirubicin and its active and inactive metabolites, and also of endogenous cellular metabolites that are linked to cell survival.

Finally, an original aim of this study was to identify whether resistance to epirubicin induced collateral resistance to other drugs. This collateral effect could undermine the efficacy of second-line treatments that may be given if the epirubicin-containing regimen fails. If the long-term epirubicin-selected cell population developed in this study was found to have elevated epirubicin resistance, it would be a relatively simple process to test its sensitivity to other commonly used drugs for TNBC.

BIBLIOGRAPHY

1. Al-Hajj, M, Wicha, MS, Benito-Hernandez, A, Morrison, SJ & Clarke, MF 2003, 'Prospective identification of tumorigenic breast cancer cells', *Proceedings of the National Academy of Sciences*, vol. 100, no. 7, pp. 3983-8.
2. Al-Hussaini, H, Subramanyam, D, Reedijk, M & Sridhar, SS 2011, 'Notch signaling pathway as a therapeutic target in breast cancer', *Molecular cancer therapeutics*, vol. 10, no. 1, pp. 9-15.
3. Alkaraki, A, Alshaer, W, Wehaibi, S, Gharaibeh, L, Abuarqoub, D, Alqudah, DA, Al-Azzawi, H, Zureigat, H, Souleiman, M & Awidi, A 2020, 'Enhancing chemosensitivity of wild-type and drug-resistant MDA-MB-231 triple-negative breast cancer cell line to doxorubicin by silencing of STAT 3, Notch-1, and β -catenin genes', *Breast Cancer*, pp. 1-10.
4. Allain, EP, Rouleau, M, Lévesque, E & Guillemette, C 2020, 'Emerging roles for UDP-glucuronosyltransferases in drug resistance and cancer progression', *British journal of cancer*, vol. 122, no. 9, pp. 1277-87.
5. Allen, KE & Weiss, GJ 2010, 'Resistance may not be futile: microRNA biomarkers for chemoresistance and potential therapeutics', *Molecular cancer therapeutics*, vol. 9, no. 12, pp. 3126-36.
6. Althobiti, M, El Ansari, R, Aleskandarany, M, Joseph, C, Toss, MS, Green, AR & Rakha, EA 2020a, 'The prognostic significance of ALDH1A1 expression in early invasive breast cancer', *Histopathology*, vol. 77, no. 3, pp. 437-48.
7. Arnold, KM, Flynn, NJ & Sims-Mourtada, J 2015, 'Activation of inflammatory responses correlate with hedgehog activation and precede expansion of cancer stem-like cells in an animal model of residual triple negative breast cancer after neoadjuvant chemotherapy', *Cancer studies and molecular medicine: open journal*, vol. 2, no. 2, p. 80.
8. Atalay, C, Demirkazik, A & Gunduz, U 2008, 'Role of ABCB1 and ABCC1 gene induction on survival in locally advanced breast cancer', *Journal of chemotherapy*, vol. 20, no. 6, pp. 734-9.
9. Baguley, BC 2010, 'Multiple drug resistance mechanisms in cancer', *Molecular biotechnology*, vol. 46, no. 3, pp. 308-16.

10. Bao, B & Prasad, AS 2019, 'Targeting CSC in a Most Aggressive Subtype of Breast Cancer TNBC', *Breast Cancer Metastasis and Drug Resistance*, pp. 311-34.
11. Barltrop, JA, Owen, TC, Cory, AH & Cory, JG 1991, '5-(3-carboxymethoxyphenyl)-2-(4, 5-dimethylthiazolyl)-3-(4-sulfophenyl) tetrazolium, inner salt (MTS) and related analogs of 3-(4, 5-dimethylthiazolyl)-2, 5-diphenyltetrazolium bromide (MTT) reducing to purple water-soluble formazans as cell-viability indicators', *Bioorganic & Medicinal Chemistry Letters*, vol. 1, no. 11, pp. 611-4.
12. Battle, E & Clevers, H 2017, 'Cancer stem cells revisited', *Nature medicine*, vol. 23, no. 10, p. 1124.
13. Bellon, JR, Burstein, HJ, Frank, ES, Mittendorf, EA & King, TA 2020, 'Multidisciplinary considerations in the treatment of triple-negative breast cancer', *CA: a cancer journal for clinicians*, vol. 70, no. 6, pp. 432-42.
14. Braunstein, M, Liao, L, Lyttle, N, Lobo, N, Taylor, KJ, Krzyzanowski, PM, Kalatskaya, I, Yao, CQ, Stein, LD & Boutros, PC 2016, 'Downregulation of histone H2A and H2B pathways is associated with anthracycline sensitivity in breast cancer', *Breast Cancer Research*, vol. 18, no. 1, pp. 1-16.
15. Burger, H, Foekens, JA, Look, MP, Meijer-van Gelder, ME, Klijn, JG, Wiemer, EA, Stoter, G & Nooter, K 2003, 'RNA expression of breast cancer resistance protein, lung resistance-related protein, multidrug resistance-associated proteins 1 and 2, and multidrug resistance gene 1 in breast cancer: correlation with chemotherapeutic response', *Clinical cancer research*, vol. 9, no. 2, pp. 827-36.
16. Cailleau, R, Young, R, Olive, M & Reeves Jr, W 1974, 'Breast tumor cell lines from pleural effusions', *Journal of the National Cancer Institute*, vol. 53, no. 3, pp. 661-74.
17. Carlisi, D, De Blasio, A, Drago-Ferrante, R, Di Fiore, R, Buttitta, G, Morreale, M, Scerri, C, Vento, R & Tesoriere, G 2017, 'Parthenolide prevents resistance of MDA-MB231 cells to doxorubicin and mitoxantrone: the role of Nrf2', *Cell death discovery*, vol. 3, no. 1, pp. 1-12.
18. Chang, PM-H, Chen, C-H, Yeh, C-C, Lu, H-J, Liu, T-T, Chen, M-H, Liu, C-Y, Wu, AT, Yang, M-H & Tai, S-K 2018, 'Transcriptome analysis and prognosis of ALDH isoforms in human cancer', *Scientific Reports*, vol. 8, no. 1, pp. 1-10.

19. Chen, C, Zhao, S, Karnad, A & Freeman, JW 2018, 'The biology and role of CD44 in cancer progression: therapeutic implications', *Journal of hematology & oncology*, vol. 11, no. 1, pp. 1-23.
20. Chen, X, Zhong, S-l, Lu, P, Wang, D-d, Zhou, S-y, Yang, S-j, Shen, H-y, Zhang, L, Zhang, X-h & Zhao, J-h 2016, 'miR-4443 participates in the malignancy of breast cancer', *PloS one*, vol. 11, no. 8, p. e0160780.
21. Cheng, C-C, Shi, L-H, Wang, X-J, Wang, S-X, Wan, X-Q, Liu, S-R, Wang, Y-F, Lu, Z, Wang, L-H & Ding, Y 2018, 'Stat3/Oct-4/c-Myc signal circuit for regulating stemness-mediated doxorubicin resistance of triple-negative breast cancer cells and inhibitory effects of WP1066', *International Journal of Oncology*, vol. 53, no. 1, pp. 339-48.
22. Cheng, W-J, Zhang, P-P, Luo, Q-Q, Deng, S-M & Jia, A-Q 2020, 'The chemosensitizer ferulic acid enhances epirubicin-induced apoptosis in MDA-MB-231 cells', *Journal of Functional Foods*, vol. 73, p. 104130.
23. Chittaranjan, S, Bortnik, S, Dragowska, WH, Xu, J, Abeyundara, N, Leung, A, Go, NE, DeVorkin, L, Wepler, SA & Gelmon, K 2014, 'Autophagy inhibition augments the anticancer effects of epirubicin treatment in anthracycline-sensitive and-resistant triple-negative breast cancer', *Clinical cancer research*, vol. 20, no. 12, pp. 3159-73.
24. Chmielecki, J, Foo, J, Oxnard, GR, Hutchinson, K, Ohashi, K, Somwar, R, Wang, L, Amato, KR, Arcila, M & Sos, ML 2011, 'Optimization of dosing for EGFR-mutant non-small cell lung cancer with evolutionary cancer modeling', *Science translational medicine*, vol. 3, no. 90, pp. 90ra59-90ra59.
25. Chomczynski, P & Sacchi, N 1987, 'Single step method of RNA isolation by acid guanidinium thiocyanate-phenol-chloroform extraction *Anal Biochem* 162: 156–159', *Find this article online*.
26. Chou, M-Y, Hu, F-W, Yu, C-H & Yu, C-C 2015, 'Sox2 expression involvement in the oncogenicity and radiochemoresistance of oral cancer stem cells', *Oral oncology*, vol. 51, no. 1, pp. 31-9.
27. Christie, EL, Pattnaik, S, Beach, J, Copeland, A, Rashoo, N, Fereday, S, Hendley, J, Alsop, K, Brady, SL & Lamb, G 2019, 'Multiple ABCB1 transcriptional fusions in drug resistant high-grade serous ovarian and breast cancer', *Nature communications*, vol. 10, no. 1, pp. 1-10.
28. Cioce, M, Gherardi, S, Viglietto, G, Strano, S, Blandino, G, Muti, P & Ciliberto, G 2010, 'Mammosphere-forming cells from breast cancer cell lines as a tool for the

- identification of CSC-like-and early progenitor-targeting drugs', *Cell cycle*, vol. 9, no. 14, pp. 2950-9.
29. D'Angelo, RC, Ouzounova, M, Davis, A, Choi, D, Tchienkam, SM, Kim, G, Luther, T, Quraishi, AA, Senbabaoglu, Y & Conley, SJ 2015, 'Notch reporter activity in breast cancer cell lines identifies a subset of cells with stem cell activity', *Molecular cancer therapeutics*, vol. 14, no. 3, pp. 779-87.
 30. Dagogo-Jack, I & Shaw, AT 2018, 'Tumour heterogeneity and resistance to cancer therapies', *Nature reviews Clinical oncology*, vol. 15, no. 2, p. 81.
 31. De Sousa e Melo, F & Vermeulen, L 2016, 'Wnt signaling in cancer stem cell biology', *Cancers*, vol. 8, no. 7, p. 60.
 32. Dellinger, RW, Matundan, HH, Ahmed, AS, Duong, PH & Meyskens Jr, FL 2012, 'Anti-cancer drugs elicit re-expression of UDP-glucuronosyltransferases in melanoma cells', *PLoS one*, vol. 7, no. 10, p. e47696.
 33. Dongre, A & Weinberg, RA 2019, 'New insights into the mechanisms of epithelial-mesenchymal transition and implications for cancer', *Nature reviews Molecular cell biology*, vol. 20, no. 2, pp. 69-84.
 34. Dontu, G, Abdallah, WM, Foley, JM, Jackson, KW, Clarke, MF, Kawamura, MJ & Wicha, MS 2003, 'In vitro propagation and transcriptional profiling of human mammary stem/progenitor cells', *Genes & development*, vol. 17, no. 10, pp. 1253-70.
 35. Douville, J, Beaulieu, R & Balicki, D 2009, 'ALDH1 as a functional marker of cancer stem and progenitor cells', *Stem cells and development*, vol. 18, no. 1, pp. 17-26.
 36. Eiraku, M, Hirata, Y, Takeshima, H, Hirano, T & Kengaku, M 2002, 'Delta/notch-like epidermal growth factor (EGF)-related receptor, a novel EGF-like repeat-containing protein targeted to dendrites of developing and adult central nervous system neurons', *Journal of Biological Chemistry*, vol. 277, no. 28, pp. 25400-7.
 37. Ejlertsen, B, Mouridsen, HT, Langkjer, ST, Andersen, J, Sjöström, J & Kjaer, M 2004, 'Phase III study of intravenous vinorelbine in combination with epirubicin versus epirubicin alone in patients with advanced breast cancer: a Scandinavian Breast Group Trial (SBG9403)', *Journal of clinical oncology*, vol. 22, no. 12, pp. 2313-20.
 38. Ferlay J, Ervik M, Lam F, Colombet M, Mery L, Piñeros M, Znaor A, Soerjomataram I, Bray F (2020). Global Cancer Observatory: Cancer Today. Lyon, France: International

- Agency for Research on Cancer. Available from: <https://gco.iarc.fr/today>, accessed 1 February 2021.
39. Filipits, M 2004, 'Mechanisms of cancer: multidrug resistance', *Drug Discovery Today: Disease Mechanisms*, vol. 1, no. 2, pp. 229-34.
 40. Fultang, N, Chakraborty, M & Peethambaran, B 2021, 'Regulation of cancer stem cells in triple negative breast cancer', *Cancer Drug Resistance*, vol. 4.
 41. Garcia-Mayea, Y, Mir, C, Masson, F, Paciucci, R & LLeonart, M 2020, 'Insights into new mechanisms and models of cancer stem cell multidrug resistance', in *Seminars in cancer biology*, vol. 60, pp. 166-80.
 42. Gatenby, RA & Brown, JS 2020, 'Integrating evolutionary dynamics into cancer therapy', *Nature reviews Clinical oncology*, vol. 17, no. 11, pp. 675-86.
 43. Genovese, I, Ilari, A, Assaraf, YG, Fazi, F & Colotti, G 2017, 'Not only P-glycoprotein: amplification of the ABCB1-containing chromosome region 7q21 confers multidrug resistance upon cancer cells by coordinated overexpression of an assortment of resistance-related proteins', *Drug resistance updates*, vol. 32, pp. 23-46.
 44. Ginestier, C, Hur, MH, Charafe-Jauffret, E, Monville, F, Dutcher, J, Brown, M, Jacquemier, J, Viens, P, Kleer, CG & Liu, S 2007, 'ALDH1 is a marker of normal and malignant human mammary stem cells and a predictor of poor clinical outcome', *Cell stem cell*, vol. 1, no. 5, pp. 555-67.
 45. Godet, I & Gilkes, DM 2017, 'BRCA1 and BRCA2 mutations and treatment strategies for breast cancer', *Integrative cancer science and therapeutics*, vol. 4, no. 1.
 46. Gonzalez-Angulo, AM, Morales-Vasquez, F & Hortobagyi, GN 2007, 'Overview of resistance to systemic therapy in patients with breast cancer', *Breast cancer chemosensitivity*, pp. 1-22.
 47. Goodison, S, Urquidi, V & Tarin, D 1999, 'CD44 cell adhesion molecules', *Molecular pathology*, vol. 52, no. 4, p. 189.
 48. Group, EBCTC 2012, 'Comparisons between different polychemotherapy regimens for early breast cancer: meta-analyses of long-term outcome among 100 000 women in 123 randomised trials', *The Lancet*, vol. 379, no. 9814, pp. 432-44.

49. Guiu, S, Michiels, S, André, F, Cortes, J, Denkert, C, Di Leo, A, Hennessy, B, Sorlie, T, Sotiriou, C & Turner, N 2012, 'Molecular subclasses of breast cancer: how do we define them? The IMPAKT 2012 Working Group Statement', *Annals of oncology*, vol. 23, no. 12, pp. 2997-3006.
50. Gusterson, BA, Ross, DT, Heath, VJ & Stein, T 2005, 'Basal cytokeratins and their relationship to the cellular origin and functional classification of breast cancer', *Breast Cancer Research*, vol. 7, no. 4, pp. 1-6.
51. Gwak, JM, Kim, M, Kim, HJ, Jang, MH & Park, SY 2017, 'Expression of embryonal stem cell transcription factors in breast cancer: Oct4 as an indicator for poor clinical outcome and tamoxifen resistance', *Oncotarget*, vol. 8, no. 22, p. 36305.
52. Györfy, B, Surowiak, P, Kiesslich, O, Denkert, C, Schäfer, R, Dietel, M & Lage, H 2006, 'Gene expression profiling of 30 cancer cell lines predicts resistance towards 11 anticancer drugs at clinically achieved concentrations', *International journal of cancer*, vol. 118, no. 7, pp. 1699-712.
53. Habib, JG & O'Shaughnessy, JA 2016, 'The hedgehog pathway in triple-negative breast cancer', *Cancer medicine*, vol. 5, no. 10, pp. 2989-3006.
54. Hamburger, AW & Salmon, SE 1977, 'Primary bioassay of human tumor stem cells', *science*, vol. 197, no. 4302, pp. 461-3.
55. Harbeck, N, Penault-Llorca, F, Cortes, J, Gnant, M, Houssami, N, Poortmans, P, Ruddy, K, Tsang, J & Cardoso, F 2019, 'Breast cancer (Primer)', *Nature Reviews: Disease Primers*.
56. He, Y, Zhu, Q, Chen, M, Huang, Q, Wang, W, Li, Q, Huang, Y & Di, W 2016, 'The changing 50% inhibitory concentration (IC50) of cisplatin: A pilot study on the artifacts of the MTT assay and the precise measurement of density-dependent chemoresistance in ovarian cancer', *Oncotarget*, vol. 7, no. 43, p. 70803.
57. Hembruff, SL, Laberge, ML, Villeneuve, DJ, Guo, B, Veitch, Z, Cecchetto, M & Parissenti, AM 2008, 'Role of drug transporters and drug accumulation in the temporal acquisition of drug resistance', *BMC cancer*, vol. 8, no. 1, p. 318.
58. Honeth, G, Bendahl, P-O, Ringnér, M, Saal, LH, Gruberger-Saal, SK, Lövgren, K, Grabau, D, Fernö, M, Borg, Å & Hegardt, C 2008, 'The CD44+/CD24-phenotype is enriched in basal-like breast tumors', *Breast Cancer Research*, vol. 10, no. 3, pp. 1-12.

59. Hu, DG, Nair, PC, Haines, AZ, McKinnon, RA, Mackenzie, PI & Meech, R 2019, 'The UGTome: The expanding diversity of UDP glycosyltransferases and its impact on small molecule metabolism', *Pharmacology & therapeutics*, vol. 204, p. 107414.
60. Hu, DG, Rogers, A & Mackenzie, PI 2014, 'Epirubicin upregulates UDP glucuronosyltransferase 2B7 expression in liver cancer cells via the p53 pathway', *Molecular pharmacology*, vol. 85, no. 6, pp. 887-97.
61. Hu, J, Li, G, Zhang, P, Zhuang, X & Hu, G 2017, 'A CD44v+ subpopulation of breast cancer stem-like cells with enhanced lung metastasis capacity', *Cell Death & Disease*, vol. 8, no. 3, pp. e2679-e.
62. Hu, J, Qin, K, Zhang, Y, Gong, J, Li, N, Lv, D, Xiang, R & Tan, X 2011, 'Downregulation of transcription factor Oct4 induces an epithelial-to-mesenchymal transition via enhancement of Ca²⁺ influx in breast cancer cells', *Biochemical and biophysical research communications*, vol. 411, no. 4, pp. 786-91.
63. Ibiyeye, KM, Zuki, ABZ, Nordin, N & Ajat, M 2019, 'Ultrastructural Changes and Antitumor Effects of Doxorubicin/Thymoquinone-Loaded CaCO₃ Nanoparticles on Breast Cancer Cell Line', *Frontiers in Oncology*, vol. 9, p. 599.
64. Ishiyama, M, Miyazono, Y, Sasamoto, K, Ohkura, Y & Ueno, K 1997, 'A highly water-soluble disulfonated tetrazolium salt as a chromogenic indicator for NADH as well as cell viability', *Talanta*, vol. 44, no. 7, pp. 1299-305.
65. Jang, G-B, Kim, J-Y, Cho, S-D, Park, K-S, Jung, J-Y, Lee, H-Y, Hong, I-S & Nam, J-S 2015, 'Blockade of Wnt/ β -catenin signaling suppresses breast cancer metastasis by inhibiting CSC-like phenotype', *Scientific Reports*, vol. 5, no. 1, pp. 1-15.
66. Justilien, V & Fields, AP 2015, 'Molecular pathways: novel approaches for improved therapeutic targeting of Hedgehog signaling in cancer stem cells', *Clinical cancer research*, vol. 21, no. 3, pp. 505-13.
67. Kadioglu, O, Cao, J, Kosyakova, N, Mrasek, K, Liehr, T & Efferth, T 2016, 'Genomic and transcriptomic profiling of resistant CEM/ADR-5000 and sensitive CCRF-CEM leukaemia cells for unravelling the full complexity of multi-factorial multidrug resistance', *Scientific Reports*, vol. 6, no. 1, pp. 1-18.
68. Kam, Y, Das, T, Tian, H, Foroutan, P, Ruiz, E, Martinez, G, Minton, S, Gillies, RJ & Gatenby, RA 2015, 'Sweat but no gain: inhibiting proliferation of multidrug resistant cancer cells with "ersatzdroges"', *International journal of cancer*, vol. 136, no. 4, pp. E188-E96.

69. Karakaş, D, Ari, F & Ulukaya, E 2017, 'The MTT viability assay yields strikingly false-positive viabilities although the cells are killed by some plant extracts', *Turkish Journal of Biology*, vol. 41, no. 6, pp. 919-25.
70. Khasraw, M, Bell, R & Dang, C 2012, 'Epirubicin: is it like doxorubicin in breast cancer? A clinical review', *The Breast*, vol. 21, no. 2, pp. 142-9.
71. Kida, K, Ishikawa, T, Yamada, A, Shimada, K, Narui, K, Sugae, S, Shimizu, D, Tanabe, M, Sasaki, T & Ichikawa, Y 2016, 'Effect of ALDH1 on prognosis and chemoresistance by breast cancer subtype', *Breast cancer research and treatment*, vol. 156, no. 2, pp. 261-9.
72. Kim, R-J & Nam, J-S 2011, 'OCT4 expression enhances features of cancer stem cells in a mouse model of breast cancer', *Laboratory animal research*, vol. 27, no. 2, p. 147.
73. King, TD, Suto, MJ & Li, Y 2012, 'The wnt/ β -catenin signaling pathway: A potential therapeutic target in the treatment of triple negative breast cancer', *Journal of cellular biochemistry*, vol. 113, no. 1, pp. 13-8.
74. Knowlden, JM, Hutcheson, IR, Jones, HE, Madden, T, Gee, JM, Harper, ME, Barrow, D, Wakeling, AE & Nicholson, RI 2003, 'Elevated levels of epidermal growth factor receptor/c-erbB2 heterodimers mediate an autocrine growth regulatory pathway in tamoxifen-resistant MCF-7 cells', *Endocrinology*, vol. 144, no. 3, pp. 1032-44.
75. Kong, Y, Lyu, N, Wu, J, Tang, H, Xie, X, Yang, L, Li, X, Wei, W & Xie, X 2018, 'Breast cancer stem cell markers CD44 and ALDH1A1 in serum: distribution and prognostic value in patients with primary breast cancer', *Journal of Cancer*, vol. 9, no. 20, p. 3728.
76. Korde, LA, Somerfield, MR, Carey, LA, Crews, JR, Denduluri, N, Hwang, ES, Khan, SA, Loibl, S, Morris, EA & Perez, A 2021, 'Neoadjuvant chemotherapy, endocrine therapy, and targeted therapy for breast cancer: ASCO guideline', *Journal of clinical oncology*, vol. 39, no. 13, pp. 1485-505.
77. Kozovska, Z, Patsalias, A, Bajzik, V, Durinikova, E, Demkova, L, Jargasova, S, Smolkova, B, Plava, J, Kucerova, L & Matuskova, M 2018, 'ALDH1A inhibition sensitizes colon cancer cells to chemotherapy', *BMC cancer*, vol. 18, no. 1, pp. 1-11.
78. Kreso, A, O'Brien, CA, Van Galen, P, Gan, OI, Notta, F, Brown, AM, Ng, K, Ma, J, Wienholds, E & Dunant, C 2013, 'Variable clonal repopulation dynamics influence chemotherapy response in colorectal cancer', *science*, vol. 339, no. 6119, pp. 543-8.

79. Lang, F, Wojcik, B & Rieger, MA 2015, 'Stem cell hierarchy and clonal evolution in acute lymphoblastic leukemia', *Stem Cells International*, vol. 2015.
80. Larsson, P, Engqvist, H, Biermann, J, Rönnerman, EW, Forssell-Aronsson, E, Kovács, A, Karlsson, P, Helou, K & Parris, TZ 2020, 'Optimization of cell viability assays to improve replicability and reproducibility of cancer drug sensitivity screens', *Scientific Reports*, vol. 10, no. 1, pp. 1-12.
81. Leccia, F, Del Vecchio, L, Mariotti, E, Di Noto, R, Morel, A-P, Puisieux, A, Salvatore, F & Ansieau, S 2014, 'ABCG2, a novel antigen to sort luminal progenitors of BRCA1-breast cancer cells', *Molecular cancer*, vol. 13, no. 1, p. 213.
82. Lee, K-L, Kuo, Y-C, Ho, Y-S & Huang, Y-H 2019, 'Triple-negative breast cancer: current understanding and future therapeutic breakthrough targeting cancer stemness', *Cancers*, vol. 11, no. 9, p. 1334.
83. Li, CH, Karantza, V, Aktan, G & Lala, M 2019, 'Current treatment landscape for patients with locally recurrent inoperable or metastatic triple-negative breast cancer: a systematic literature review', *Breast Cancer Research*, vol. 21, no. 1, pp. 1-14.
84. Li, H, Ma, F, Wang, H, Lin, C, Fan, Y, Zhang, X, Qian, H & Xu, B 2013, 'Stem cell marker aldehyde dehydrogenase 1 (ALDH1)-expressing cells are enriched in triple-negative breast cancer', *The International journal of biological markers*, vol. 28, no. 4, pp. 357-64.
85. Liu, F-S 2009, 'Mechanisms of chemotherapeutic drug resistance in cancer therapy—a quick review', *Taiwanese Journal of Obstetrics and Gynecology*, vol. 48, no. 3, pp. 239-44.
86. Liu, P, Tang, H, Song, C, Wang, J, Chen, B, Huang, X, Pei, X & Liu, L 2018, 'SOX2 promotes cell proliferation and metastasis in triple negative breast cancer', *Frontiers in pharmacology*, vol. 9, p. 942.
87. Liu, S, Dontu, G, Mantle, ID, Patel, S, Ahn, N-s, Jackson, KW, Suri, P & Wicha, MS 2006, 'Hedgehog signaling and Bmi-1 regulate self-renewal of normal and malignant human mammary stem cells', *Cancer research*, vol. 66, no. 12, pp. 6063-71.
88. Livak, KJ & Schmittgen, TD 2001, 'Analysis of relative gene expression data using real-time quantitative PCR and the $2^{-\Delta\Delta CT}$ method', *methods*, vol. 25, no. 4, pp. 402-8.

89. Lombardo, Y, de Giorgio, A, Coombes, CR, Stebbing, J & Castellano, L 2015, 'Mammosphere formation assay from human breast cancer tissues and cell lines', *Journal of visualized experiments: JoVE*, no. 97.
90. Lundin, A, Hasenson, M, Persson, J & Pousette, Å 1986, '[4] Estimation of biomass in growing cell lines by adenosine triphosphate assay', *Methods in enzymology*, vol. 133, pp. 27-42.
91. Ma, F, Li, H, Wang, H, Shi, X, Fan, Y, Ding, X, Lin, C, Zhan, Q, Qian, H & Xu, B 2014, 'Enriched CD44+/CD24- population drives the aggressive phenotypes presented in triple-negative breast cancer (TNBC)', *Cancer letters*, vol. 353, no. 2, pp. 153-9.
92. Mamaeva, V, Niemi, R, Beck, M, Özliseli, E, Desai, D, Landor, S, Gronroos, T, Kronqvist, P, Pettersen, IK & McCormack, E 2016, 'Inhibiting notch activity in breast cancer stem cells by glucose functionalized nanoparticles carrying γ -secretase inhibitors', *Molecular Therapy*, vol. 24, no. 5, pp. 926-36.
93. Mansoori, B, Mohammadi, A, Davudian, S, Shirjang, S & Baradaran, B 2017, 'The different mechanisms of cancer drug resistance: a brief review', *Advanced pharmaceutical bulletin*, vol. 7, no. 3, p. 339.
94. Mayer, EL & Burstein, HJ 2016, 'Chemotherapy for triple-negative breast cancer: is more better?', *Journal of clinical oncology: official journal of the American Society of Clinical Oncology*, vol. 34, no. 28, pp. 3369-71.
95. Medrano-González, PA, Rivera-Ramírez, O, Montañó, LF & Rendón-Huerta, EP 2021, 'Proteolytic Processing of CD44 and Its Implications in Cancer', *Stem Cells International*, vol. 2021.
96. Meech, R, Hu, DG, McKinnon, RA, Mubarakah, SN, Haines, AZ, Nair, PC, Rowland, A & Mackenzie, PI 2019, 'The UDP-glycosyltransferase (UGT) superfamily: new members, new functions, and novel paradigms', *Physiological reviews*, vol. 99, no. 2, pp. 1153-222.
97. Metz, EP & Rizzino, A 2019, 'Sox2 dosage: A critical determinant in the functions of Sox2 in both normal and tumor cells', *Journal of cellular physiology*, vol. 234, no. 11, pp. 19298-306.
98. Milani, M, Venturini, S, Bonardi, S, Allevi, G, Strina, C, Cappelletti, MR, Corona, SP, Aguggini, S, Bottini, A & Berruti, A 2017, 'Hypoxia-related biological markers as predictors of epirubicin-based treatment responsiveness and resistance in locally advanced breast cancer', *Oncotarget*, vol. 8, no. 45, p. 78870.

99. Mohammed, F, Rashid-Doubell, F, Taha, S, Cassidy, S & Fredericks, S 2020, 'Effects of curcumin complexes on MDA-MB-231 breast cancer cell proliferation', *International Journal of Oncology*, vol. 57, no. 2, pp. 445-55.
100. Mohiuddin, IS, Wei, S-J & Kang, MH 2020, 'Role of OCT4 in cancer stem-like cells and chemotherapy resistance', *Biochimica et Biophysica Acta (BBA)-Molecular Basis of Disease*, vol. 1866, no. 4, p. 165432.
101. Mondal, S, Bhattacharya, K & Mandal, C 2018, 'Nutritional stress reprograms dedifferentiation in glioblastoma multiforme driven by PTEN/Wnt/Hedgehog axis: a stochastic model of cancer stem cells', *Cell death discovery*, vol. 4, no. 1, pp. 1-16.
102. Monteiro, J, Gaspar, C, Richer, W, Franken, PF, Sacchetti, A, Joosten, R, Idali, A, Brandao, J, Decraene, C & Fodde, R 2014, 'Cancer stemness in Wnt-driven mammary tumorigenesis', *Carcinogenesis*, vol. 35, no. 1, pp. 2-13.
103. Moore, N, Houghton, J & Lyle, S 2012, 'Slow-cycling therapy-resistant cancer cells', *Stem cells and development*, vol. 21, no. 10, pp. 1822-30.
104. Mosmann, T 1983, 'Rapid colorimetric assay for cellular growth and survival: application to proliferation and cytotoxicity assays', *Journal of immunological methods*, vol. 65, no. 1-2, pp. 55-63.
105. Mukherjee, P, Gupta, A, Chattopadhyay, D & Chatterji, U 2017, 'Modulation of SOX2 expression delineates an end-point for paclitaxel-effectiveness in breast cancer stem cells', *Scientific Reports*, vol. 7, no. 1, pp. 1-16.
106. Munson, ME 2010, 'An improved technique for calculating relative response in cellular proliferation experiments', *Cytometry Part A*, vol. 77, no. 10, pp. 909-10.
107. Najafi, M, Mortezaee, K & Majidpoor, J 2019, 'Cancer stem cell (CSC) resistance drivers', *Life sciences*, vol. 234, p. 116781.
108. Nam, K, Oh, S, Lee, K-m, Yoo, S-a & Shin, I 2015, 'CD44 regulates cell proliferation, migration, and invasion via modulation of c-Src transcription in human breast cancer cells', *Cellular signalling*, vol. 27, no. 9, pp. 1882-94.

109. Ni, T, Li, X-Y, Lu, N, An, T, Liu, Z-P, Fu, R, Lv, W-C, Zhang, Y-W, Xu, X-J & Rowe, RG 2016, 'Snail1-dependent p53 repression regulates expansion and activity of tumour-initiating cells in breast cancer', *Nature cell biology*, vol. 18, no. 11, pp. 1221-32.
110. Nielsen, D, Dombernowsky, P, Larsen, SK, Hansen, OP & Skovsgaard, T 2000, 'Epirubicin or epirubicin and cisplatin as first-line therapy in advanced breast cancer. A phase III study', *Cancer chemotherapy and pharmacology*, vol. 46, no. 6, pp. 459-66.
111. Nowell, PC 1976, 'The clonal evolution of tumor cell populations', *science*, vol. 194, no. 4260, pp. 23-8.
112. Ormrod, D, Holm, K, Goa, K & Spencer, C 1999, 'Epirubicin: A Review of its Efficacy as Adjuvant Therapy and in the Treatment of Metastatic Disease in Breast Cancer', *Drugs Aging*, vol. 15, no. 5, pp. 389-416.
113. Park, S-Y, Choi, J-H & Nam, J-S 2019, 'Targeting cancer stem cells in triple-negative breast cancer', *Cancers*, vol. 11, no. 7, p. 965.
114. Peng, J, Wang, Z, Li, Y, Lv, D, Zhao, X, Gao, J & Teng, H 2020, 'Identification of differential gene expression related to epirubicin-induced cardiomyopathy in breast cancer patients', *Human & experimental toxicology*, vol. 39, no. 4, pp. 393-401.
115. Perou, CM, Sørlie, T, Eisen, MB, Van De Rijn, M, Jeffrey, SS, Rees, CA, Pollack, JR, Ross, DT, Johnsen, H & Akslen, LA 2000, 'Molecular portraits of human breast tumours', *Nature*, vol. 406, no. 6797, pp. 747-52.
116. Pfeiffer, RM, Webb-Vargas, Y, Wheeler, W & Gail, MH 2018, 'Proportion of US trends in breast cancer incidence attributable to long-term changes in risk factor distributions', *Cancer Epidemiology and Prevention Biomarkers*, vol. 27, no. 10, pp. 1214-22.
117. Plosker, GL & Faulds, D 1993, 'Epirubicin', *Drugs*, vol. 45, no. 5, pp. 788-856.
118. Prat, A, Parker, JS, Karginova, O, Fan, C, Livasy, C, Herschkowitz, JI, He, X & Perou, CM 2010, 'Phenotypic and molecular characterization of the claudin-low intrinsic subtype of breast cancer', *Breast Cancer Research*, vol. 12, no. 5, pp. 1-18.
119. Rabinovich, I, Sebastião, APM, Lima, RS, de Andrade Urban, C, Schunemann Jr, E, Anselmi, KF, Elifio-Esposito, S, De Noronha, L & Moreno-Amaral, AN 2018, 'Cancer stem cell markers ALDH1 and CD44+/CD24–phenotype and their prognosis impact in invasive ductal carcinoma', *European journal of histochemistry: EJH*, vol. 62, no. 3.

120. Raha, D, Wilson, TR, Peng, J, Peterson, D, Yue, P, Evangelista, M, Wilson, C, Merchant, M & Settleman, J 2014, 'The cancer stem cell marker aldehyde dehydrogenase is required to maintain a drug-tolerant tumor cell subpopulation', *Cancer research*, vol. 74, no. 13, pp. 3579-90.
121. Reed, K, Hembruff, S, Sprowl, J & Parissenti, A 2010, 'The temporal relationship between ABCB1 promoter hypomethylation, ABCB1 expression and acquisition of drug resistance', *The pharmacogenomics journal*, vol. 10, no. 6, pp. 489-504.
122. Robert, J & Bui, N 1992, 'Pharmacokinetics and metabolism of epirubicin administered as iv bolus and 48-h infusion in patients with advanced soft-tissue sarcoma', *Annals of oncology*, vol. 3, no. 8, pp. 651-6.
123. Rodrigues, MFSD, Xavier, FCdA, Andrade, NP, Lopes, C, Miguita Luiz, L, Sedassari, BT, Ibarra, AMC, López, RVM, Kliemann Schmerling, C & Moyses, RA 2018, 'Prognostic implications of CD44, NANOG, OCT4, and BMI1 expression in tongue squamous cell carcinoma', *Head & neck*, vol. 40, no. 8, pp. 1759-73.
124. Saito, S-Y & Takeshima, H 2006, 'DNER as key molecule for cerebellar maturation', *The Cerebellum*, vol. 5, no. 3, pp. 227-31.
125. Saygin, C, Wiechert, A, Rao, VS, Alluri, R, Connor, E, Thiagarajan, PS, Hale, JS, Li, Y, Chumakova, A & Jarrar, A 2017, 'CD55 regulates self-renewal and cisplatin resistance in endometrioid tumors', *Journal of Experimental Medicine*, vol. 214, no. 9, pp. 2715-32.
126. Schaefer, T & Lengerke, C 2020, 'SOX2 protein biochemistry in stemness, reprogramming, and cancer: the PI3K/AKT/SOX2 axis and beyond', *Oncogene*, vol. 39, no. 2, pp. 278-92.
127. Schmid, P, Cortes, J, Puztai, L, McArthur, H, Kümmel, S, Bergh, J, Denkert, C, Park, YH, Hui, R & Harbeck, N 2020, 'Pembrolizumab for early triple-negative breast cancer', *New England journal of medicine*, vol. 382, no. 9, pp. 810-21.
128. Sen, U, Gowda, A, Rachamalla, HK, Banerjee, R, Shenoy, S & Bose, B 2021, 'Significance of Oct-4 transcription factor as a pivotal therapeutic target for CD44+/24-mammary tumour initiating cells; aiming at the root of the recurrence', *bioRxiv*.
129. Shaw, FL, Harrison, H, Spence, K, Ablett, MP, Simões, BM, Farnie, G & Clarke, RB 2012, 'A detailed mammosphere assay protocol for the quantification of breast stem cell activity', *Journal of mammary gland biology and neoplasia*, vol. 17, no. 2, pp. 111-7.

130. Sheridan, C, Kishimoto, H, Fuchs, RK, Mehrotra, S, Bhat-Nakshatri, P, Turner, CH, Goulet, R, Badve, S & Nakshatri, H 2006, 'CD44+/CD24-breast cancer cells exhibit enhanced invasive properties: an early step necessary for metastasis', *Breast Cancer Research*, vol. 8, no. 5, pp. 1-13.
131. Shibata, M & Hoque, MO 2019, 'Targeting cancer stem cells: a strategy for effective eradication of cancer', *Cancers*, vol. 11, no. 5, p. 732.
132. Shibue, T & Weinberg, RA 2017, 'EMT, CSCs, and drug resistance: the mechanistic link and clinical implications', *Nature reviews Clinical oncology*, vol. 14, no. 10, p. 611.
133. Siddharth, S, Goutam, K, Das, S, Nayak, A, Nayak, D, Sethy, C, Wyatt, MD & Kundu, CN 2017, 'Nectin-4 is a breast cancer stem cell marker that induces WNT/ β -catenin signaling via Pi3k/Akt axis', *The international journal of biochemistry & cell biology*, vol. 89, pp. 85-94.
134. Siegel, RL, Miller, KD & Jemal, A 2020, 'Cancer statistics, 2020', *CA Cancer J Clin*, vol. 70, no. 1, pp. 7-30.
135. Spiess, A-N & Neumeyer, N 2010, 'An evaluation of R² as an inadequate measure for nonlinear models in pharmacological and biochemical research: a Monte Carlo approach', *BMC pharmacology*, vol. 10, no. 1, pp. 1-11.
136. Spoerri, L, Beaumont, KA, Anfosso, A & Haass, NK 2017, 'Real-time cell cycle imaging in a 3D cell culture model of melanoma', in *3D Cell Culture*, Springer, pp. 401-16.
137. Sridharan, S, Howard, CM, Tilley, A, Subramaniyan, B, Tiwari, AK, Ruch, RJ & Raman, D 2019, 'Novel and alternative targets against breast cancer stemness to combat chemoresistance', *Frontiers in Oncology*, vol. 9, p. 1003.
138. Sung, H, Ferlay, J, Siegel, RL, Laversanne, M, Soerjomataram, I, Jemal, A & Bray, F 2021, 'Global cancer statistics 2020: GLOBOCAN estimates of incidence and mortality worldwide for 36 cancers in 185 countries', *CA: a cancer journal for clinicians*, vol. 71, no. 3, pp. 209-49.
139. Symmans, WF, Wei, C, Gould, R, Yu, X, Zhang, Y, Liu, M, Walls, A, Bousamra, A, Ramineni, M & Sinn, B 2017, 'Long-term prognostic risk after neoadjuvant chemotherapy associated with residual cancer burden and breast cancer subtype', *Journal of clinical oncology*, vol. 35, no. 10, p. 1049.

140. Tarpgaard, LS, Qvortrup, C, Nielsen, SL, Stenvang, J, Detlefsen, S, Brünner, N & Pfeiffer, P 2021, 'New use for old drugs: Epirubicin in colorectal cancer', *Acta Oncologica*, pp. 1-3.
141. Toledo-Guzmán, ME, Hernandez, MI, Gómez-Gallegos, AA & Ortiz-Sánchez, E 2019, 'ALDH as a Stem Cell Marker in Solid Tumors', *Current stem cell research & therapy*, vol. 14, no. 5, pp. 375-88.
142. Tomita, H, Tanaka, K, Tanaka, T & Hara, A 2016, 'Aldehyde dehydrogenase 1A1 in stem cells and cancer', *Oncotarget*, vol. 7, no. 10, p. 11018.
143. Trudeau, M, Sinclair, S & Clemons, M 2005, 'Neoadjuvant taxanes in the treatment of non-metastatic breast cancer: a systematic review', *Cancer treatment reviews*, vol. 31, no. 4, pp. 283-302.
144. Tse, T, Sehdev, S, Seely, J, Gravel, DH, Clemons, M, Cordeiro, E & Arnaout, A 2021, 'Neoadjuvant Chemotherapy in Breast Cancer: Review of the Evidence and Conditions That Facilitated Its Use during the Global Pandemic', *Current Oncology*, vol. 28, no. 2, pp. 1338-47.
145. Viale, G 2012, 'The current state of breast cancer classification', *Annals of oncology*, vol. 23, pp. x207-x10.
146. Von Minckwitz, G, Untch, M, Blohmer, J-U, Costa, SD, Eidtmann, H, Fasching, PA, Gerber, B, Eiermann, W, Hilfrich, J & Huober, J 2012, 'Definition and impact of pathologic complete response on prognosis after neoadjuvant chemotherapy in various intrinsic breast cancer subtypes', *J Clin Oncol*, vol. 30, no. 15, pp. 1796-804.
147. Wahba, HA & El-Hadaad, HA 2015, 'Current approaches in treatment of triple-negative breast cancer', *Cancer biology & medicine*, vol. 12, no. 2, p. 106.
148. Wang, L, Wu, Q, Li, Z, Sun, S, Yuan, J, Li, J, Zhang, Y, Yu, D, Wang, C & Sun, S 2019, 'Delta/notch-like epidermal growth factor-related receptor promotes stemness to facilitate breast cancer progression', *Cellular signalling*, vol. 63, p. 109389.
149. Wang, M-L, Chiou, S-H & Wu, C-W 2013, 'Targeting cancer stem cells: emerging role of Nanog transcription factor', *OncoTargets and therapy*, vol. 6, p. 1207.

150. Wang, R, Lv, Q, Meng, W, Tan, Q, Zhang, S, Mo, X & Yang, X 2014, 'Comparison of mammosphere formation from breast cancer cell lines and primary breast tumors', *Journal of thoracic disease*, vol. 6, no. 6, p. 829.
151. Wang, X, Zhang, H & Chen, X 2019, 'Drug resistance and combating drug resistance in cancer', *Cancer Drug Resistance*, vol. 2, no. 2, pp. 141-60.
152. Wang, Z, Li, Z, Wu, Q, Li, C, Li, J, Zhang, Y, Wang, C, Sun, S & Sun, S 2020, 'DNER promotes epithelial–mesenchymal transition and prevents chemosensitivity through the Wnt/ β -catenin pathway in breast cancer', *Cell Death & Disease*, vol. 11, no. 8, pp. 1-16.
153. Ward, MC, Vicini, F, Al-Hilli, Z, Chadha, M, Abraham, A, Recht, A, Hayman, J, Thaker, N, Khan, AJ & Keisch, M 2021, 'Cost-Effectiveness Analysis of No Adjuvant Therapy Versus Partial Breast Irradiation Alone Versus Combined Treatment for Treatment of Low-Risk DCIS: A Microsimulation', *JCO oncology practice*, p. OP. 20.00992.
154. Ween, M, Armstrong, M, Oehler, M & Ricciardelli, C 2015, 'The role of ABC transporters in ovarian cancer progression and chemoresistance', *Critical reviews in oncology/hematology*, vol. 96, no. 2, pp. 220-56.
155. Wegler, C, Ölander, M, Wiśniewski, JR, Lundquist, P, Zettl, K, Åsberg, A, Hjelmæsæth, J, Andersson, TB & Artursson, P 2020, 'Global variability analysis of mRNA and protein concentrations across and within human tissues', *NAR Genomics and Bioinformatics*, vol. 2, no. 1, p. lqz010.
156. Wren, BG 2007, 'The origin of breast cancer', *Menopause*, vol. 14, no. 6, pp. 1060-8.
157. Xiao, Y-S, Zeng, D, Liang, Y-K, Wu, Y, Li, M-F, Qi, Y-Z, Wei, X-L, Huang, W-H, Chen, M & Zhang, G-J 2019, 'Major vault protein is a direct target of Notch1 signaling and contributes to chemoresistance in triple-negative breast cancer cells', *Cancer letters*, vol. 440, pp. 156-67.
158. Xu, X, Zhang, L, He, X, Zhang, P, Sun, C, Xu, X, Lu, Y & Li, F 2018, 'TGF- β plays a vital role in triple-negative breast cancer (TNBC) drug-resistance through regulating stemness, EMT and apoptosis', *Biochemical and biophysical research communications*, vol. 502, no. 1, pp. 160-5.
159. Yang, L, Shi, P, Zhao, G, Xu, J, Peng, W, Zhang, J, Zhang, G, Wang, X, Dong, Z & Chen, F 2020, 'Targeting cancer stem cell pathways for cancer therapy', *Signal transduction and targeted therapy*, vol. 5, no. 1, pp. 1-35.

160. Yousefnia, S, Ghaedi, K, Seyed Forootan, F & Nasr Esfahani, MH 2019, 'Characterization of the stemness potency of mammospheres isolated from the breast cancer cell lines', *Tumor Biology*, vol. 41, no. 8, p. 1010428319869101.
161. Zhang, J-M, Wei, K & Jiang, M 2018, 'OCT4 but not SOX2 expression correlates with worse prognosis in surgical patients with triple-negative breast cancer', *Breast Cancer*, vol. 25, no. 4, pp. 447-55.
162. Zhang, M, Lee, AV & Rosen, JM 2017, 'The cellular origin and evolution of breast cancer', *Cold Spring Harbor perspectives in medicine*, vol. 7, no. 3, p. a027128.
163. Zhang, M, Mathur, A, Zhang, Y, Xi, S, Atay, S, Hong, JA, Datrice, N, Upham, T, Kemp, CD & Ripley, RT 2012, 'Mithramycin represses basal and cigarette smoke-induced expression of ABCG2 and inhibits stem cell signaling in lung and esophageal cancer cells', *Cancer research*, vol. 72, no. 16, pp. 4178-92.
164. Zhang, X, Powell, K & Li, L 2020, 'Breast Cancer Stem Cells: Biomarkers, Identification and Isolation Methods, Regulating Mechanisms, Cellular Origin, and Beyond', *Cancers*, vol. 12, no. 12, p. 3765.
165. Zhao, G, Wang, X, Qu, L, Zhu, Z, Hong, J, Hou, H, Li, Z, Wang, J & Lv, Z 2021, 'The Clinical and Molecular Characteristics of Sex-Determining Region Y-Box 2 and its Prognostic Value in Breast Cancer: A Systematic Meta-Analysis', *Breast Care*, vol. 16, no. 1, pp. 16-26.
166. Zhong, S, Chen, X, Wang, D, Zhang, X, Shen, H, Yang, S, Lv, M, Tang, J & Zhao, J 2016, 'MicroRNA expression profiles of drug-resistance breast cancer cells and their exosomes', *Oncotarget*, vol. 7, no. 15, p. 19601.
167. Zhou, H-M, Zhang, J-G, Zhang, X & Li, Q 2021, 'Targeting cancer stem cells for reversing therapy resistance: mechanism, signaling, and prospective agents', *Signal transduction and targeted therapy*, vol. 6, no. 1, pp. 1-17.
168. Zhou, J, Chen, Q, Zou, Y, Chen, H, Qi, L & Chen, Y 2019, 'Stem cells and cellular origins of breast cancer: updates in rationale, controversies and therapeutic implications', *Frontiers in Oncology*, vol. 9, p. 820.

APPENDICES

5.1.0.0. Material, Equipment and Software Tools Utilised in This Study

Table 5.1. The Composition of the Reagents and Buffers used in this study

<p>DMEM Media Sodium Pyruvate 5% 100 x MEM Non-essential amino acids 5% 10,000 units/mL Pen Strep 5 ml</p> <p>DMSO Freezing Media DMSO 90% FBS 10%</p> <p>1 x Phosphate Buffered Saline (PBS) NaCl 137mM Na₂HPO₄ 10 mM KCL 2.7 mM KH₂PO₄ 2 mM pH 7.4</p>	<p>Mammosphere Media SF DMEM/F12 B27 Supplement 1 x hEGF 20ng/ml bFGF 10ng/ml ITS 1 x</p> <p>MTT Solvent NP40 0.1% 4 mM HCL In Isopropanol</p>
---	--

Table 5.2. Equipment's and Apparatus Used in this Study

Equipment's/ Apparatus	Manufacturer
Rotor- Gene 3000	Corbett Research
Rotor- Gene 6000	Corbett Research
NanoDrop™ 2000 spectrophotometer	Thermo Fisher Scientific™
DNA Thermal Cycler 480	Perkin Elmer
CKX53 Cell Culture Microscope	Olympus (United States)
Laminar Floor Hoods	AES Environment/ Gelman Sciences
Bio-safety Cabinet	Labconco

Haemocytometer	Hausser Scientific
Pipettors (P2, P20, P200, P1000)	Gilson
pH Meter	Hanna Instruments
Pipette Controllers	Thermo Fisher Scientific™
EVOS® FL Cell Imaging Microscope	Thermo Fisher Scientific™
Multi-channel Pipettor	
Fume Hood	
Centrifuge	
CO2 Thermoregulatory Incubator	SANYO
-70oC Freezer	Kelvinator (Series 100)
Liquid Nitrogen Freezer	
Orbital Shaker	Thermo Fisher Scientific™

Table 5.3. Consumables used in this study

Consumable	Manufacturer
Nunc™ EasYFlask™ Cell Culture Flasks with filter cap (25 cm ² , 75 cm ²)	Thermo Fisher Scientific™
Nunc™ Cell-Culture Treated Multi-dishes (6 wells, 24 wells, 96 wells)	Thermo Fisher Scientific™
Cryo Tubes (1 ml)	Sigma-Aldrich
PCR Tubes (0.1 ml)	Corning® Axygen®
Serological Pipettes (2 ml, 5 ml, 10 ml, 25 ml)	Sarstedt, South Australia
Centrifuge Tubes (10 ml, 15 ml, 50 ml)	Sarstedt, South Australia
Micro Tubes (0.5 ml, 1.5 ml)	Sarstedt, South Australia
Syringes and needles	BD
Sterile aerosol barrier tips 10 µl, 200 µl, 1250 µl	Interpath, Victoria, Australia

Pasteur Pipettes	Adelab Scientific, South Australia
Sterile Filter 0.22 µm	Pall Australia, Victoria, Australia
High Absorbency Sheet Protector	Halyard Health, New South Wales, Australia

Table 5.4. Oligonucleotides used in mRNA quantification

Gene	Accession No	Primer	Sequence (5' → 3')
House Keeping Genes			
<i>18S</i>	M10098.1	Forward	CGATGCTCTTAGCTGAGTGT
		Reverse	GGTCCAAGAATTTACCTCT
Stemness Markers			
<i>ALDH1A1</i>	NM_000689.5	Forward	TAAGCATCTCCTTACAGTCAC
		Reverse	TGTTAAGTACTTCAAGAGTCAC
<i>CD44</i>	NM_000610.4	Forward	GACACCATGGACAAGTTTTGG
		Reverse	CGGCAGGTTATATTCAAATCG
<i>OCT4</i>	KY781166.1	Forward	GAAACCCACACTGCAGATCA
		Reverse	CGGTTACAGAACCACACTCG
<i>SOX2</i>	NM_003106.4	Forward	GCTAGTCTCCAAGCGACGAA
		Reverse	GCAAGAAGCCTCTCCTTGAA
<i>DNER</i>	NM_139072.4	Forward	ACCACGAAGCCGTCAGAG
		Reverse	ATCGTATTCTTCACAGAAAGTACCC
ABC Transporters			
<i>ABCB1</i>	NM_001348946.2	Forward	GCCATCAGTCCTGTTCTTGG
		Reverse	GCTTTTGCATACGCTAAGAGTTC
<i>ABCC1</i>	NM_004996.4	Forward	Not Available
		Reverse	Not Available
<i>ABCG2</i>	NM_004827.3	Forward	TGCAACAGGAAACAATCCTTGT
		Reverse	GATCGATGCCCTGCTTACC
UGT Enzymes			
UGT2B7	NM_001074	Forward	AGTTGGAGAATTTTCATCATGCAACAGA
		Reverse	TCAGCCAGCAGCTCACCACAGGG

UGT2B10	NM_001075	Forward	TGACATCGTTTTTGCAGATGCTTA
		Reverse	CAGGTACATAGGAAGGAGGGAA
UGT2B15	NM_001076.3	Forward	GTGTTGGGAATATTATGACTACAGTAAC
		Reverse	TCAGCCAGCAGCTCACACAGGG

Table 5.5. Software Tools Used in the Study

Software	Application in the study
Microsoft Excel 2010	Calculation of fold increase in the RT qPCR results and T-test analysis
NanoDrop 2000 software 1.6	Determination of preliminary nucleic acid concentrations in the samples
Rotor-Gene 6000 Series Software 1.7	Analysing Rt qPCR results
GraphPad Prism 9.1.2.	IC50 Determination
SoftMax Pro 7	Plate reading in the proliferation assay
EVOS FL Auto 2 Software 2.0.2094.0	Cell cultures and mammosphere imaging

5.2.0.0. Methods Elaborated

5.2.1.0. Estimation of RNA Yield and the Purity using the NanoDrop™ 2000 Spectrophotometer

The NanoDrop™ 2000 spectrophotometer (Thermo Scientific™) was used to determine the RNA concentration and the purity prior to cDNA synthesis. The system was initialised by blanking the instrument with nuclease-free water (1µl). Samples were measured after selecting RNA settings in the NanoDrop 2000 software 1.6.

5.2.2.0. Establishment of the Standard Curve for the MTT Assay

Serial diluted MDA-MB-231 cells were seeded in quadruplicates in a transparent 96 well plate. The following steps were carried out as given in the MTT assay protocol (Methods 2.4.7.0). A

background control, Media (200 μ l) + MTT solution (20 μ l) + MTT solvent (150 μ l) was incorporated in the standard curve readings to avoid the background generated from the serum and the phenol red present in the media. Next, the culture medium background was subtracted from the assay reading to obtain the corrected absorbance. Data from three biological replicates were used to establish the standard curve below.

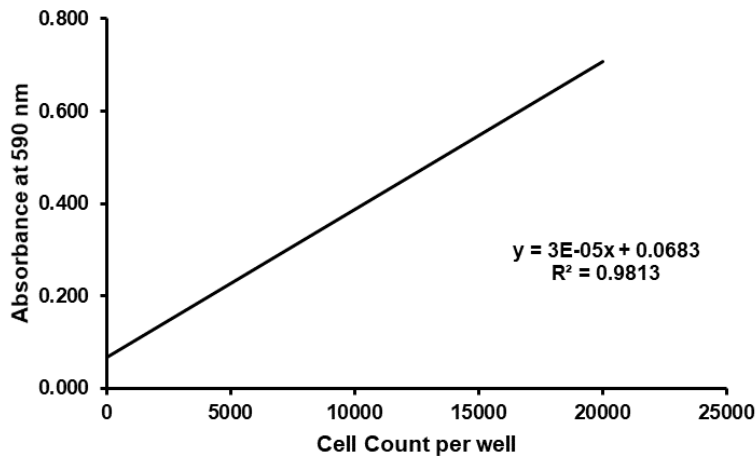


Figure 5.1. Standard Curve for the MTT Assay

5.3.0.0. Calculations

5.3.1.0. Cell Seeding At Specific Densities

Seeding a six well plate with 6.25×10^5 cells per well in 2 ml DMEM was achieved using a haemocytometer for counting and then appropriate dilution as defined in the example below.

Example: Average cell count of 16 small squares in the haemocytometer= 55

Cell density in the cell suspension= 5.5×10^5 cells per ml

Required Amount of cells= 6.25×10^5 cells per well x 7 wells in (7 x 2= 14 ml DMEM).

$$\begin{aligned} \text{Required cell suspension volume} &= \frac{6.25 \times 10^5 \times 7}{5.5 \times 10^5} \\ &= 8 \text{ ml} \end{aligned}$$

8 mls from cells suspension should be diluted with 6 ml (14 ml -8 ml = 6 ml) media.

5.3.2.0. Treating a Six Well Plate With Epirubicin

Control: 0.1% Ethanol (vehicle) in 2 ml DMEM in each well

Required media volume with ethanol = (2 ml x 2) + 1 ml extra = 5 ml

Ethanol volume = 5 ml x 0.1% = 5 μ l

A volume of 5 ml DMEM was combined with 5 μ l 100% ethanol. Media in two wells of the six-well plate replaced was with 2 ml of vehicle-containing DMEM.

Treatment 1: 250 nM epirubicin in 2 ml DMEM in each well

Required media volume with ethanol = (2 ml x 2) + 1 ml extra = 5 ml

Concentration of epirubicin stock solution = 50 μ M

$$C_1 \times V_1 = C_2 \times V_2$$

$$(250 \text{ nM} \times 10^{-3}) \times (5 \text{ ml} \times 1 \times 10^3) = 50 \text{ } \mu\text{M} \times V_2$$

$$V_2 = 25 \text{ } \mu\text{l}$$

A volume of 25 μ l from the 50 μ M epirubicin stock solution was added to 5 ml DMEM making 250 nM epirubicin solution. Media in two wells of the six-well plate was replaced with 2 ml of drug-containing DMEM for each.

Epirubicin treatments at 100, 200, and 500 nM concentrations were carried out in a similar way.

5.3.3.0. Calculation of RNA Input Volume for Dnase Treatment

Example: 250 nM epirubicin treated cells with 800 ng/μL mRNA concentration

$$\begin{aligned}\text{RNA Volume to obtain } 5 \mu\text{g of mRNA} &= \frac{5 \mu\text{g} \times 1000}{800 \text{ ng}/\mu\text{L}} \\ &= 6.25 \mu\text{L}\end{aligned}$$

A volume of 6.25 μL mRNA solution was diluted in 10.25 μL (16.5 μL – 6.25 μL) nuclease free water.

5.3.4.0. Delta Delta Calculation of the Gene Expression Fold Change

$$\begin{aligned}\text{Average Ct Value} &= \frac{\text{Ct Rep1} + \text{Ct Rep2}}{\text{Number of Replicates}} \\ &= \frac{22.28 + 22.51}{2} \\ &= 22.40\end{aligned}$$

$$\begin{aligned}\Delta\text{Ct value} &= \text{Average Ct value} - \text{Average 18S Ct value} \\ &= 22.40 - 7.20 \\ &= 15.2\end{aligned}$$

Fold Change in Expression (Relative to the vehicle treated)

$$\begin{aligned}&= \frac{\text{Power}(2, -[\Delta\text{Ct value}])}{\text{Power}(2, -[\Delta\text{Ct value of the control}])} \\ &= \frac{\text{Power}(2, -15.2)}{\text{Power}(2, -18.3)} \\ &= 8.57\end{aligned}$$

5.3.5.0. Calculation of the Mammosphere formation Efficiency

Mammosphere Formation Efficiency

$$= \frac{\text{Average Number of Mammospheres Formed per Well}}{\text{Original Number of Cells Seeded per Well}} \times 100\%$$

$$= \frac{33}{4000} \times 100\%$$

$$= 0.82\%$$

5.3.6.0. Calculation of the Proliferation Index

Example: Average OD reading of 0.349 at 590 nm wavelength (Corrected to the background)

Standard Curve Equation $y = 3E-05x + 0.0683$

Cell Number (x) = $(OD(y) - 0.0683) / 3E-05$

$$= (0.349 - 0.0683) / 3E-05$$

$$= 9360$$

$$\text{Proliferation Index (PI)} = \frac{\text{Sum of the Cells}}{\text{Number of Originally Seeded Cells}}$$

$$= \frac{9360}{5000}$$

$$= 1.87$$

5.4.0.0 Epirubicin Treatment Alters UGT Enzyme Gene Expression Levels

Uridine 5'-diphospho-glucuronosyltransferase (UGT) are a family of enzymes that play a major role in detoxifying an array of dissimilar carcinogens and the xenobiotics (Hu, DG et al. 2019). Researching UGTs have a critical role in anti-cancer drug clearance. Conjugation of glucuronic acid to lipophilic drug molecules impairs the biological potency of drugs and increases elimination by enhancing the water solubility (Meech et al. 2019). Multiple preclinical studies have reported drug induced overexpression of UGTs in many cancer cell lines (Allain et al. 2020). This can be linked to enhanced drug inactivation and elimination which leads to subsequent reduction of drug sensitivity and emergence of resistance.

In mammals, UGT superfamily comprising four main families; UGT1, UGT2, UGT3 and UGT 8 are expressed in a tissue specific manner (Meech et al. 2019). Out of these, UGT1 and UGT2 subfamilies gain the highest research attention driven by their significant role in drug metabolism. Dellinger et al. in their 2012 study reported an UGT2B7, UGT2B10 and UGT2B15 mediated epirubicin resistance in melanoma cells (Dellinger et al. 2012). This led these UGT enzymes to be assessed in epirubicin treated TNBC cells.

All three assessed UGT enzymes indicated a dose dependent upregulation with approximate fold inductions at 250 and 500 nM epirubicin concentrations as follows: UGT2B7: 5 and 16; UGT2B10: 26 and 109; and UGT2B15 22 and 63 -fold. Due to the low and variable baseline levels of gene expression, only UGT2B10 at 250 nM and UGT2B15 at 500 nM epirubicin demonstrated significance compared to the control. However, the drug treatment induced induction emphasise the role of UGT enzymes in epirubicin resistance in TNBC cells.

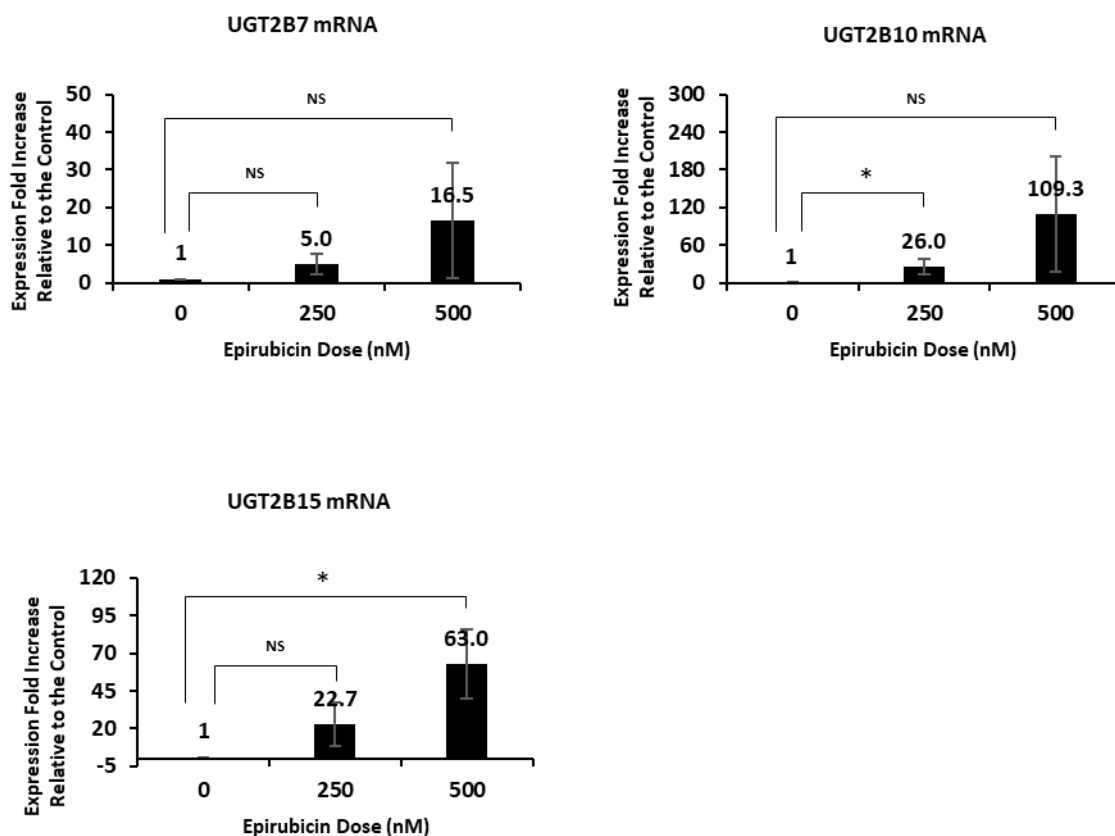


Figure 5.2. Differential expression of *UGT2B7*, *UGT2B10* and *UGT2B15* in MDA-MB-231 cells after treating with 250 nM and 500 nM epirubicin for 48 hours. Ethanol vehicle control is indicated as 0 nM epirubicin treatment in the graphs. The cells at an initial density of 6.25×10^5 cells per well in 2 mL media were seeded in a six-well plate. Cells were treated after a 24-hour adherence period. The target genes were amplified in duplicates. The Human 18S gene was used as the endogenous control in the double delta calculation.

The standard deviation is represented by the error bars (+/-). For all data, statistical significance from the controlled condition was assessed using Student's t-test denoted as * when $p < 0.05$ and ** when $p < 0.01$. The graphs indicate the results of three independent biological replicates with two technical replicates

UGT: Uridine 5'-diphospho-glucuronosyltransferase

5.5.0.0. MDA-MB-231 Spheroid Generation By Liquid Overlay

Method

Method 1: Before the experiment, Matrigel was thawed submerged in an ice bucket for 3-4 hours. Pre-chilled pipette tips and Poly-HEMA coated culture plates were used to avoid premature gelling of the Matrigel. The bottom of the wells of a 24-well plate was coated with undiluted Matrigel (200 $\mu\text{L}/\text{cm}^2$). The plate was incubated at 37°C for 30 mins to allow the matrix to polymerise. The cell suspension containing 2% Matrigel was added on top of the Matrigel bed.

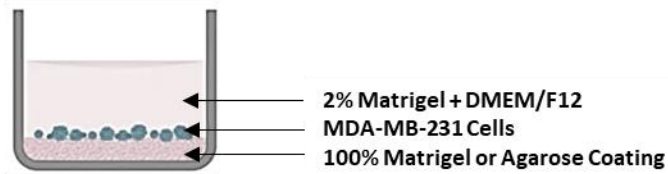
MDA-MB-231 monolayer cultures were trypsinized, and the cells in the suspension were counted using the haemocytometer. The cells to be plated (4×10^4 cells per well) were aliquoted in a centrifuge tube and was pelleted by centrifuging at $\sim 115g$. The supernatant was removed carefully, minimizing the cell loss. The cells were resuspended in half of the media volume (250 μL per well) of precooled DMEM/F12 with 2.5% Matrigel. The cell suspension was plated onto the Matrigel-coated surface. The cells were allowed to settle down for 30 mins in the incubator. The second 250 μL volume of DMEM/F12 containing 2.5% Matrigel was added to each well through the wall with minimal disturbance to the plated cells. Figure 5.3 (A) indicates the diagram of a crosscut of a well prepared for the spheroid formation.

Method 2: In the second attempt to grow spheroids from MDA-MB-231s, the Matrigel bed was replaced with an agarose coating to avoid monolayer cell growth. Also, a 96-well plate was used to obtain spheroids consistent in size. The wells of a 96-well plate were coated with liquified agarose before the experiment. This step could be omitted with the use of poly-HEMA treated plates. Agarose was preferred to avoid the drying time associated with poly-HEMA

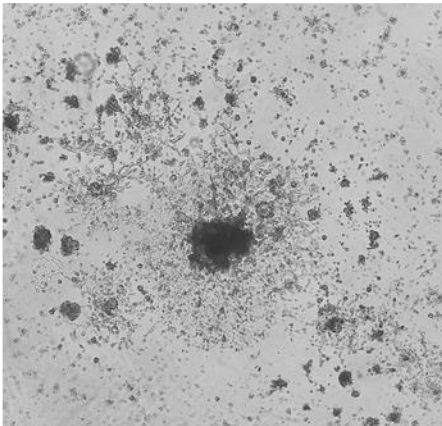
coating. Liquified agarose was kept in a water bath at 60 °C while coating. The cells suspended in 2.5% Matrigel containing DMEM/F12 was plated. Each well contained 10000 cells per well in 200 µl media. The plate was centrifuged at 1000g for 10 mins and moved to the incubator. The plate was kept undisturbed for five days, and media was replenished once every five days until 20 days after the initial cell plating.

Results: The attempt of using the liquid overlay method on the Matrigel proved unsuccessful as the MDA-MB-231 cells with enhanced invasive and migratory capacity started to grow into the Matrigel extracellular matrix (ECM) [Figure 5.3 (B)] rather than forming spheroids on top of the Matrigel bed. Thus, the cells were not studied further. The final attempt of growing spheroids from the MDA-MB-231 cells gave disc-like formations rather than three-dimensional clusters. Upon maintaining the culture for three weeks, this disc-like formation did not form spheroids as shown in Figure 5.3 (C) and the cells were not studied further.

(A)



(B)



(C)

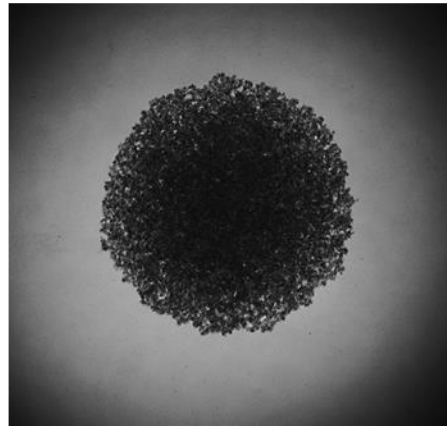


Figure 5.3. MDA-MB-231 spheroid culturing (A) a diagram showing the general structure of the liquid overlay culturing. (B) MDA-MB-231 cells invading the Matrigel bed (Magnification at 40x). (C) The disc like formation of the MDA-MB-231 cells after 20 days in culture in an agarose coated well of a 96-well plate (Magnification at 2x).

Table 5.6. Cross Analysis of the stemness marker mRNA levels in the untreated MDA-MB-231 cells

Gene	Epirubicin Dose (nM)	mRNA Fold Induction*	Expression level of the untreated *
<i>ABCB1</i>	250	77.8	0.1
	500	288.4	
<i>ALDH1</i>	250	112.5	0.5
	500	191.0	
<i>OCT4</i>	250	6.4	7.4
	500	9.9	
<i>SOX2</i>	250	2.6	18.8
	500	5.0	
<i>ABCG2</i>	250	2.2	58.5
	500	1.3	
<i>ABCC1</i>	250	2.2	87.4
	500	1.6	
<i>DNER</i>	250	1.8	232.2
	500	1.4	
<i>CD44</i>	250	1.2	12047.9
	500	1.0	

*Expression level of the untreated (as a function of the cycle threshold value corrected to the 18S Ct)

Expression Level= Power [2, $-(\Delta Ct \text{ value})$] x 10^7